THE JOURNAL
OF
CHEMICAL PHYSICS

VOLUME 12, NUMBER 12 DECEMBER, 1944

Bromination of Hydrocarbons. I. Photochemical and Thermal Bromination of Methane and Methyl Bromine. Carbon-Hydrogen Bond Strength in Methane

G. B. KISTIAKOWSKY* AND E. R. VAN ARTSDALEN**
Department of Chemistry, Harvard University, Cambridge, Massachusetts
(Received October 12, 1944)

The photochemical bromination of methane was studied in the temperature range 423–503°K and found to proceed through the following chain mechanism:

$$\begin{aligned}
&(1) && Br_2+h\nu=Br+Br\\
&(2) && Br+CH_4=CH_3+HBr\\
&(3) && CH_3+Br_2=CH_3Br+Br\\
&(4) && CH_3+HBr=CH_4+Br\\
&(5) && Br+Br+M=Br_2+M.
\end{aligned}$$

Bromination of methyl bromide is analogous and from 7.5 to 10 times more rapid in this temperature range. Hydrogen bromide inhibits bromination of methane but not of methyl bromide. Thermal bromination was studied at 570°K and found to follow the same mechanism as photochemical reaction, except that bromine atoms are produced thermally. The activation energy of photochemical bromination of methane is 17.8 kcal./mole and that of methyl bromide is 15.6 kcal./mole. Varying efficiencies of different molecules as third bodies in the homogeneous recombination of bromine atoms are discussed. Configurations of activated complexes have been assigned and by statistical mechanical calculations shown to be reasonable. Activation energies and other data have been combined to arrive at a value for the C−H bond strength in methane of 102 kcal./mole at room temperature.

SUBSTITUTION reactions of bromine with paraffins are known to yield bromo-paraffins and hydrogen bromide. They have not been studied kinetically heretofore. Coehn and Cordes[1] have investigated the photochemical chlorination of methane and reported that it is analogous to the hydrogen chloride reaction. Other writers[2] have suggested that bromination should take place in a similar type of chain mechanism. It was felt that a thorough study of the bromination of paraffins might lead to valuable methods for determining strengths of several carbon-hydrogen and carbon-carbon bonds. This has proved to be the case.[3]

REAGENTS AND MATERIALS

Methane of extremely high purity was prepared jointly with Dr. E. E. Roper by decomposition of a methyl grignard reagent with

* On leave.

** Department of Chemistry, Lafayette College, Easton, Pennsylvania: at present on leave of absence to Department of Physiological Chemistry, Johns Hopkins School of Medicine, Baltimore, Maryland.

[1] A. Coehn and H. Cordes, Zeits. f. physik. Chemie **B9**, 1 (1930).

[2] H. J. Schumacher, X. Congr. Int. di Chimica **IV**, 464 (1938); J. W. T. Spinks, Chem. Rev. **26**, 129 (1940).

[3] Andersen, Kistiakowsky, and Van Artsdalen, J. Chem. Phys. **10**, 305 (1942). E. R. Van Artsdalen, *ibid.* **10**, 653 (1942); H. C. Andersen and G. B. Kistiakowsky, *ibid.* **11**, 6 (1943).

ethanol. It was anticipated that oxygen would inhibit photochemical bromination, hence great pains were taken to exclude air, preparation being accomplished under vacuum conditions using reagents repurified especially. The methane was distilled from a trap in liquid air to one in liquid nitrogen (−188° to −197°) and showed a distillation pressure between 12 and 12.5 mm. Vapor pressure determinations with different amounts vaporized indicated that the methane was extremely pure.

Mallinckrodt bromine, A.R. grade, was purified further by storing over pure potassium bromide to eliminate chlorine. It then was distilled under vacuum through a drying tube containing P_2O_5. Alternate freezing and melting of the sample under high vacuum was carried out to eliminate traces of air. In a final distillation the middle third was retained for this investigation.

A sample of methyl bromide, about 99.8 percent pure, was donated for this work by The Dow Chemical Company. It was purified further by repeated bulb-to-bulb distillations under vacuum until no further change in its vapor pressure in a dry-ice acetone bath could be detected. Its vapor pressure at 0°C was 677 mm. Approximately 95 percent was distilled from a dry-ice bulb into a reservoir flask. The vapor pressure of the 5 percent residuum was 674 mm. Kemp and Egan[4] give 675.8 mm as the vapor pressure at 0°C.

Hydrogen bromide was prepared by the direct union of electrolytic hydrogen and A.R. grade bromine, according to the method outlined by Ruhoff, Burnett, and Reid.[5] Repeated bulb-to-bulb distillations (dry-ice to liquid air) were made of the product under vacuum, voiding considerable hydrogen bromide. The purified material formed a clear, colorless liquid and a perfectly white solid. Its vapor pressure was 320 mm at −81°C.

EXPERIMENTAL METHOD

Bromination was followed by observing the rate of disappearance of bromine from the reaction system. For this purpose a photoelectric photometer of balanced construction was used. Light of wave-length greater than 4360A was eliminated by Corning violet filter, No. 511. Immediately prior to each set of measurements, the photometer was calibrated against known pressures of bromine measured with a quartz spiral null-point manometer against a glass scale mercury manometer. In general it was possible to reproduce bromine partial pressures to ±0.1 mm. Ability to rotate the photometer between two fixed paths, one of which passed through the reaction cell and the other through a comparison cell, made it possible to check the zero setting of the photometer immediately before and after each individual determination of bromine concentration.

A Pyrex glass reaction cell of about 82-cc volume and 106-cm² wall area was supported in a fixed position in an electrically heated glass air bath which was made large in comparison with the cell in order to minimize thermal gradients. Temperature was measured to 0.1° with a thermocouple and controlled to ±0.2°–0.3°. Dead space was about 2–2.5 cc which is not serious for these bromination reactions in which there is no volume change.

The reaction mixture was illuminated in the photo experiments by blue light (from a 750-watt Mazda projection lamp) filtered through 0.5″ of water and 4.54-mm Corning blue-green filter No. 430 to eliminate red and infra-red radiation. Constant amperage through the lamp circuit was maintained by manual rheostat control. The axis of illumination was perpendicular to the photometer path. All lamps, air bath windows, and filters were cleaned with alcohol prior to each set of measurements.

Bromine predissociation in the band region yields two normal bromine atoms, while dissociation in the continuum gives one normal atom and one excited atom. Jost[6] has shown that there is no very appreciable difference between using light in the band region or in the continuum to activate photochemical formation of hydrogen bromide, indicating that the electronic excitation energy is not useful in the reaction. Most of the radiation in our experiments was in the continuum. Bromine was the only substance present which absorbed any light of the wave-lengths used.

[4] J. D. Kemp and C. J. Egan, J. Am. Chem. Soc. **60**, 2097 (1938).

[5] Ruhoff, Burnett, and Reid, *Organic Syntheses* (John Wiley & Sons, Inc., New York, 1935), Vol. XV, p. 35.

[6] W. Jost, Zeits. f. physik. Chemie **B3**, 95 (1929).

It is known that at the temperatures employed in this research no thermal decomposition of either methane or methyl bromide occurs.[7] An *a posteriori* calculation indicates that dark reaction (thermal bromination) should be undetectable in the course of an hour at 483°K. Experimentally no dark reaction at this temperature was observed over a period of half an hour, in which time photochemical bromination was practically complete. Therefore the photoreaction was stopped by inserting a metal shield between light source and reaction cell while bromine concentrations were determined with the photometer. In this way repeated measurements of bromine concentration could be made after each desired interval of illumination. In the case of thermal brominations photometer readings had

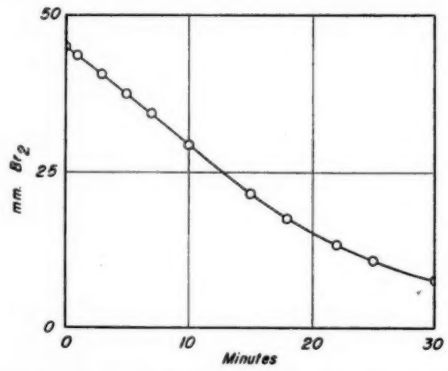

FIG. 1. Photochemical bromination of methane. 483°K. Initial pressures, CH_4 641 mm; Br_2 45.0 mm.

to be taken "on the fly," that is, while the reading was changing. In all cases reproducibility was satisfactory.

Bromine concentrations were measured at suitable times and from them rates of reaction during small time intervals were determined and an extrapolation made to obtain the rate at zero time. Rate constants were calculated from this rate at zero time. This method was employed because at the start of the reaction there are no products of reaction present to complicate the kinetics. It is known that all of the bromomethanes can be produced by photobromination, hence it is essential in a kinetic study to measure the rate of formation of a particular compound. The plot of a typical experiment is given in Fig. 1.

[7] H. P. Meissner and H. J. Schumacher, Zeits. f. physik. Chemie **A185**, 435 (1940).

EXPERIMENTAL RESULTS

It was found experimentally that the rate of photobromination of methane was proportional to methane concentration, to the square root of bromine concentration, and inversely proportional to the square root of total pressure. In analogy with the hydrogen bromide synthesis it is plausible to expect the rate determining step in methane bromination to involve the reaction of a bromine atom, produced either thermally or photochemically, with a methane molecule. On this basis the initial rate should be proportional to methane concentration and to the square root of bromine concentration, or in the case of the photoreaction, to the square root of absorbed light intensity. The Lambert-Beer law is known to apply quite accurately in the case of bromine up to a partial pressure of 50 mm,[8] about the maximum employed here, hence absorbed light intensity is proportional to bromine concentration. The inverse proportionality with total pressure in the photochemical bromination is in accord with a three-body mechanism for destruction of bromine atoms.

Table I gives values of initial rate constants (k') for photobromination calculated by means of the equation

$$-d[Br_2]/dt = k'[CH_4][Br_2]^{\frac{1}{2}}[1/P]^{\frac{1}{2}}. \quad (A)$$

k' is a rate constant multiplied by absorption coefficient and an apparatus constant. P is the total pressure. The three series of experiments are not comparable in terms of absolute rate because design and adjustment of the optical system were altered slightly between them. Series A and B show clearly that the initial rate constant remains unchanged over a threefold variation in both CH_4 and Br_2 partial pressures as well as total pressure. However, this equation cannot be used to evaluate rate constants during any appreciable part of the reaction because of secondary reactions and inhibition by the hydrogen bromide produced.

A direct test of the dependence of rate on the intensity of incident radiation was made by inserting between the light source and reaction cell a screen calibrated to transmit 44.5 percent

[8] M. Bodenstein and H. Lütkemeyer, Zeits. f. physik. Chemie **114**, 208 (1924).

TABLE I. Photobromination of methane.

	T°K	Initial pressures (mm at T°K) CH_4	Br_2	k'(sec.$^{-1}$) $\times 10^4$
Series A	503	547	53.5	7.0
		618	41.7	7.3
		613	40.5	7.3
		555	41.1	7.2
		553	41.1	7.0
		456	41.5	7.2
		311	43.0	7.3
		284	40.5	7.2
		279	40.8	7.0
		210	40.9	7.7
		473	25.1	7.8
		280	21.5	7.0
		497	16.3	7.3
				7.25
Series B	483	641	45.0	1.38
		514	44.4	1.39
		210	44.4	1.41
				1.40
Series C	483	492	44.4	2.94
		488	45.1	3.03
		486	46.2	2.89
		486	43.6	2.53
		483	44.1	2.84
		450	45.8	2.71
				2.82
	453	424	45.7	0.816
		419	51.1	.816
		418	45.5	.830
		418	45.4	.764
				0.807
	423	406	45.2	0.196
		400	44.9	.185
				0.190

of incident radiation. If the rate is proportional to the square root of absorbed light and with validity of the Lambert-Beer law this screen should reduce the velocity of bromination to $(0.445)^{\frac{1}{2}}=0.667$ or 66.7 percent of its value in absence of the screen. Experimentally the rate was reduced to 68.3 percent of its normal value. This is within experimental error of 66.7 percent and is considered as additional proof that the rate depends upon the square root of absorbed light intensity, which latter is proportional to the bromine concentration.

It was found that hydrogen bromide, a product of the reaction, inhibits bromination. The following equation was found to apply to photobromination of methane in the presence of HBr,

$$-\frac{d[Br_2]}{dt}=\frac{k'[CH_4][Br_2]^{\frac{1}{2}}[1/P]^{\frac{1}{2}}}{1+\dfrac{k_4[HBr]}{k_3[Br_2]}}. \qquad (B)$$

Table II shows results of experiments made to study the effect of inhibition by HBr. Values of k' were taken from experiments run in absence of HBr. The experiments at 310°K were of very long duration (two months), and were carried out in sealed tubes, analysis being made chemically instead of photometrically. They are subject to lower accuracy than those at the two higher temperatures. In any case it is difficult to determine the ratio k_4/k_3 with high accuracy because the rate is rather insensitive to relatively large changes in HBr concentration.

Bodenstein and Lütkemeyer,[8] employing an analogous expression, found for the hydrogen-bromine reaction a value of $k_4/k_3=0.10$ which is temperature independent. It is seen in Table II that at high temperature HBr inhibits bromination of CH_4 more strongly than that of H_2 and that this inhibition has a definite temperature coefficient.

An experiment was performed at 453°K to determine whether oxygen exerts an inhibitory action. To a reaction mixture of 371 mm of CH_4 and 45.7 mm of Br_2, carefully dried and CO_2-free air was admitted corresponding to 1.6 mm of O_2. A calculation using $k'=0.807$ $\times 10^{-4}$ sec.$^{-1}$ showed that if this behaved as an inert gas the initial rate of disappearance of Br_2 should have been 0.60 mm/min. The experimental value was 0.4 mm/min., indicating strong inhibition by oxygen. However, this inhibition

TABLE II. Photobromination of methane. Inhibition by HBr.

T°K	Initial pressures (mm at T°) CH_4	HBr	Br_2	k_4/k_3
483	363	121	46.6	0.212
	385	96	47.7	.204
423	254	138	41.6	.154
	248	116	42.1	.111
310	298	143	48.4	.089
	281	135	48.4	.064

was present at the start of the reaction only, the rate having increased to 0.6 mm/min. after about 1.5 mm of Br_2 had been consumed. The reaction was normal from then on. This experiment is in agreement with known behavior of oxygen in other brominations and bromine sensitized oxidations.[2]

Series C of Table I gives data for a 60° temperature interval which have been used to calculate the activation energy of photochemical bromination of methane. Before such data may be employed with assurance it is necessary to answer two questions: (1) Does the absorption coefficient of bromine vary appreciably over the temperature range in question, and (2) is the ideal gas law sufficiently exact under the conditions of the experiment? The second question was tested by applying the Berthelot equation to Br_2. Deviations between it and the ideal gas law in our pressure ranges were considerably less than 0.5 percent, hence the ideal gas law was used. Bodenstein and Lütkemeyer[8] have shown that the absorption coefficient of bromine varies about 5 percent between room temperature and 490°K at 5350A, decreasing with shorter wave-length to 1 percent variation at 5000A. Relatively little light of wave-length greater than 5000A was used. Consequently no correction was made for temperature dependence of the absorption coefficient over our smaller temperature interval. In Fig. 2, log k' has been plotted against $1/T$ giving a good straight line. The slope of this line gives 18.25 kcal. for the uncorrected energy of activation. Taking the mean temperature of 453°K, $RT/2=0.45$ kcal. leaving 17.8 kcal. by subtraction from 18.25 for the corrected energy of activation.[9]

The photochemical bromination of methyl bromide corresponds to the second step in the over-all bromination of methane. It was studied kinetically in the same manner as was methane. The rate of disappearance of bromine follows the kinetic expression

$$-d[Br_2]/dt=k''[CH_3Br][Br_2]^{\frac{1}{2}}[1/P]^{\frac{1}{2}}. \quad (C)$$

Rate constants are given for three series of experiments in Table III. Series C has been used to evaluate the activation energy as in the case of methane, the data being plotted in Fig. 2. The corrected value for the activation energy is 15.6 kcal./mole. The effect of hydrogen bromide was investigated at both 483°K and 423°K. No inhibition was observed.

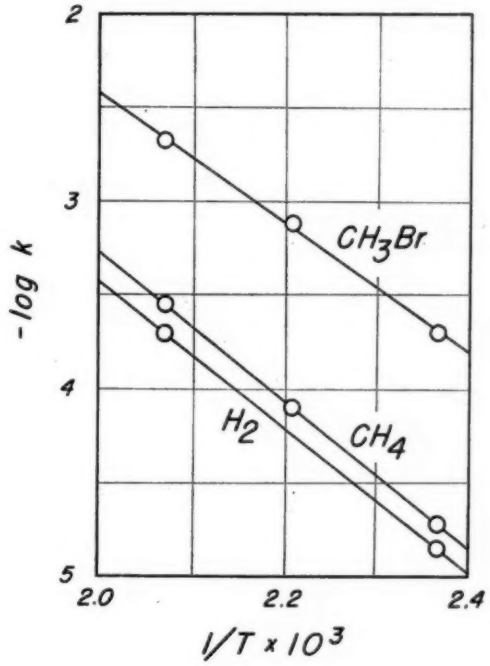

FIG. 2. Temperature coefficients. Each circle represents average of all runs at that particular temperature.

The rate constants for bromination of methane and methyl bromide being known separately, it is possible to calculate what the rate should be in mixtures of methane and methyl bromide. Satisfactory agreement was obtained between experiment and calculation when tested.

Several experiments at both 483 and 423°K were made on the photochemical hydrogen-bromine reaction in order to check our method on a very well studied reaction. Good reproducibility was obtained. The activation energy calculated from these experiments was 17.5 kcal./mole in agreement with Bodenstein's value of 17.6 kcal./mole. The data are plotted in Fig. 2.

The rates of thermal bromination of methane, methyl bromide and hydrogen were measured at 570°K. The method of measurement was essentially the same as that used in the photochemical experiments. Data are recorded in Table IV.

[9] This correction is based on the simple bimolecular rate equation, $k=Z'T^{\frac{1}{2}}e^{-E/RT}$.

Rate constants were calculated from the initial rate of reaction using the equation:

$$-d[Br_2]/dt = k[CH_4][Br_2]^{\frac{1}{2}}. \qquad (D)$$

It is observed that the rate is independent of total pressure and that concordant values of k are obtained over a twofold variation of partial pressures.

The data of Bodenstein and Lind[10] were used to calculate a rate constant for the hydrogen reaction at 570°K of $k=0.022$ which is in good agreement with our value of $k=0.0196$. A difference of 1 to 1.5° in the temperature scales would bring the two values into excellent agreement.

DISCUSSION

The following chain is postulated as the reaction mechanism operative in bromination of methane.

$$Br_2+h\nu \rightarrow Br+Br \qquad (1)$$

or

$$Br_2+M \rightarrow Br+Br+M \qquad (1a)$$

$$Br+CH_4 \rightarrow CH_3+HBr \qquad (2)$$

$$CH_3+Br_2 \rightarrow CH_3Br+Br \qquad (3)$$

$$CH_3+HBr \rightarrow CH_4+Br \qquad (4)$$

$$Br+Br+M \rightarrow Br_2+M \qquad (5)$$

. . . . . .

$$Br+CH_3Br \rightarrow CH_2Br+HBr \qquad (2a)$$

$$CH_2Br+Br_2 \rightarrow CH_2Br_2+Br \qquad (3a)$$

$$CH_2Br+HBr \rightarrow CH_3Br+Br \qquad (4a)$$

etc.

At sufficiently low pressures one would expect chain termination to result from diffusion of bromine atoms to the wall followed by heterogeneous recombination. This is not the case in our experiments, for the rate then would be first order with respect to Br_2 concentration instead of 0.5 order.

Reactions involving production of hydrogen atoms have been ruled out on the basis of energetic considerations. Some would involve Walden type inversions which are known to have high activation energies. For example, it has been shown[11] that the reaction $CH_4+H \rightarrow CH_3+H_2$ requires 8 to 11 kcal. activation energy while the Walden inversion $CH_4+H \rightarrow CH_4+H$ requires 35 to 40 kcal. Thus there is good evidence against reactions of the type $CH_4+Br \rightarrow CH_3Br+H$.

Using the above reaction mechanism and assuming steady state concentrations of chain-propagating radicals, one can derive the ex-

[10] M. Bodenstein and S. C. Lind, Zeits. f. physik. Chemie **57**, 168 (1906).

[11] Gorin, Kauzmann, Walter, and Eyring, J. Chem. Phys. **7**, 633 (1939).

TABLE III. Photobromination of methyl bromide.

	T°K	Initial pressures (mm at T°K) CH_3Br	Br_2	k''(sec.$^{-1}$) $\times 10^3$
Series A	503	337	52.4	5.36
		159	41.8	5.15
		347	40.6	5.19
Series B	483	381	43.2	1.07
		453	42.8	1.02
		398	42.6	1.08
		298	32.9	1.15
		211	29.0	1.17
Series C	483	259	48.5	2.07
		287	45.9	2.21
		255	45.2	2.25
		472	44.1	1.93
				2.12
	453	331	45.5	0.754
		336	44.5	.769
				0.762
	423	317	45.0	0.209
		308	44.4	.199
		295	42.8	.198
				0.202

TABLE IV. Thermal brominations at 570°K.

	Initial pressures (mm at 570°K) X	Br_2	k(cc mole^{-1})$^{\frac{1}{2}}$ sec.$^{-1}$
A. $-CH_4$	517	53.0	0.0247
	331	55.5	.0250
	317	48.1	.0249
	227	51.0	.0240
	353	25.0	.0253
	325	22.0	.0247
			0.0248
B. $-H_2$	431	51.2	0.0193
	405	52.0	.0198
			0.0196
C. $-CH_3Br$	352	52.7	0.156
	210	53.2	.163
	342	25.6	.162
			0.160

pression

$$\frac{d[CH_3Br]}{dt}=\frac{k_2[CH_4](n/k_5[M])^{\frac{1}{2}}}{1+\dfrac{k_4[HBr]}{k_3[Br_2]}}, \quad (E)$$

where n represents the number of absorbed light quanta and $[M]$ is the total concentration of all molecules present. It is clear that $n=k_{ap}\alpha I[Br_2]$, where k_{ap} is a temperature independent apparatus constant, I is the intensity of incident radiation, and α is the absorption coefficient of bromine. Because I was a constant in any set of experiments we may write $k'=k_2(k_{ap}\alpha I/k_5)^{\frac{1}{2}}$. Hence, Eq. (E) is seen to be equivalent to Eq. (B). It is based on methyl bromide as the only bromomethane formed and is, therefore, a first-order approximation only. Considering secondary bromination to produce methylene bromide with negligible inhibition of this step

TABLE V. Frequency factor and entropy of activation at 570°K.

Reaction	A Expt.	Z' Collision theory	S Expt.	S Calc.
$Br+H_2$	1.14×10^{12}	11.7×10^{12}	−2.31	
$Br+CH_4$	1.48×10^{12}	7.2×10^{12}	−1.81	−1.84
$Br+CH_3Br$	1.35×10^{12}	5.9×10^{12}	−1.98	−1.94

by hydrogen bromide, the second-order approximation for the rate becomes

$$\frac{d[CH_3Br]}{dt}=\frac{k'[CH_4][Br_2]^{\frac{1}{2}}[1/P]^{\frac{1}{2}}}{1+\dfrac{k_4[HBr]}{k_3[Br_2]}}-k''[CH_3Br][Br_2]^{\frac{1}{2}}[1/P]^{\frac{1}{2}}, \quad (F)$$

where $k''=k_{2a}(k_{ap}\alpha I/k_5)^{\frac{1}{2}}$. The rate of disappearance of bromine clearly will be the sum of the two terms on the right. This equation was found to fit our experimental data when applied by means of successive approximations.

From the postulated mechanism one derives the first-order approximation for the thermal reaction:

$$\frac{d[CH_3Br]}{dt}=\frac{k[CH_4][Br_2]^{\frac{1}{2}}}{1+\dfrac{k_4[HBr]}{k_3[Br_2]}}, \quad (G)$$

in which $k=k_2(K_{eq})^{\frac{1}{2}}$ where K_{eq} is the equilibrium constant for dissociation of bromine. This reduces to Eq. (D) at zero time when the concentration of hydrogen bromide is zero.

Qualitatively we may observe that the rate of disappearance of bromine will increase for a time after the reaction begins because of the gradual increase in concentration of methyl bromide which is brominated from 7.5 to 10 times more rapidly than methane in the temperature range we investigated. Inhibition by hydrogen bromide becomes progressively more pronounced in the latter stages of bromination when its concentration becomes relatively high in respect to bromine. Acceleration by methyl bromide is more important than inhibition by hydrogen bromide. However, decreasing bromine concentration of itself also causes a decreasing rate of bromination. These effects are seen in Fig. 1.

It is evident from the form of the kinetic equation that the rate determining step is reaction (2) in the case of methane and (2a) in the case of methyl bromide. If this were not true the rate would depend on some other concentration functions. Energetic considerations also are in agreement. Reaction (3) will be exothermic to an appreciable extent because the C−Br bond is stronger than the Br−Br bond (45.2 kcal.) and because it is a free radical reaction it should require very low or zero activation energy. On the other hand, reaction (2) should be endothermic because the C−H bond is certainly stronger than the H−Br bond (85.6 kcal.). It must, therefore, require an activation energy at least equal to its endothermicity. On the basis of these considerations the activation energy of bromination of methane, 17.8 kcal., has been ascribed to reaction (2), while the corresponding value of methyl bromide, 15.6 kcal., has been assigned to reaction (2a).

The temperature dependence of inhibition by hydrogen bromide enables a determination of the difference in activation energies between reactions (3) and (4) and a reliable estimate of the activation energy of reaction (4). Employing the usual, simple bimolecular equation $k=AT^{\frac{1}{2}}e^{-E/RT}$, where A is a temperature independent frequency factor and E the activation energy, we express the logarithmic ratio of the rate constants of reactions (3) and (4) in the

TABLE VI. Rate constant ratios.

T°K	k_{CH_4}/k_{H_2} Experimental	Calc'd with efficiency 1:1	3.6:2.2	k_{CH_3Br}/k_{H_2} Experimental	Calc'd with efficiency 1:1	2.7:2.2	k_{CH_3Br}/k_{CH_4} Experimental	Calc'd with efficiency 1:1	2.7:3.6
Thermal 570	1.26			8.2			6.4		
Photo 483	1.39	1.05	1.35	10.5	9.6	10.5	7.5	9.0	7.7
453							9.3	10.9	9.4
423	1.33	1.01	1.30	14.2	12.8	14.0	10.6	12.5	10.7

form

$$\ln\frac{k_4}{k_3}=\ln\frac{A_4}{A_3}-\frac{E_4-E_3}{RT}.$$

For these two similar reactions the assumption is made that the quantity (E_4-E_3) does not vary appreciably with temperature. Since A also is essentially temperature independent, the expression can be differentiated to give

$$d\ln\frac{k_4}{k_3}=\frac{E_4-E_3}{RT^2}dT$$

which combined with inhibition data (Table II) yields $(E_4-E_3)=2$ kcal. For reasons already mentioned it is not unreasonable to assume that the activation energy of reaction 3 is zero, making 2 kcal. the activation energy of reaction 4 in good agreement with the value of 1.5 kcal. obtained by Andersen and Kistiakowsky[12] from experiments on the photolysis of methyl iodide in the presence of hydrogen bromide.

Absolute rates of thermal bromination at 570°K and data of Gordon and Barnes[13] on the thermal dissociation of molecular bromine have been used to calculate the temperature independent frequency factor A in the equation $k=AT^{\frac{1}{2}}e^{-E/RT}$ as applied to the rate determining single reactions of bromine atoms with hydrogen, methane, and methyl bromide. Experimental values of E determined in the photochemical brominations were used. The collision number Z was calculated by classical collision theory employing the following molecular diameters, $H_2=2.76$A, $CH_4=3.2$A, $CH_3Br=4.5$A, $Br=3.0$A. Values of A and Z' $(=Z/T^{\frac{1}{2}})$ are given in Table V. It is interesting that A and Z' differ little from one another, the steric factor being approximately 0.1 to 0.2. This is in contrast to the reaction of hydrogen atoms with methane where a steric factor of the order of 10^{-2} to 10^{-3} is required.[11] A possible explanation of this difference may be found by considering the relative sizes of bromine and hydrogen atoms. The hydrogen atom presumably must approach the methane molecule more precisely oriented along the axis of a C−H bond than is required in the case of the bromine atom.

Experimental entropies of activation were calculated from the data of thermal experiments at 570°K using a formula of Kistiakowsky and Ransom,[14]

$$k=\frac{k_BT}{h}e^2e^{S/R}e^{-E/RT},$$

where S is the entropy of activation, k_B the Boltzmann constant, and h Planck's constant. "Theoretical" entropies of activation were calculated by statistical mechanical methods. Configurations of activated complexes were assigned by analogy with those calculated by Gorin, Kauzmann, Walter, and Eyring[11] for reaction between hydrogen atoms and methane. It was assumed that the minimum activation energy is required when a bromine atom approaches a methane molecule along the axis of a C−H bond. No change in configuration of the CH_3 part of the molecule was assumed. Interatomic distances and vibrational frequencies were as-

[12] H. C. Andersen and G. B. Kistiakowsky, J. Chem. Phys. **11**, 6 (1943).
[13] A. P. Gordon and C. Barnes, J. Chem. Phys. **1**, 692 (1933).
[14] G. B. Kistiakowsky and W. W. Ransom, J. Chem. Phys. **7**, 725 (1939).

signed as follows,

$$\underset{1.09A}{H_3}\text{———}\underset{1.17A}{C}\text{------}\underset{1.86A}{H}\text{----------Br}$$

C–H stretching	3000 cm^{-1}	(4)
CH_3 torsional	1440	(6)
H–Br stretching	2200	(1)
Br–H–CH_3 bending	500	(2).

In the case of methyl bromide the assignments were

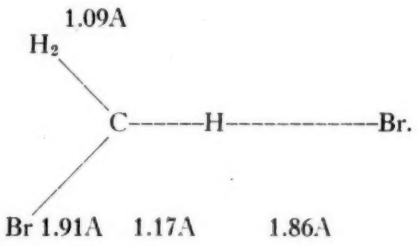

Frequencies of methyl bromide[15] plus others for bromine atom assignments were 3061 (2), 2900 (1), 2200 (1), 1450 (2), 1305 (1), 957 (2), 610 (2), and 105 (2). A comparison of experimental and "theoretical" entropies of activation is given in Table V. It is observed that these complexes have low, doubly degenerate bending frequencies which make large contributions to the entropy. Unfortunately they cannot be estimated with high precision. However, agreement between experimental and calculated entropies of activation indicates that the structures assigned to the activated complexes are reasonable.

Ratios of the experimental rate constants for thermal and photochemical reactions are shown in Table VI. Clearly in the case of thermal bromination these are ratios of the rate constants of reaction (2) and its prototypes, the equilibrium constant for dissociation of bromine cancelling out. However, for photochemical bromination they would represent the ratios of the bromine atom reactions only if all molecules were equally effective third bodies for homogeneous recombination of bromine atoms. That such is not the case is shown in Table VI. Ratios for photobromination calculated from thermal absolute rates and experimental activation energies on the assumption of equal efficiencies do not agree with experiment. Rabinowitch and Wood[16] have studied the influence of various molecules on recombination of bromine atoms and report that the efficiencies of hydrogen and methane are in the ratio 2.2:3.6, respectively. When these values are used in calculating rate constant ratios excellent agreement with experiment is obtained as shown in Table VI. We deduced from our experiments that the efficiency of methyl bromide on the same basis as hydrogen and methane was 2.7, the results being indicated in the table. It is surprising that methyl bromide efficiency should be less than that of methane. However, this quantity is very susceptible to a small difference in the values of activation energies. A recalculation assuming an activation energy of 16.2 kcal., i.e., 0.6 kcal. above our accepted value of 15.6 kcal., for bromination of methyl bromide yields an efficiency of 3.9. It can be said that our experiments confirm the work of Rabinowitch and Wood and indicate that the efficiencies of methyl bromide and methane are roughly equal. In the inhibition experiments with hydrogen bromide no account has been taken of varying efficiency of methane and hydrogen bromide. Work of Hilferding and Steiner[17] combined with that of Rabinowitch and Wood indicates that the efficiencies of methane and hydrogen bromide are equal. Differing efficiencies would change the absolute value of the inhibition constant but should not affect its temperature coefficient.

The experimental rate constant ratios of photochemical bromination in Table VI can be used as an estimate of the relative quantum yields. If the quantum yield for hydrogen bromide synthesis is one[18] then it is about 1.4 for formation of methyl bromide.

CARBON-HYDROGEN BOND STRENGTH

Values for activation energies of reactions (2) and (4) may be combined to obtain the heat of reaction at the mean experimental temperature

[15] D. P. Stevenson and J. Y. Beach, J. Chem. Phys. **6**, 25 (1938).

[16] E. Rabinowitch and W. C. Wood, Trans. Faraday Soc. **32**, 907 (1936).

[17] K. Hilferding and W. Steiner, Zeits. f. physik. Chemie **B30**, 399 (1935).

[18] See, for example, W. A. Noyes, Jr., and P. A. Leighton, *The Photochemistry of Gases* (Reinhold Publishing Corporation, New York, 1941).

453°K for $CH_4+Br\rightarrow CH_3+HBr$. Because the numbers of molecules of products and reactants are equal, we may write

$$\Delta H^0_{453}=\Delta E^0_{453}=(E_2-E_4)=(17.8-2)=15.8 \text{ kcal.}$$

$\Delta H_0{}^0$ was calculated using the following values of $(H^0_{453}-H_0{}^0)$.

	$H^0_{453}-H_0{}^0$
CH_4	3.83 kcal./mole
CH_3	3.75 kcal./mole
HBr	3.15 kcal./mole
Br	2.25 kcal./mole
H	2.25 kcal./mole.

Values for CH_4 and HBr are from a review by Pitzer,[19] H and Br were calculated for free atoms with translational degree of freedom only, and the value for CH_3 is that for CH_4 diminished by 0.3 times the vibrational contribution. We thus obtain $\Delta H_0{}^0=15.0$ kcal. This may be combined with the value 85.8 kcal. for the heat of dissociation of hydrogen bromide[20] to obtain the carbon-hydrogen bond strength as follows:

$CH_4+Br\rightarrow CH_3+HBr$	$\Delta H_0{}^0=$ 15.0 kcal.
$HBr\rightarrow H+Br$	$\Delta H_0{}^0=$ 85.8 kcal.
$CH_4\rightarrow CH_3+H$	$\Delta H_0{}^0=100.8$ kcal.

The value of ΔH^0 at any temperature may be calculated in similar manner. We obtain the following rounded values for the carbon-hydrogen bond strength at the indicated temperatures.

T°K	$D(CH_3-H)$
0	101 kcal.
293	102 kcal.
453	103 kcal.

Although quite divergent values of the carbon-hydrogen bond strength in methane have been reported, a considerable body of evidence points to its being in the range 100 to 104 kcal./mole.[21] The agreement between our value and that of Stevenson[21g] derived from electron impact critical potentials is particularly impressive. Thus two entirely different experimental methods of determining the carbon-hydrogen bond strength agree within their experimental errors (about 1 kcal.). Semi-empirical calculations of H. A. Taylor and Burton[21e] by the Voge method yield the value of 102.1 kcal. if one assumes the zero-point energy of CH_3 to be three-quarters that of methane.

Similar assumptions regarding activation energies lead to the conclusion that the substitution of bromine for one hydrogen in methane lowers the bond strength by about 2 to 3 kcal. von Braunwarth and Schumacher[22] found an activation energy of the order of 10 kcal. for bromination of bromoform, which indicates that the introduction of 3 bromine atoms into methane lowers its C−H bond strength by about 7–8 kcal. Probably the introduction of two bromine atoms lowers this bond strength about 5–6 kcal.

[19] K. Pitzer, Chem. Rev. **27**, 39 (1940).

[20] $D(H-Br)=85.8$ kcal. by combination of the heat of dissociation of $H_2=102.48$ kcal. [H. Beutler, Zeits. f. physik. Chemie **B29**, 315 (1935)] with that for $Br_2=45.22$ kcal. and heat of formation of HBr from its elements = 11.99 kcal. (reference 13).

[21] (a) L. Pauling and J. Sherman, J. Chem. Phys. **1**, 606 (1933), 100 kcal.; (b) R. G. W. Norrish, Trans. Faraday Soc. **30**, 103 (1934), 103 kcal.; (c) F. O. Rice and K. K. Rice, *Aliphatic Free Radicals* (Johns Hopkins Press, Baltimore, 1935), p. 75, 100 kcal.; (d) F. Patat, Zeits. f. physik. Chemie **B32**, 290 (1936), 102.5 kcal.; (e) H. A. Taylor and M. Burton, J. Chem. Phys. **7**, 572 (1939), 102.1–103.7; (f) E. C. Baughan and M. Polanyi, Nature **146**, 685 (1940), 103.6 kcal.; (g) D. P. Stevenson, J. Chem. Phys. **10**, 291 (1942)—101 kcal.

[22] von Braunwarth and H. J. Schumacher, Kolloid Zeits. **89**, 184 (1939).

THE JOURNAL OF CHEMICAL PHYSICS VOLUME 12, NUMBER 12 DECEMBER, 1944

Bromination of Hydrocarbons. II. Photochemical Bromination of Ethane and Ethyl Bromide. Carbon-Hydrogen Bond Strength in Ethane

HOLGER C. ANDERSEN* AND E. R. VAN ARTSDALEN**
Department of Chemistry, Harvard University, Cambridge, Massachusetts

(Received October 12, 1944)

The kinetics of the photochemical bromination of ethane was determined. The mechanism is very similar to the analogous brominations of hydrogen and methane:

(1) $Br_2+h\nu=Br+Br$
(2) $Br+C_2H_6=C_2H_5+HBr$
(3) $C_2H_5+Br_2=C_2H_5Br+Br$
(4) $C_2H_5+HBr=C_2H_6+Br$
(5) $Br+Br+M=Br_2+M$.

Rate constants computed by assuming various efficiencies for ethane as the third body in step (5) are presented, as well as those calculated by considering heterogeneous recombination of bromine atoms. The rate of bromination of ethyl bromide is about the same as that for ethane, but its exact determination was precluded by the presence of rapidly brominated impurities. The experimental activation energy, 13.6±0.5 kcal., is quite insensitive to the several variations in mechanism discussed, and indicates a value of 98±2 kcal. for the upper limit of the strength of the C_2H_5-H bond. This figure is in good agreement with absolute values reported by other workers.

KINETIC studies of the bromination of methane[1] having proved successful, it was decided to extend the method to ethane.

EXPERIMENTAL

Ethane was prepared by catalytic hydrogenation with cobalt-nickel catalyst of 99.5 percent ethylene, a standard product of the Ohio Chemical Company. The hydrogen was purified carefully to remove traces of oxygen and passed through in twofold excess. Any unsaturates remaining after the hydrogenation were removed by fuming sulfuric acid; potassium hydroxide was used to free the ethane from acid gases. The ethane was condensed in liquid nitrogen. It was then given a batch distillation with efficient stirring followed by several bulb-to-bulb distillations under high vacuum to remove permanent gases and passed through a glass wool filter at dry ice temperature to remove mercury. Purity tests described by Nickle,[2] indicated about 0.01 percent unsaturates, as ethylene, and 0.02 mole percent high boiling material, calculated as butane. The ethane registered an equilibrium pressure of 0.02 mm Hg when immersed in liquid air. (Compare Kistiakowsky and Nazmi:[3] 0.95×10^{-2} at liquid oxygen temperature.)

Two samples of ethyl bromide were used. The first sample was prepared from Baker's "purified" ethyl bromide by distilling through a 9-foot glass-helix packed column and recovering the fraction boiling at 38.6–38.8°C. This fraction was further purified by three bulb-to-bulb high vacuum distillations. It had to be stored behind a stopcock lubricated with Shawinigan low melting resin because of solubility in ordinary grease. The second sample was prepared from the same "Purified" grade by treatment with liquid bromine for one-half hour, subsequent removal of bromine by 20 percent sodium hydroxide and drying of the product over calcium bromide. The dried material was distilled as above; a fraction boiling at 38.4–38.5° being redistilled and a middle cut boiling at 38.3° (758 mm corr.) taken for final bulb-to-bulb vacuum distillation. It was stored behind a glass valve. It will be shown that

* Present address: Kellex Corporation, New York, New York.
** Department of Chemistry, Lafayette College, Easton, Pennsylvania. At present on leave of absence to Department of Physiological Chemistry, Johns Hopkins School of Medicine, Baltimore, Maryland.
[1] G. B. Kistiakowsky and E. R. Van Artsdalen, J. Chem. Phys. 12, 469 (1944), hereafter termed I.
[2] A. G. Nickle, Thesis (Harvard University, 1941).
[3] G. B. Kistiakowsky and F. Nazmi, J. Chem. Phys. 6, 18 (1938).

these samples of ethyl bromide apparently contained appreciable amounts of impurity, probably ethanol.

Bromine and hydrogen bromide were prepared and purified as described in I.

The experimental method was essentially the same as described in I. However, one important change was made. Small pressures were measured with the quartz spiral null-point manometer against a butyl-phthalate manometer instead of a mercury manometer. Special pains were taken to outgas the butyl-phthalate thoroughly before each set of measurements. Butyl-phthalate pressures were converted to mm of mercury employing measured absolute densities of the butyl-phthalate over the temperature range 20–31°C.

In the kinetic experiments, partial pressures of bromine were measured after various periods of illumination. The rate of reaction was determined over the first ten percent of reaction only, during which interval interference by products of reaction is at a minimum. It was found that the rate during the first ten percent was practically linear. Constants in this paper properly are termed initial constants in the same way as those cited in I.

RESULTS

Bromination of ethane conceivably could lead to a considerably greater diversity of products than in the case of bromination of methane. It was necessary to prove the assumption that during the first 10 percent of reaction essentially only ethyl bromide is formed by photo-bromination of ethane. For this purpose a 2-liter mixture of 43.5 mm of bromine and 495 mm of ethane was illuminated until reaction was practically complete and an analysis made of the reaction products. From average determinations of vapor pressure and refractive index it was concluded that the product of reaction consisted of a minimum of 65 percent of ethyl bromide. Under the experimental conditions employed this corresponds to a minimum of 97 percent of ethyl bromide during the first 10 percent of reaction. It was on this basis that constants were calculated from rates during the initial 10 percent of reaction.

The measured thermal, or "dark," rate of bromination at 96°C was 0.02 mm/min. Such "dark" reaction was negligible, since rates of photobromination were of the order of 5–10 mm/min. at 90°C.

TABLE I. Photobromination of ethane.

Temp. (°C)	Initial pressure (mm at t°C) Br_2	C_2H_6	Measured rate (mm/min.)	k	k' (sec.$^{-1}$×10^9)	k''
				(corrected to 89.8°)		
90.1	17.40	660.0	10.4	161	44	174
89.6	17.38	608.8	9.3	155	43	172
90.2	17.64	319.6	5.92	132	42	174
89.4	16.52	317.1	6.11	147	46	183
89.9	16.35	310.0	5.69	136	43	166
				(corrected to 59.7°)		
59.9	32.7	664.9	2.18	25	7.6	26
59.4	14.7	648.0	1.60	28	7.4	30
59.3	15.25	733.5	1.63	26	6.9	28
59.5	9.48	721.8	1.70	34	8.6	37
59.7	9.52	741.4	1.99	39	9.8	42
59.5	16.82	288.5	1.09	27	8.6	33
59.1	16.05	288.2	.96	25	7.8	31
59.1	15.92	287.8	1.06	28	8.7	35
60.1	15.9	290.4	1.10	27	8.4	36
60.2	10.82	278.5	.98	29	8.5	39
59.7	31.42	174.1	.81	20	8.7	26
58.6	29.55	188.2	.77	20	8.3	26
59.5	16.2	187.4	.76	24	8.5	36
59.9	9.80	192.8	.72	28	8.5	47
59.3	30.52	53.5	.226	12	7.4	31
				(corrected to 35.6°)		
35.1	14.1	272.3	.17	4.7	1.5	6.3
35.2	14.80	282.1	.221	5.9	1.88	7.4
36.7	14.68	281.5	.231	5.6	1.77	7.5
35.4	14.50	274.6	.213	5.8	1.82	7.8

If bromination of ethane, in its early stages, involves a mechanism analogous to that for bromination of methane, the rate of the photochemical reaction should be proportional to the square root of light intensity. An experiment performed to check this gave fair agreement with prediction (observed rate = 0.62 mm per min.; calculated rate = 0.70 mm per min.), but indicated that the rate probably depends upon a power of the light intensity between 0.5 and 1.

Data for a series of experiments at three mean temperatures are presented in Table I. All rate constants in this paper have been corrected to mean temperatures with the aid of temperature coefficients calculated from the experimentally evaluated activation energy. The coefficients were 1.073 at 35°, 1.062 at 60°, and 1.052 at 90°. This procedure will be justified later when it will be shown that the activation energy is only slightly subject to the "constant" used in calculating it. The corrections rarely exceeded 2 percent.

k was calculated from the following rate

equation in analogy with the methane-bromine reaction.

$$\frac{-d[Br_2]}{dt}=\frac{d[C_2H_5Br]}{dt}=\frac{k[C_2H_6][Br_2]^{\frac{1}{2}}}{[P]^{\frac{1}{2}}} \quad (A)$$

where P = total pressure. This equation is valid for initial rates only, where reaction products do not interfere.

Definite trends are observed in k, *viz.*, decreasing k with decreasing ethane pressure and increasing k with decreasing bromine pressure, indicating that the power of ethane concentration should be greater than one and that of bromine less than 0.5. Let us consider the following reaction mechanism in analogy with the bromination of methane.

$$Br_2+h\nu\rightarrow Br+Br \quad (1)$$

$$Br+C_2H_6\rightarrow C_2H_5+HBr \quad (2)$$

$$C_2H_5+Br_2\rightarrow C_2H_5Br+Br \quad (3)$$

$$C_2H_5+HBr\rightarrow C_2H_6+Br \quad (4)$$

$$Br+Br+M\rightarrow Br_2+M. \quad (5)$$

Equation (A) can be derived from this mechanism for the condition that $[HBr]=0$. $k=k_2(k_{ap}\alpha I/k_5)^{\frac{1}{2}}$ where α = absorption coefficient, I is the incident light intensity, and k_{ap} is a temperature independent apparatus constant. Two effects may be important in accounting for the observed trends in k, namely, different efficiencies of molecules in promoting reaction (5) and heterogeneous reaction.

If the efficiency of the third body M in reaction (5) is not the same for all molecules in the reacting system the rate of this reaction will not be given by $k_5[M][Br]^2$ but rather by a summation over individual effects of the various molecular species, such as $k_5[nA+nB+\cdots][Br]^2$. That different molecules have different efficiencies in this respect is well known,[4] and has been demonstrated in the case of the methane reaction.[1] However, it is quite general that more complicated molecules are better able to absorb translational energy of colliding bromine atoms than are simpler molecules, methane being shown to be more effective than hydrogen. The derivation of the rate equation is such that ethane would have to be considered less efficient than bromine to account for the observed effect. By assuming that each three-body collision between two bromine atoms and a bromine molecule is as effective as n such collisions in which ethane is the third body the following rate expression is derived when no HBr is present.

$$\frac{-d[Br_2]}{dt}=\frac{k'[Br_2]^{\frac{1}{2}}[C_2H_6]}{\left([Br_2]+\frac{[C_2H_6]}{n}\right)^{\frac{1}{2}}} \quad (B)$$

where $k'=k_2'(k_{ap}\alpha I/k_5)^{\frac{1}{2}}$. The constants k' in Table I have been calculated with $n=20$ which gave the best set of values. This would indicate that ethane is only about one twentieth as effective a third body as bromine, which is a rather surprising result. It should be noted, however, that fairly large changes in n, e.g., $n=25$ instead of 20, reflect only moderate changes in k'.

Heterogeneous recombination of bromine atoms on the walls of the reaction vessel would account for a decrease in rate constant with decreasing total pressure. Rabinowitch and Wood[4] have demonstrated this effect, but in general such heterogeneous recombination is not important at pressures above 200 mm, although subject to reaction vessel dimensions and intensity of illumination. It is possible to make an empirical correction for the wall reaction. We add to the above reaction scheme the following recombination reaction.

$$Br+Br\xrightarrow{\text{wall}}Br_2. \quad (6)$$

The rate of disappearance of Br atoms is increased by the quantity $2k_6[Br]/[M]$, where k_6 is a constant which depends upon vessel dimensions, diffusion coefficient, etc. The rate of reaction derivable from this scheme for zero HBr concentration is

$$\frac{-d[Br_2]}{dt}=\frac{k''[C_2H_6]\left\{\left(\frac{C^2}{[M]^2}+[M][Br_2]\right)^{\frac{1}{2}}-\frac{C}{[M]}\right\}}{[M]}, \quad (C)$$

[4] E. Rabinowitch and W. C. Wood, Trans. Faraday Soc. **32**, 907 (1936); E. Rabinowitch and S. C. Lehmann, *ibid.* **31**, 689 (1935).

where $k''=k_2''(k_{ap}\alpha I)^{\frac{1}{2}}/k_5^{\frac{1}{2}}$ and shows the temperature dependence of bromination, ascribed to k_2, and $C^2=k_6^2/4k_1k_5$. We are left with an adjustable constant C which was evaluated from two experiments in which total pressure varied by a factor of about 8. The value found was $C=11$ which was used to compute k'' in Table I. The effect of varying C was tested and found to be small for $C=9$ and 13. It is observed that this treatment gives good constancy for high and low total pressures, but there is a marked trend toward higher constants for decreasing bromine pressure.

Perhaps a combination of the two modes of correction (varying third-body efficiency and wall recombination) would improve the situation, but the use of two adjustable parameters would be involved and scarcely justified.

Constants calculated according to the three methods outlined above, and presented in Table I, have been used to compute activation energies. Considerations concerning computation of activation energy of photobromination of methane outlined in I are applicable in this case also. The following results were obtained:

from k $E=13.4\pm0.7$ kcal.

from k' $E=13.3\pm0.4$ kcal.

from k'' $E=14.0\pm0.4$ kcal.

The average experimental value, $E=13.6\pm0.5$ kcal., seems quite certain. It is noted that although absolute magnitudes of rate constants calculated by the several methods vary greatly, their temperature coefficients remain practically unchanged. The experimental energy of activation has been corrected to the true value by subtracting the term $\frac{1}{2}RT$ which yields a final value of 13.3 ± 0.5 kcal. Since in the proposed reaction scheme the temperature dependence may be ascribed to the endothermic reaction (2) between Br atoms and C_2H_6 molecules, we have assigned an activation energy of 13.3 kcal. to this reaction.

Various experiments were made to measure the extent of inhibition by HBr, which would occur through reaction (4) $C_2H_5+HBr\rightarrow C_2H_6+Br$. The rate equation in the presence of HBr is

$$\frac{-d[Br_2]}{dt}=\frac{k[Br_2]^{\frac{1}{2}}[C_2H_6][1/P]^{\frac{1}{2}}}{1+\frac{k_4}{k_3}\frac{[HBr]}{[Br_2]}}, \qquad (C)$$

where $k=k_2(k_{ap}\alpha I/k_5)^{\frac{1}{2}}$. In actual practice experiments with HBr were made in pairs bracketed alternately between those with no HBr present. Data at three temperatures are presented in Table II. It is evident that inhibition by hydrogen bromide is temperature independent, in contrast with the effect observed in bromination of methane.[1] Temperature independence of the ratio of these two specific reaction rate constants k_4/k_3 indicates that the activation energies of the two reactions are essentially equal. The magnitude of k_4/k_3 is considerably larger than in hydrogen bromide synthesis[5] or methane bromination,[1] from which one may surmise that the steric factors of the two reactions are more nearly equal in the case of ethane than in the case of hydrogen or methane.

A few experiments at 60–61°C were made of the photobromination of ethyl bromide. It was found that there was an extremely rapid initial reaction in which approximately 7 percent of the ethyl bromide appeared to react. This was followed by a nearly linear reaction taking place at a rate about equal to the rate of bromination of ethane under similar conditions. Upon readmitting fresh ethyl bromide to the reaction mixture a second rapid reaction corresponding to about 7 percent of the readmitted ethyl bromide occurred. The initial rapid reaction was shown also by the sample of ethyl bromide treated with bromine as described above. The literature[6] reveals that ethyl bromide and ethanol form an azeotrope boiling at 37.6° and containing 93 percent ethyl bromide. If our sample of ethyl bromide contained 7 percent ethanol, the initial,

TABLE II. Photobromination of ethane. Inhibition by HBr.

	Initial pressures (mm at t°C)			
t°C	C_2H_6	HBr	Br_2	k_4/k_3
90.0	326.3	102.3	16.2	0.68
89.9	325.7	103.0	16.97	.74
89.8	323.1	103.9	16.39	.68
89.9	312.9	104.0	16.2	.58
89.9	309.5	103.5	16.6	.58
60.6	195.7	98.5	15.40	.64
35.2	266.0	82.8	14.2	.7

[5] M. Bodenstein and H. Lütkemeyer, Zeits. f. physik. Chemie **114**, 208 (1924); M. Bodenstein and S. C. Lind, *ibid.* **57**, 168 (1906).

[6] *International Critical Tables*, Vol. III, p. 320.

rapid bromination would be explained quantitatively if it is assumed that ethanol is brominated much more rapidly than ethyl bromide. In view of the strength of the C−OH bond (some 30 kcal. less than that of the C−H bond), this is quite plausible. Probably a small amount of oxygen would be released and would be expected to inhibit bromination of ethyl bromide. Therefore no quantitative reliance can be placed on the experiments with ethyl bromide, although they indicate that the rate is not very different from that with ethane.

CARBON-HYDROGEN BOND STRENGTH

It is possible to utilize data presented in this paper to calculate with considerable accuracy the carbon-hydrogen bond strength in ethane. At the mean temperature of the experiments, 333°K, the heat of reaction of $C_2H_6+Br\rightarrow C_2H_5+HBr$ will be the activation energy of the reaction as written, diminished by the activation energy of the reverse, i.e., $13.3-E_4$ kcal. While no measurements of E_4 have been made, it can be estimated with close approximation. In the case of methane,[1] E_4 was shown to be about 1–2 kcal. In general it is known that such reactions occur on almost every collision and require very low energies of activation. We shall assume that in this case $E_4=0.8$ kcal., whence the heat of reaction is 12.5 kcal. at 333°K. This has been recomputed to 0°K by the method described in I, giving $\Delta H_0^0=11.9$ kcal. We now write:

	ΔH_0^0
$C_2H_6+Br=C_2H_5+HBr$	11.9 kcal.
$HBr=H+Br$	85.8 kcal.
$C_2H_6=C_2H_5+H$	97.7 kcal.

A probable error of about ±2 kcal. is assigned to this value. We find the following rounded values of this C−H bond strength

°K	$D_{(C_2H_5-H)}$
0	98 kcal.
298	99 kcal.

Steacie and Phillips[7] have estimated the C−H bond in ethane to be 95 kcal., while Stevenson[8] has obtained the value of 96 kcal. from electron impact potentials. Our value of 98 kcal. would approach these more closely if it should develop that the activation energy of reaction (4) were larger than 1 kcal.

Comparison with the C−H bond strength obtained for methane in I shows that the bond strength of ethane is about 3 kcal. lower, a result one might anticipate. It is interesting that the substitution of either a bromine atom or a methyl radical for an hydrogen atom in methane causes about the same decrease in carbon-hydrogen bond strength.

We wish to thank Professor G. B. Kistiakowsky and Dr. R. S. Halford for their interest and suggestions in this research.

[7] E. W. R. Steacie and N. W. F. Phillips, J. Chem. Phys. **6**, 179 (1938); Can. J. Research **B16**, 303 (1938).
[8] D. P. Stevenson, J. Chem. Phys. **10**, 291 (1942).

THE JOURNAL OF CHEMICAL PHYSICS VOLUME 12, NUMBER 12 DECEMBER, 1944

The Mercury Photosensitized Polymerization and Hydrogenation of Butadiene*

H. E. GUNNING AND E. W. R. STEACIE
National Research Laboratories, Ottawa, Canada

(Received November 3, 1944)

An investigation has been made of the mercury ($^3P_1$) photosensitized polymerization and hydrogenation of butadiene. The main products of the reaction of butadiene with mercury ($^3P_1$) atoms are hydrogen, an acetylenic compound in the C_4 fraction, dimer, and polymer. In the presence of excess hydrogen, the products are mainly butane, butene, and octanes. The variation of the rate of the polymerization reaction with time, and with the pressure of butadiene, suggests the following mechanism: $C_4H_6+Hg(^3P_1)\rightarrow C_4H_6^*+Hg(^1S_0)$, followed by $C_4H_6^*+C_4H_6\rightarrow 2C_4H_6$, or $C_4H_6^*+C_4H_6\rightarrow(C_4H_6)_2$ or $C_4H_6^*\rightarrow C_4H_4+H_2$. Polymerization arises largely by a free radical mechanism $H_2+Hg(^3P_1)\rightarrow 2H+Hg(^1S_0)$, $H+C_4H_6\rightarrow C_4H_7$, $C_4H_7+C_4H_6\rightarrow C_8H_{13}$, etc. The mechanism is shown to be consistent with the value found for the quantum yield.

INTRODUCTION

ALTHOUGH the mercury [$^3P_1$] photosensitized reactions of many of the lower paraffins and olefins have been studied,[1] no papers have as yet appeared on either the mercury photosensitized polymerization or hydrogenation of butadiene. This conjugated alkadiene is of very considerable interest, and the work described herein was undertaken in the hope that some light might be thrown on the mechanisms involved in its reactions.

PART I. THE MERCURY PHOTOSENSITIZED POLYMERIZATION OF BUTADIENE

Static Runs

Both static and single-pass runs were made, the former at 30°C, and the latter at room temperature.

In the earlier part of the work with a static system a quartz annular cell was employed having a volume of 342 cc. The mercury "resonance" lamp used in conjunction with this cell was fashioned in the form of a trap. The trap was constructed entirely of Pyrex glass with the exception of the lower half of the outer tube, which was of quartz and joined to the Pyrex portion by means of a graded seal. The electrodes were sealed to the inlet and outlet tubes by means of uranium glass seals. The lamp was filled with neon at 3-mm pressure, and was operated at about 120 milliamp. from a 6000-volt sign transformer. The lamp and cell were immersed in a thermostat containing distilled water, and maintained at 30.0±0.1°C, the quartz portion of the lamp being placed in the center of the annular cell. The temperature was controlled in the thermostat by means of a thermoregulator of the DeKhotinsky type connected to a knife-blade heater. It was found necessary to run the lamp continuously for at least 48 hours before its light intensity became constant. During this time the intensity fell to about 50 percent of its original value.

In order to facilitate the determination of the quantum yield, and of the effect of light intensity on the rate, the cell system was modified to some extent. A cylindrical fused quartz cell, 10 cm in length, with windows 5 cm in diameter, was substituted for the annular cell. Its volume was 240 cc. The cell was immersed in a metal water bath provided with a fused quartz window. The distilled water in the bath was kept at 30.00 ±0.01°C, by means of a thermoregulating system consisting of a mercury thermoregulator, a knife-blade heater, and a thermionic relay employing a 117L7GT rectifier-beam, power amplifier tube in its circuit as recommended by Serfass.[2] The mercury resonance lamp was made by fusing two Pyrex-to-quartz, 13-mm O.D., graded seals together at the quartz ends, and bending the tube in the form of a U. The electrodes were fused to the Pyrex ends by uranium glass seals. The lamp was filled with neon at a pressure of 3 mm and clamped securely outside

* Contribution No. 1248 from The National Research Laboratories, Ottawa, Canada.

[1] For references, see: D. J. Le Roy and E. W. R. Steacie, J. Chem. Phys. **10**, 676, 683 (1942).

[2] E. J. Serfass, Ind. Eng. Chem. Anal. Ed. **13**, 262 (1941).

the thermostat about 2 cm from the fused quartz window.

The butadiene used in the experiments was obtained from the Ohio Chemical and Manufacturing Company and was shown by analysis to be 98.5 percent butadiene. It was further purified by several trap-to-trap distillations, and finally stored in a one-liter flask, connected to the manifold of the system. The storage flask was provided with a modified Stock valve, as designed by Warrick and Fugassi.[3] This valve proved to be a very convenient method of introducing definite quantities of gas into the cell system.

The nitric oxide used in the work was prepared by the action of mercury on a 2 percent solution of sodium nitrite in concentrated sulphuric acid.[4] The other oxides of nitrogen present were removed by passing the gas through two long glass spirals, the first immersed in a dry-ice acetone mixture at −78.5°C, and the second in petroleum ether at −148°C. The nitric oxide was then frozen out in a trap with liquid air, and subjected to several trap-to-trap distillations, the middle fraction being collected and stored in a similar storage flask to the one used for butadiene.

Pressure changes were followed on McLeod gauges covering the range from 2×10^{-5} to 110 mm of mercury.

Analytical Methods

The analytical methods employed underwent several modifications during the course of the work. Non-condensable gas was drawn off through a "pumped down" liquid air trap, by means of a two-stage diffusion pump, backed by a Toepler pump. The hydrogen in the non-condensable gas was measured either by circulation over copper oxide deposited on glass wool, and maintained at 300°C, or by transferring the sample to a Blacet-Leighton gas analysis apparatus, if its volume was small.

Isolation of the fractions of various carbon numbers in the products was accomplished by a method of fractional condensation and vaporization, using the Ward apparatus,[5] as modified by Savelli, Seyfried, and Filbert.[6] Four traps were connected in series, and separated from each other by stopcocks. This trap system was connected at one end to the system through a modified Stock valve,[3] and to the other end were connected a two-stage diffusion pump, an all-mercury Toepler pump, a gas measuring burette, and a copper oxide tube for determining hydrogen. Each trap was provided with internal and external copper-constantan thermocouples. The traps were maintained at the desired temperature either by surrounding them with the appropriate substance at its freezing point, or by the modified Ward method.[6] In this method a copper cylinder wrapped with resistance wire was slipped over the trap, and the ends of the resistance wire attached to binding posts on a control panel. These binding posts were connected to General Radio 200-CM Variac transformers, giving a variable voltage from 0–135 volts. The copper cylinder was then filled with a light gasoline. A glass cylinder, filled with gasoline, and a Dewar flask were then slipped concentrically over the copper cylinder. The Dewar flask was kept filled to the top with liquid air during the analysis. By a careful adjustment of the Variac it was found possible to keep the temperature constant to 0.5°C over the range from −10°C to −175°C.

The acetylene compound found in the C_4 fraction was estimated by the method of Ross and Trumbull,[7] as modified by Le Roy and Steacie[8] for their determination of acetylene. Butadiene did not react with the neutral 2.5 percent silver nitrate solution, used to absorb the acetylene compound.

The temperatures used in the traps and the cutting pressures are given in reference 6. The cutting pressures were determined with a McLeod gauge. An atmospheric Toepler pump was attached to the system for transferring fractions for analysis in the Blacet-Leighton apparatus.

Single-Pass Runs

About a dozen single-pass runs were made in order to study the initial products of the reac-

[3] E. Warrick and P. Fugassi, Ind. Eng. Chem. Anal. Ed. **15**, 13 (1943).
[4] A. Klemenc, *Die Behandlung und Reindarstellung von Gasen* (Akad. Verlagsges., m. b. H., Leipzig, 1938), p. 166.
[5] E. C. Ward, Ind. Eng. Chem. Anal. Ed. **10**, 169 (1938).
[6] J. J. Savelli, W. D. Seyfried and B. M. Filbert, Ind. Eng. Chem. Anal. Ed. **13**, 868 (1941).
[7] W. H. Ross and H. L. Turnbull, J. Am. Chem. Soc. **41**, 1180 (1919).
[8] D. J. Le Roy and E. W. R. Steacie, J. Chem. Phys. **9**, 829 (1941).

tion without the complications arising from secondary reactions. The system consisted of a large trap connected to a quartz annular cell through a fine capillary. The cell contained a drop of mercury, and was attached to the system with ground glass joints in order to facilitate removal for cleaning. The lamp used was a Hanovia Sc 2537, of the double-U type. It was inserted through the annulus. The cell was connected in turn to the analytical unit described above.

In these runs the butadiene was first frozen out with liquid air in the large trap, after which, the system was pumped down to a pressure of 10^{-5} mm of mercury, in order to remove any traces of air or other permanent gases that might have been present. The temperature of the trap was then raised to -78.5°C, by immersing it in dry-ice acetone. Butadiene has a vapor pressure of 11.2 mm of mercury at this temperature. The system was then left for six hours in order that the vapor pressure of the mercury might attain its equilibrium value. To start the run the lamp was turned on and the valve connecting the cell

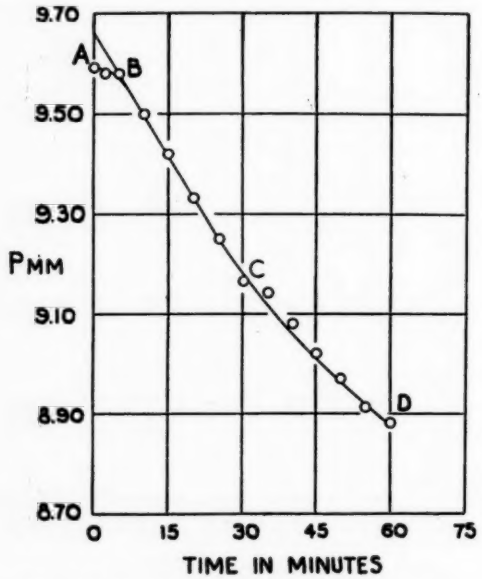

FIG. 1. Pressure *vs.* time for a typical static run.

to the analytical unit was opened. The butadiene flowed in turn through the cell, then through a trap at -85°C, and finally was condensed in a liquid air trap. The dimer formed in the reaction was frozen out in the trap at -85°C. The acetylene compound condensed with the butadiene in the liquid air trap. The mercury vapor pump on the analytical unit served to pump off the hydrogen formed, which was collected in a gas burette and analyzed by combustion over copper oxide at 300°C.

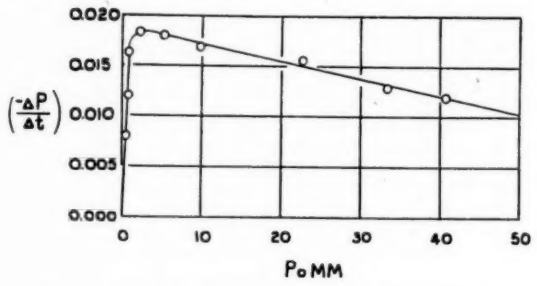

FIG. 2. The initial rate *vs.* the initial pressure for the static runs.

RESULTS

Static Runs

The Effect of Pressure on the Rate

Figure 1 shows a typical one-hour run at an initial pressure of 10 mm of butadiene. As can be seen from the diagram, the curve consists of three portions. There is a period of induction *AB*, during which time the pressure decrease is very small. This is followed by a linear portion *BC*, and the slope of this line is considered as the rate of the over-all reaction. Finally *CD* represents a falling off of the rate, caused, as has been shown, by the accumulation of polymer on the window of the cell. The length of the period of induction *AB* is directly proportional to the initial pressure of butadiene in the system, being about 10 minutes at 10 mm and increasing to about 28 minutes at 30 mm.

Taking, then, the rate of the over-all reaction as the slope of the portion *BC* of the curve, this value is plotted in Fig. 2 against the initial pressure of the butadiene. The fact that the rate of the reaction as defined in this manner reaches a maximum at about 2 mm is undoubtedly caused by the incomplete quenching of the $Hg(^3P_1)$ atoms by the butadiene at lower pressures.

That the falling off of the rate in the *CD* portion of the curve in Fig. 1 is caused entirely by the accumulation of a polymer on the window of the cell can be shown by pumping off the

butadiene after a run, and then making another run at the same pressure, without cleaning the cell. The rate is reduced to a value equal to the slope of the *CD* portion of the curve.

The polymer, which was clearly discernible on the window of the cell through which the light entered, was removed between runs with a hot saturated solution of chromic oxide in concentrated sulphuric acid. In certain cases it was found necessary to flame out the cell in order to ensure the complete removal of polymer. This was imperative in the case of the runs made with nitric oxide-butadiene mixtures, suggesting that the character of the polymer was different in this case.

Kublitskii[9] found that the polymer formed upon illuminating butadiene sealed in quartz ampules with light from the mercury arc, absorbed λ2537, in agreement with our observations. Another interesting characteristic of the polymer is that it seems to exhibit the phenomenon of "dark growth." If the butadiene and products are pumped off at the end of a run, and the cell again filled with butadiene, without removing the cell from the system for cleaning, it was found that the rate for the second run decreased the longer the cell was left before making the second run.

The Effect of Nitric Oxide on the Rate

Rate-inhibition by nitric oxide is usually taken to be an indication that free radical chains play an important part in a reaction. For this reason the effect of nitric oxide on the rate of the butadiene reaction was studied. Figure 3 shows a typical run with a mixture of 8 vol. percent of nitric oxide in butadiene. There is no period of induction in the reaction, and the falling off of the rate is caused by an accumulation of polymer on the wall. The rate of the reaction in Fig. 3, as measured by the rate of pressure decrease, is about 2½ times as great as the rate with pure butadiene at the same pressure.

The rate was measured over a concentration range of 0.2 percent to 20 percent of added nitric oxide, and it was found that the rate of this reaction, with a constant partial pressure of butadiene, was directly proportional to the amount of nitric oxide present. Analysis of the products of the reaction showed that the nitric oxide had been used up in the course of the reaction. All the above facts seem to suggest that we are dealing here with the mercury photosensitized reaction of nitric oxide with butadiene, and for our purpose, therefore, these results are irrelevant.

[9] K. M. Kublitskii, Sintet. Kauchuk (U.S.S.R.), No. 7/8, 30–32 (1936).

THE PRODUCTS OF THE REACTION

(a) Static Runs

Small amounts of hydrogen and ethane were formed in the reaction, together with a large amount of a dimer and of course the polymer which forms on the window of the cell, through which the light entered.

Analysis of the gas non-condensable in liquid air from several one-hour runs, made at an initial pressure of 25 mm of butadiene, showed 0.06 mole of hydrogen formed for every mole of butadiene decomposed. Two-hour runs at the same initial pressure yielded only 0.01 mole of hydrogen for each mole of butadiene decomposed, showing that the hydrogen formed initially was being used up in the course of the reaction.

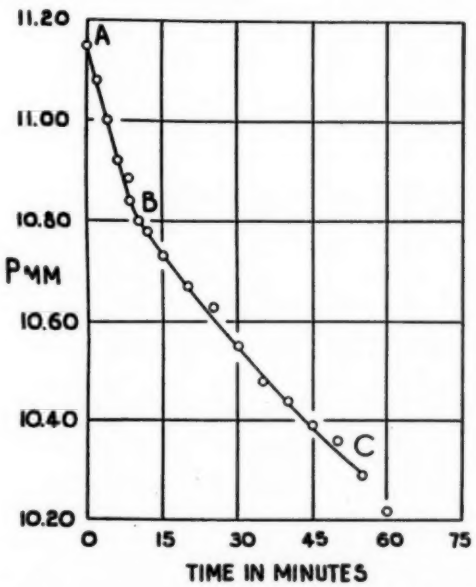

FIG. 3. Pressure *vs.* time for a static run with 8 vol. percent of nitric oxide and 92 vol. percent of butadiene.

By freezing out the condensable products in liquid air in a small bulb attached to a capillary manometer, and then pumping off the butadiene

from dry-ice acetone at −78.5°C, a colorless dimer was isolated. By surrounding the bulb with various freezing mixtures a series of vapor pressure measurements were made after the manner described by Benson.[10] Measurements were made from −78.5°C to 50.0°C. An extrapolation of the plot, log (vapor pressure) *vs.* $1/T$ to 760 mm gave a value of 95°C for the normal boiling point of the dimer. Gravimetric microanalysis gave C = 88.2 percent, H = 11.7 percent. Calculated for C_8H_{12}, C = 88.8 percent, H = 11.2 percent.

The dimer showed a great tendency to polymerize both in vacuum and in air. In both cases a yellow transluscent solid is formed, which slowly loses the "double bond" odor of the original dimer. Oxygen does not seem to affect the rate of the polymerization.

About 0.6 mole of dimer were formed for every mole of butadiene decomposed. This was the average of 5 two-hour runs at a pressure of 25 mm.

A small amount of an acetylenic compound was found in the C_4 fraction by using the method of Ross and Trumbull,[4] as adapted by Le Roy and Steacie.[8] This may be vinyl acetylene.

The amount of the polymer formed decreases markedly with increasing pressure. At an initial pressure of 100 mm there is no falling off of the rate even after two hours illumination. Furthermore, there is no visible evidence of polymer on the window of the cell.

(b) Single-Pass Runs

The products from these runs were hydrogen, an acetylenic compound in the C_4 fraction, a dimer, and a trace of polymer. The mean of four 12-hour runs gave:

Products	*Millimoles*
Hydrogen	2.0
Acetylenic c.p.d.	0.5 (as C_4H_4)
Dimer	0.37 (as C_8H_{12})
Polymer	trace.

The Effect of Light Intensity

The effect of light intensity on the rate was determined by inserting a calibrated copper screen between the lamp and the cell, which reduced the light intensity to 0.32 of its full value. The rate at this intensity was 0.39 of the value obtained by using the full output of the lamp. From this it can be seen that the rate is approximately directly proportional to the light intensity.

The Quantum Yield

A rough determination of the quantum yield was made by comparison with the initial pressure rise in the Hg-photosensitized reaction of ethylene.[8] Le Roy and Steacie found that the quantum yield of the ethylene reaction was 0.37 at 13-mm pressure of ethylene.[8] The quantum yield of the butadiene reaction calculated on this basis was 0.8±0.5 at 25-mm pressure. According to Gee, as quoted by Bolland and Melville,[11] the quantum yield of the mercury photosensitized reaction of butadiene is in the neighborhood of unity. This is in agreement with our results within the limit of error.

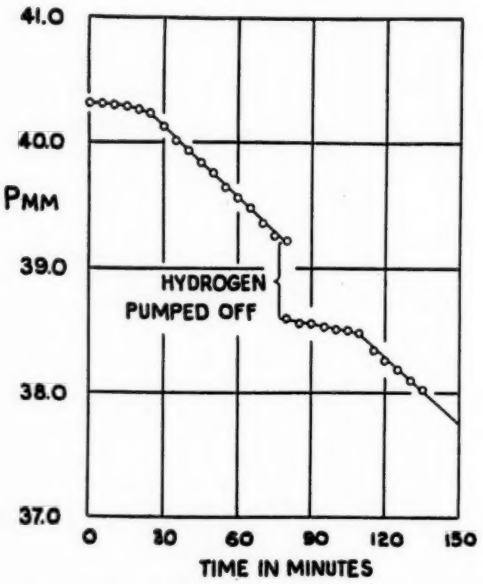

FIG. 4. The effect of pumping off the hydrogen in a static run.

The Effect of Hydrogen on the Rate

Two sets of runs were made in order to find out whether any relation existed between the

[10] S. W. Benson, Ind. Eng. Chem. Anal. Ed. **14**, 189 (1942).

[11] J. L. Bolland and H. W. Melville, Proc. Rubber Tech. Conf., No. 90, p. 248 (1938).

period of induction and the hydrogen found in the products. Figure 4 shows a typical run in which the hydrogen has been pumped off after the reaction had reached the linear part of the curve. It is obvious from Fig. 4 that a new period of induction is begun when the reaction is resumed after pumping off the hydrogen.

Another series of runs was made in which a small amount of hydrogen was added to the butadiene before starting the run. The period of induction was completely eliminated in these runs. The same effect is produced by stopping the reaction in its period of induction and adding a small amount of hydrogen.

The slope of the linear portion of the curve increased with the percentage of added hydrogen. This is in accordance with the results from the hydrogenation of butadiene with $Hg[^3P_1]$ atoms; the rate of this reaction for a 10:1 ratio of hydrogen to butadiene is about ten times as fast as the reaction with pure butadiene.

Discussion

(*a*) *Static Runs*

Any mechanism proposed to explain the reactions of butadiene photosensitized by $Hg(^3P_1)$ atoms must be consistent with the following facts.

(a) There is a period of induction in the reaction the length of which is directly proportional to the initial pressure of the butadiene.

(b) Small amounts of hydrogen and an acetylenic C_4 compound are found in the products of the reaction. The hydrogen disappears slowly upon prolonged illumination.

(c) If the reaction is stopped, after the linear portion of the pressure-time curve has been reached, and the hydrogen pumped off from liquid air, the period of induction reappears when the reaction is resumed.

(d) Adding a small amount of hydrogen to the butadiene eliminates the period of induction, and the resultant rate increases with increasing amounts of added hydrogen.

(e) The rate as defined above decreases slowly with increasing pressure.

(f) Appreciable amounts of a liquid dimer are formed.

(g) A highly unsaturated polymer is formed which absorbs λ2537. The amount of the polymer formed decreases with increasing pressure.

(h) The quantum yield of the reaction is approximately unity.

By analogy with the results found by Le Roy and Steacie[10] for the mercury photosensitized reactions of ethylene, the formation of an activated molecule seems the most probable primary step:

$$C_4H_6+Hg(^3P_1)\rightarrow C_4H_6^*+Hg(^1S_0). \qquad (a)$$

Indeed, the formation of an activated butadiene molecule of relatively long life by the collision of a butadiene molecule with a mercury ($^3P_1$) atom would seem even more likely than with ethylene since butadience has a larger number of degrees of freedom over which the energy imparted upon collision might distribute itself.

Since the C−H bond strength in the olefins probably is not much different from that in the paraffins, the reactions

$$C_4H_6+Hg(^3P_1)\rightarrow C_4H_5+H+Hg(^1S_0) \qquad (b)$$

and

$$C_4H_6^*\rightarrow C_4H_5+H \qquad (c)$$

may occur to some extent, although these reactions do not seem to be of importance as initial steps at room temperature.

The period of induction in the reaction is presumably the result of competition between a pressure-increasing and a pressure-decreasing reaction. By analogy with the ethylene reaction, and in the light of our own findings, these would be:

$$C_4H_6^*\rightarrow C_4H_4+H_2 \qquad (d)$$

and

$$C_4H_6^*+C_4H_6\rightarrow(C_4H_6)_2. \qquad (e)$$

Reaction (d) would explain the small amounts of hydrogen found in the products, and the presence of an acetylenic compound in the C_4 fraction. The acetylenic compound would most probably be vinyl acetylene. The dimer formed by reaction (e) would explain how the liquid dimer is formed which was found in the products. According to Wasserman,[12] the Diels-Alder bimolecular dimerization of butadiene results in the formation of 4-vinylcyclohexene. Vaughan[13] isolated what appeared to be a bicyclooctadiene.

[12] A. Wasserman, J. Chem. Soc., p. 612 (1942).
[13] W. E. Vaughan, J. Am. Chem. Soc. **54**, 3863 (1932).

It is probable that the dimer formed in the photosensitized reaction is of a similar nature to these compounds.

Reactions (d) and (e) are probably the only reactions of importance occurring during the period of induction which would have any effect upon the over-all pressure. Increasing pressures would favor reaction (e), and consequently the pressure decrease in the induction period is more apparent at higher pressures. The quantum yield of 0.8, together with the decrease in rate with increasing pressure, strongly suggests that a deactivating reaction also occurs:

$$C_4H_6^* + C_4H_6 \rightarrow 2C_4H_6, \qquad (f)$$

as in the case of the ethylene reaction (8).

During the period of induction, then, reaction (d) will result in the accumulation of hydrogen in the system. Eventually the hydrogen will reach a high enough concentration to quench the $Hg(^3P_1)$ atoms to an appreciable extent:

$$H_2 + Hg(^3P_1) \rightarrow 2H + Hg(^1S_0). \qquad (g)$$

The hydrogen atoms formed by (g) will then be used up by hydrogenating the butadiene:

$$C_4H_6 + H \rightarrow C_4H_7. \qquad (h)$$

By analogy with the ethylene reaction (h) should have an activation energy of 5 kcal. or less. Polymerization would then occur by

$$C_4H_6 + C_4H_7 \rightarrow C_8H_{13}, \text{ etc.} \qquad (i)$$

The end of the induction period will occur when the hydrogen has built up to a high enough concentration to quench the $Hg(^3P_1)$ atoms to an appreciable extent, by reaction (g). The fact that a very small amount of hydrogen will bring about a large pressure decrease, and result in the formation of considerably more polymer is additional and convincing evidence that at least part of the polymerization occurs by means of a free radical reaction.

The above mechanism is also in accordance with the fact that the length of the induction period increases with increasing pressure. At higher pressure it would take a proportionately longer time for the hydrogen formed by (d) to attain a sufficiently high concentration to be able to quench an appreciable number of the $Hg(^3P_1)$ atoms, and thereby initiate polymerization, by (g), (h), and (i).

The runs done on the effect of hydrogen upon the rate also afford a striking confirmation of the above mechanism. The fact that the period of induction can be reproduced by pumping off the hydrogen present, when the reaction has reached a stage where the pressure is varying linearly with the time, shows that the main part of the polymerization must be initiated by H atoms, as in the case with the mercury photosensitized ethylene reaction (8).

Moreover, in the light of the above mechanism, one would expect that at higher pressures the polymerization would be depressed in favor of the dimerization. This would result in a smaller yield of polymer at higher pressures, a larger yield of dimer, and a decrease in rate. All this is in complete agreement with our findings. The quantum yield will always be small since deactivation by (f) will always remove a large proportion of activated molecules.

The small amount of ethane identified in the products may have been formed by some sequence such as

$$C_4H_7 + H \rightarrow 2C_2H_4, \qquad (j)$$

$$C_2H_4 + H \rightarrow C_2H_5, \qquad (k)$$

$$C_2H_5 + C_4H_7 \rightarrow C_2H_6 + C_4H_6. \qquad (l)$$

(*b*) *Single-Pass Runs*

In the single-pass runs the rate of flow of butadiene through the cell was so adjusted that the reaction remained essentially in its period of induction throughout the course of the run. Under these conditions the main reactions would be (a), (d), (e), and (f). The hydrogen formed by (d) would never reach a high enough concentration in the cell to quench the $Hg(^3P_1)$ atoms to any appreciable extent. Therefore one would expect that the ratio

moles of dimer formed/moles of hydrogen formed

would be small in the single-pass runs, and large in the static runs, where the hydrogen is being continuously used up by (g). Our analyses are in accord with this conclusion;

	Moles dimer formed/ Moles hydrogen formed
Static runs (1 hour)	10
Single-pass runs	0.2.

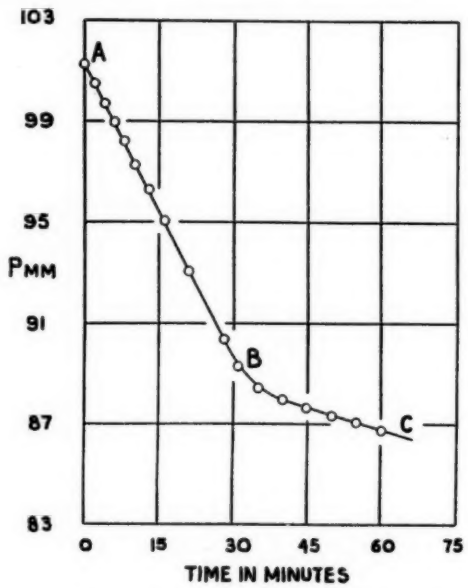

FIG. 5. Pressure *vs.* time for a static run with 15 vol. percent of butadiene and 85 vol. percent of hydrogen

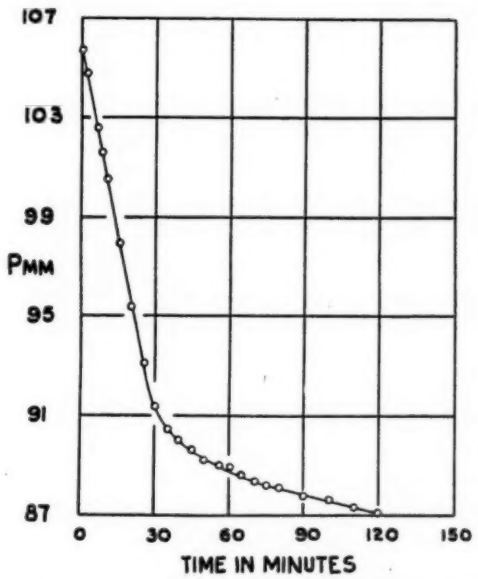

FIG. 6. Pressure *vs.* time for a static run with 9 vol. percent of butadiene and 91 vol. percent of hydrogen.

The trace of polymer formed in the single-pass runs suggests that, under these conditions, polymerization may have been initiated to some extent by C_4H_5 radicals resulting from reactions (b) and (c).

PART II. THE MERCURY-PHOTOSENSITIZED HYDROGENATION OF BUTADIENE

The work previously described on the polymerization of butadiene, sensitized by $Hg(^3P_1)$ atoms, strongly suggested that the polymerization of butadiene was initiated by hydrogen atoms in the following manner:

$$C_4H_6+Hg(^3P_1)\rightarrow C_4H_6^*+Hg(^1S_0) \quad (1)$$

$$C_4H_6^*\rightarrow C_4H_4+H_2 \quad (2)$$

$$H_2+Hg(^3P_1)\rightarrow 2H+Hg(^1S_0) \quad (3)$$

$$C_4H_6+H\rightarrow C_4H_7 \quad (4)$$

$$C_4H_7+C_4H_6\rightarrow C_8H_{13}\rightarrow \text{polymer}. \quad (5)$$

The work described herein on the mercury $(^3P_1)$ photosensitized hydrogenation of butadiene was undertaken in order to gain additional information on the polymerization reaction.

Experimental

The experiments were carried out, at 30°C, in a static system similar to the one employed above.

The hydrogen used in the runs was prepared by passing hydrogen from a cylinder through two liquid-air traps, and then through a combustion tube containing platinized asbestos at 500°C. It was stored in a two-liter flask provided with a modified Stock valve.[3]

The mixtures of butadiene and hydrogen were made up by first introducing the butadiene into the cell system and measuring its pressure on a large McLeod gauge. The hydrogen was then admitted after the butadiene had been frozen out in liquid air. The partial pressure of hydrogen in the mixture was taken as the difference between the total pressure and the pressure of the butadiene.

THE EFFECT OF TOTAL PRESSURE AND HYDROGEN CONCENTRATION ON THE OVER-ALL RATE

Figures 5 and 6 show two runs, the first made with a fivefold, and the second with a tenfold, excess of hydrogen. There is no period of induction, and the initial rate is about ten times as great as the rate obtained when no hydrogen has been added. The falling off of the rate in the *BC* portion of the curve in Fig. 5 was shown to be caused by the accumulation of a polymer on the window of the cell through which the light entered. This was done by adding more butadiene

at the end of the run and then re-illuminating the mixture. The resulting rate corresponded to a continuation of the *BC* portion of the curve.

The falling off of the rate in Fig. 6 was caused not by an accumulation of polymer on the window, but by a complete conversion of the butadiene present to saturated products. Upon adding butadiene at the end of this run, a rate was obtained which was only slightly less than the initial rate. An analysis of the products of this run is given below. Only a few patches of polymer were found on the window of the cell.

The effect of hydrogen concentration on the rate is shown in Fig. 7. The initial rate is here plotted against mm of added hydrogen, the partial pressure of the butadiene being maintained constant at 10 mm. The relation is roughly linear for mixtures containing less than 80 vol. percent of hydrogen. At higher concentrations the rate falls off as would be expected.

Increasing the total pressure at constant composition did not perceptibly affect the rate up to a total pressure of 300 mm. However, the amount of polymer formed was markedly affected —so much so that at 300 mm the accumulation of polymer was sufficient to render the window opaque to λ2537, and stop the reaction, when only 5 percent of the butadiene had reacted.

The Products of the Reaction

The products of the reaction were separated into fractions of the same carbon number by the analytical technique previously described. The C_4 fraction was analyzed by passing the gas over maleic anhydride at 100°C, to constant volume, and then determining the butene in the residue by bromination, using the method of Uhlig and Levin, in the microadaptation of Benson.[10]

The products of the runs made with mixtures containing more than 90 mole-percent of hydrogen consisted mainly of butane with smaller amounts of methane, ethane, and octanes, together with a small amount of polymer. Analysis of the run shown in Fig. 5 gave 10 percent methane, 1 percent ethane, a trace of propane, 70 percent butane, 5 percent butene, 10 percent octanes, and a small amount of polymer.

Qualitative analyses were carried out on the products of the runs from mixtures containing less than 90 percent hydrogen, and these showed that the products were preponderately butene and butane, and polymer.

Discussion

The quenching cross section for hydrogen is 8.6×10^{-16} cm², while that for butadiene should not be very far from 40×10^{-16} cm²,[14] by analogy with other unsaturated substances, although it has never been experimentally determined. Using these values in the standard kinetic theory expression for the collision number, we obtain

$$Z(H_2, Hg^*)/Z(C_4H_6, Hg^*)=[H_2]/[C_4H_6],$$

where $[H_2]$ and $[C_4H_6]$ are the molar concentrations of hydrogen and butadiene, respectively.

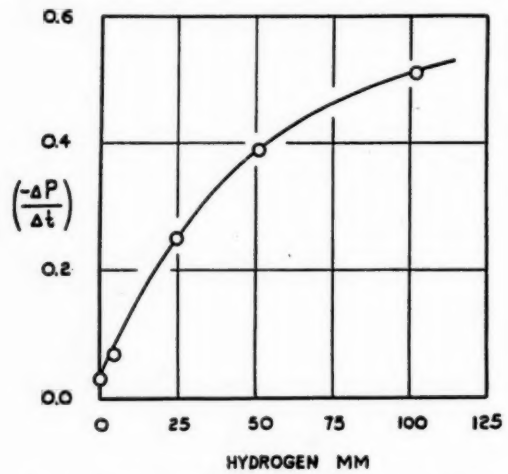

FIG. 7. The intial rate *vs.* mm of hydrogen added to 10 mm of butadiene.

In other words, the extent of quenching of $Hg(^3P_1)$ atoms done by butadiene and hydrogen in a mixture will be approximately proportional to the ratio of the molar concentration of the two substances in the mixture. It follows, then, that in a mixture of butadiene and hydrogen containing 90 mole-percent of hydrogen, the hydrogen will do about 90 percent of the quenching.

Bearing the above facts in mind, two primary steps seem likely; namely,

$$H_2+Hg(^3P_1)\rightarrow 2H+Hg(^1S_0), \quad (1)$$

$$C_4H_6+Hg(^3P_1)\rightarrow C_4H_6^*. \quad (2)$$

[14] A. C. G. Mitchell and M. W. Zemansky, *Resonance Radiation and Excited Atoms* (Cambridge University Press, 1934), p. 224.

The large amounts of polymer formed in the hydrogenation runs lend weight to our previous conclusion that the polymerization occurs through the addition of an H atom—

$$C_4H_6+H\rightarrow C_4H_7, \quad (3)$$

$$C_4H_6+C_4H_7\rightarrow C_8H_{13}\rightarrow \text{polymer}. \quad (4)$$

Another step which is energetically possible and may be important is,

$$C_4H_6^*+H_2\rightarrow C_4H_7+H. \quad (5)$$

Certainly the fact that the main product formed is butane in a mixture containing 90 mole-percent of hydrogen would seem to indicate that there is a relatively high concentration of both C_4H_7 radicals and H atoms. The butane formed, under these conditions, would likely arise from some such sequence as

$$C_4H_7+H\rightarrow C_4H_8, \quad (6)$$

$$C_4H_8+H\rightarrow C_4H_9, \quad (7)$$

followed by

$$C_4H_9+C_4H_7\rightarrow C_4H_6+C_4H_{10}, \quad (8)$$

and/or

$$C_4H_9+H_2\rightarrow C_4H_{10}+H. \quad (9)$$

Disproportionation is not considered important with normal radicals; however, the type of cross disproportionation represented in (8) may be quite important, owing perhaps to the C−H bond in the C_4H_7 being slightly weaker than it is in C_4H_9.

Reactions of radicals with hydrogen molecules seem to possess rather high activation energies, probably of the order of 8 to 15 kcal., and therefore one would expect (9) to be relatively slow. However, a butyl radical formed by the successive addition of three H atoms to butadiene might conceivably have been able to retain some of this energy of hydrogenation, and, for this reason, we might be dealing in (9) with an activated radical. Of course, if butene is formed as an intermediate, and this seems to be the case, it would quench almost as strongly as butadiene, and consequently direct photosensitized hydrogenation might occur. The octanes formed undoubtedly arise from radical recombination of butyl radicals. It is of interest to note here that Moore and Taylor[15] found that octanes were the main products in the mercury photosensitized hydrogenation of *n*-butene, while we obtained only a 10 percent conversion of butadiene to octanes, our yield of butane being correspondingly greater. This discrepancy could be explained if we assume that a large percentage of the butyl radicals formed from butadiene by hydrogenation remained in an activated state long enough to collide with a hydrogen molecule, forming butane as in (9).

Presumably the methane and ethane formed could be accounted for by a series of "atomic cracking" reactions starting with the butyl radical. However, a detailed study of these secondary reactions is beyond the scope of the present investigation.

Conclusions

The present investigation on the mercury photosensitized reactions of butadiene seems to suggest the following conclusions:

(a) Collisions of butadiene molecules with $Hg(^3P_1)$ atoms result in the formation of activated molecules of relatively long life.

(b) These activated molecules are mainly used up by the following reactions:

$$C_4H_6^*\rightarrow C_4H_4+H_2, \quad (i)$$

$$C_4H_6^*+C_4H_6\rightarrow 2C_4H_6, \quad (ii)$$

$$C_4H_6^*+C_4H_6\rightarrow (C_4H_6)_2. \quad (iii)$$

(c) Hydrogen atoms are formed when the hydrogen formed by (i) reached a high enough concentration in the system to quench the $Hg(^3P_1)$ atoms appreciably.

(d) Polymerization then occurs by the reactions:

$$C_4H_6+H\rightarrow C_4H_7, \quad (iv)$$

$$C_4H_6+C_4H_7\rightarrow C_8H_{13}, \text{ etc.} \quad (v)$$

[15] W. J. Moore and H. S. Taylor, J. Chem. Phys. **8**, 504 (1940).

THE JOURNAL OF CHEMICAL PHYSICS VOLUME 12, NUMBER 12 DECEMBER, 1944

The Tetrahedral X_2YZ_2 Molecular Model

Part I. Classical Vibration Problem

W. H. SHAFFER
Mendenhall Laboratory of Physics, The Ohio State University, Columbus, Ohio

AND

R. C. HERMAN
Applied Physics Laboratory, Johns Hopkins University, Silver Spring, Maryland

(Received October 30, 1944)

Appropriate coordinates are set up from the standpoint of group theory for describing the normal modes of oscillation in such a manner that maximum factorization of the secular determinant is accomplished. The cubic and quartic portions of the anharmonic potential function are derived. The components of vibrational angular momentum are set down. The complete valence-type potential function is discussed; explicit relations are derived between the generalized force constants occurring in the secular determinant and the valence force constants for CH_2D_2.

1. INTRODUCTION

THE tetrahedral X_2YZ_2 molecular model has symmetry C_{2v} and includes, as examples, the dihalogen substituted methanes, CH_2F_2, etc., the dideutero substituted methane, CH_2D_2, SO_2Cl_2, and others. The normal vibrations of this molecular model and the quantum-mechanical evaluation of its allowed rotation-vibration energies have not been treated extensively in the literature. Rosenthal[1,2] has studied the calculation of the normal frequencies of CH_2F_2 and CH_2D_2 type molecules, Dennison[3] has discussed the frequencies of CH_2D_2, and Ta-You Wu[4] has given a qualitative description of the normal modes. References to experimental papers on the Raman and infra-red spectra of tetrahedral X_2YZ_2 molecules are given by Dennison and Ta-You Wu.[3,4]

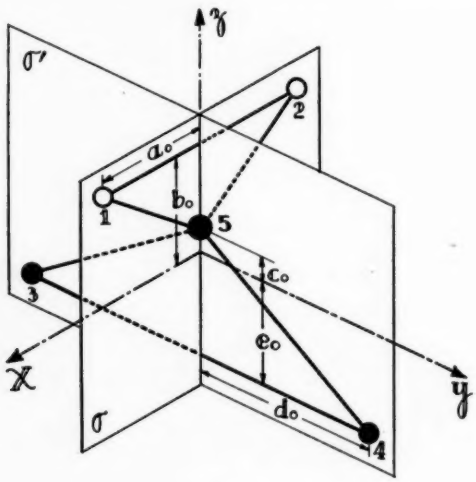

FIG. 1.

This paper is intended to form the basis for the interpretation of both the gross vibrational and fine rotational structure of the Raman and infra-red spectra of tetrahedral X_2YZ_2 molecules. Part I deals with the purely vibrational aspects of the problem and includes discussions of the molecular symmetry, characteristic modes of vibrations and potential functions. Part II deals with the evaluation to second-order approximation of the allowed energies of the rotating vibrating model and includes discussions of anharmonicities, coriolis interactions between rotation and vibration, dependence of the rotational constants on the state of vibration, effects of centrifugal stretching, etc.

2. GEOMETRY AND SYMMETRY

The equilibrium configuration of the model assumed for the tetrahedral X_2YZ_2 molecule is shown in Fig. 1. A right-handed body-fixed rectangular coordinate system *xyz*, with origin

[1] J. E. Rosenthal, Phys. Rev. **45**, 538 (1934).
[2] J. E. Rosenthal, Phys. Rev. **46**, 730 (1934).
[3] D. M. Dennison, Rev. Mod. Phys. **12**, 175 (1940).
[4] Ta-You Wu, *Vibrational Spectra and Structure of Molecules* (Prentice-Hall, Inc., New York, 1939), p. 244 ff.

TABLE I.

atom	r	m_r	x_{0r}	y_{0r}	z_{0r}
X	1	m	a_0	0	b_0
X	2	m	$-a_0$	0	b_0
Z	3	n	0	$-d_0$	$-e_0$
Z	4	n	0	d_0	$-e_0$
Y	5	M	0	0	c_0

at the center of mass of the molecule, is adopted for specifying the equilibrium positions of the 5 atoms. The coordinate system is so oriented that its axes are the principal axes of inertia. The equilibrium coordinates and masses of the respective atoms are given in Table I.

The model belongs, in the equilibrium configuration, to the symmetry point group C_{2v} whose characters are given in Table II. The symmetry elements of the point group shown in Fig. 1 are a twofold axis of rotation and two mutually perpendicular reflection planes intersecting in that axis. The symbol E denotes the identity operation, C_2 rotation by π around the twofold axis, and σ and σ' denote reflection in the respective planes. The symmetry types A and B denote quantities which are, respectively, symmetrical and antisymmetrical under rotation about the axis C_2; subscripts 1 and 2 denote quantities which are, respectively, symmetrical and antisymmetrical under reflection in the σ-plane. Several authors[5-9] have described methods of obtaining many properties of a molecular model from the table of symmetry characters. All the states of the X_2YZ_2 model are non-degenerate. The total angular momentum component P_x is of type B_2, P_y of B_1, and P_z of A_2. The coordinate x belongs to type B_1, y to B_2, and z to A_1. There are nine normal modes, 4 of which belong to type A_1, 1 to A_2, 2 to B_1, and 2 to B_2. The components of the dipole moment behave like x, y, and z; hence, only vibrations of types A_1, B_1, and B_2 will have fundamentals active in infra-red. Any combination or overtone of type A_2 will be inactive in the infra-red. All classes of vibrations have fundamentals, overtones, and combinations which are Raman active; vibrations belonging to A_1 are polarized and the others are depolarized.

[5] E. Wigner, Gottinger Nachrichten, p. 133 (1930); *Gruppentheorie* (Braunschweig, 1931).
[6] L. Tisza, Zeits. f. Physik **82**, 48 (1933).
[7] E. B. Wilson, Jr., J. Chem. Phys. **2**, 432 (1934).
[8] J. E. Rosenthal and G. M. Murphy, Rev. Mod. Phys. **8**, 317 (1936).
[9] A. G. Meister, F. F. Cleveland, and M. J. Murray, Am. J. Phys. **11**, 239 (1943).

3. INTERMEDIATE VIBRATIONAL COORDINATES

The instantaneous positions of the atoms are described during vibration by a right-handed body-fixed rectangular coordinate system, which coincides in the equilibrium configuration with the system described above. The instantaneous position of the rth atom is given by

$$(x_r, y_r, z_r) = (x_{0r}+x_r', y_{0r}+y_r', z_{0r}+z_r'),$$

where x_r', y_r', and z_r' denote components of displacement from the equilibrium position. There are $3N$(N=number of atoms) displacement coordinates x_r', y_r', and z_r' of which only $3N-6=9$, corresponding to the number of degrees of vibrational freedom, are linearly independent. Six linear relations among the displacement coordinates are given by the Eckart conditions:[10,11] (a) the center of mass remains at the origin during vibration, $\sum m_r x_r'=0$, etc., and (b) the angular momentum of vibration vanishes in zero-order approximation,

$$p_{0x}=\sum m_r(y_{0r}z_r'-z_{0r}y_r')=0, \quad \text{etc.}$$

For the tetrahedral X_2YZ_2 model the Eckart conditions are:

$$\begin{aligned} m(x_1'+x_2')+n(x_3'+x_4')+Mx_5'&=0,\\ m(y_1'+y_2')+n(y_3'+y_4')+My_5'&=0,\\ m(z_1'+z_2')+n(z_3'+z_4')+Mz_5'&=0, \end{aligned} \tag{1a}$$

TABLE II.

	E	C_2	σ	σ'
A_1	1	1	1	1
A_2	1	1	−1	−1
B_1	1	−1	1	−1
B_2	1	−1	−1	1

$$\begin{aligned} p_{0x}&=nd_0(z_1'-z_3')-mb_0(y_1'+y_2')\\ &\quad +ne_0(y_3'+y_4')-Mc_0y_5'=0,\\ p_{0y}&=mb_0(x_1'+x_2')-ne_0(x_3'+x_4')\\ &\quad +Mc_0x_5'+ma_0(z_2'-z_1')=0,\\ p_{0z}&=ma_0(y_1'-y_2')+nd_0(x_3'-x_4')=0. \end{aligned} \tag{1b}$$

[10] C. Eckart, Phys. Rev. **47**, 552 (1932).
[11] E. B. Wilson and J. B. Howard, J. Chem. Phys. **4**, 260 (1936).

A suitable set of 9 linearly independent intermediate generalized coordinates, which are mutually orthogonal and of proper symmetry, is:

$$\begin{aligned}
\xi_1&=(z_1'+z_2')/2,\\
\xi_2&=(z_3'+z_4')/2,\\
\xi_3&=(x_1'-x_2')/2,\\
\xi_4&=(y_3'-y_4')/2,\\
\sigma_5&=(x_3'-x_4')/2,\\
\eta_6&=(x_1'+x_2')/2,\\
\eta_7&=(x_3'+x_4')/2,\\
\zeta_8&=(y_1'+y_2')/2,\\
\zeta_9&=(y_3'+y_4')/2,
\end{aligned}\tag{2}$$

where ξ denotes a coordinate belonging to symmetry type A_1, σ to A_2, η to B_1, and ζ to B_2. It follows from Eqs. (1a), (1b), and (2) that the 15 displacement coordinates are the following functions of the generalized coordinates:

$$\begin{aligned}
x_1'&=\eta_6+\xi_3,\\
x_2'&=\eta_6-\xi_3,\\
x_3'&=\eta_7+\sigma_5,\\
x_4'&=\eta_7-\sigma_5,\\
x_5'&=-(2/M)[m\eta_6+n\eta_7],\\
y_1'&=\zeta_8-\phi_5\sigma_5,\\
y_2'&=\zeta_8+\phi_5\sigma_5,\\
y_3'&=\zeta_9+\xi_4,\\
y_4'&=\zeta_9-\xi_4,\\
y_5'&=-(2/M)[m\zeta_8+n\zeta_9],\\
z_1'&=\xi_1+\phi_6\eta_6-\phi_7\eta_7,\\
z_2'&=\xi_1-\phi_6\eta_6+\phi_7\eta_7,\\
z_3'&=\xi_2-\phi_8\zeta_8+\phi_9\zeta_9,\\
z_4'&=\xi_2+\phi_8\zeta_8-\phi_9\zeta_9,\\
z_5'&=-(2/M)[m\xi_1+n\xi_2],
\end{aligned}\tag{3}$$

where

$$\begin{aligned}
\phi_5&=(nd_0/ma_0),\\
\phi_6&=(b_0-c_0)/a_0,\\
\phi_7&=(n/m)(e_0+c_0)/a_0,\\
\phi_8&=(m/n)(b_0-c_0)/d_0,\\
\phi_9&=(e_0+c_0)/d_0.
\end{aligned}\tag{3a}$$

The kinetic energy of vibration,

$$T_v=(1/2)\sum_r m_r(\dot{x}_r^2+\dot{y}_r^2+\dot{z}_r^2)$$

must be of symmetry type A_1 and is given in terms of the generalized coordinates by:

$$\begin{aligned}
2T_v=&\mu_1\dot{\xi}_1^2+\mu_2\dot{\xi}_2^2+\mu_3\dot{\xi}_3^2+\mu_4\dot{\xi}_4^2+2\mu_{12}\dot{\xi}_1\dot{\xi}_2\\
&+\mu_5\dot{\sigma}_5^2+\mu_6\dot{\eta}_6^2+\mu_7\dot{\eta}_7^2+2\mu_{67}\dot{\eta}_6\dot{\eta}_7\\
&+\mu_8\dot{\zeta}_8^2+\mu_9\dot{\zeta}_9^2+2\mu_{89}\dot{\zeta}_8\dot{\zeta}_9,
\end{aligned}\tag{4}$$

where

$$\begin{aligned}
\mu_1&=(2m/M)(M+2m),\\
\mu_2&=(2n/M)(M+2n),\\
\mu_3&=2m,\quad \mu_4=2n,\\
\mu_{12}&=(4mn/M),\\
\mu_5&=(2n/ma_0^2)(ma_0^2+nd_0^2),\\
\mu_6&=\mu_1+2m\phi_6^2,\\
\mu_7&=\mu_2+2m\phi_7^2,\\
\mu_{67}&=\mu_{12}-2m\phi_6\phi_7,\\
\mu_8&=\mu_1+2n\phi_8^2,\\
\mu_9&=\mu_2+2n\phi_9^2,\\
\mu_{89}&=\mu_{12}-2n\phi_8\phi_9.
\end{aligned}\tag{4a}$$

The harmonic (quadratic) generalized potential function U_0 is of symmetry type A_1 and is given by:

$$\begin{aligned}
2U_0=&k_1\xi_1^2+k_2\xi_2^2+k_3\xi_3^2+k_4\xi_4^2+2k_{12}\xi_1\xi_2\\
&+2k_{13}\xi_1\xi_3+2k_{14}\xi_1\xi_4+2k_{23}\xi_2\xi_3+2k_{24}\xi_2\xi_4\\
&+2k_{34}\xi_3\xi_4+k_5\sigma_5^2+k_6\eta_6^2+k_7\eta_7^2\\
&+2k_{67}\eta_6\eta_7+k_8\zeta_8^2+k_9\zeta_9^2+2k_{89}\zeta_8\zeta_9,
\end{aligned}\tag{5}$$

in which the k's are generalized force constants which are given in Sections 8 and 9 as functions of the special force constants in the valence-force potential function.

4. NORMAL COORDINATES

The Lagrange secular determinant,

$$|\lambda T_v-U_0|=0,$$

for evaluation of the normal or characteristic frequencies of the model is of ninth order but factors into four steps, each of which is associated with one symmetry type. The roots λ of the determinant are related to the normal frequencies ω (measured in cm^{-1}) by the expression $\lambda=4\pi^2c^2\omega^2$, if c is the velocity of light in cm/sec. The subscripts i, j, k, and l are used in this paper in the following manner to denote the normal frequencies belonging to each symmetry type:

$i=1, 2, 3, 4$, for type A_1; $j=5$ for type A_2; $k=6, 7$ for type B_1; and $l=8, 9$ for type B_2. The subscript s is used to denote the intermediate coordinates, defined in Eq. (2), as follows: $s=1, 2, 3, 4$, for the ξ's of type A_1; $s=5$ for σ of A_2; $s=6, 7$ for the η's of B_1; and $s=8, 9$, for the ζ's of B_2.

The steps of the secular determinant associated with symmetry types A_1, A_2, B_1, and B_2, respectively, are as follows:

$$\begin{vmatrix} \lambda\mu_1-k_1 & \lambda\mu_{12}-k_{12} & -k_{13} & -k_{14} \\ \lambda\mu_{12}-k_{12} & \lambda\mu_2-k_2 & -k_{23} & -k_{24} \\ -k_{13} & -k_{23} & \lambda\mu_3-k_3 & -k_{34} \\ -k_{14} & -k_{24} & -k_{34} & \lambda\mu_4-k_4 \end{vmatrix} = 0, \quad (6a)$$

$$\lambda\mu_5-k_5 = 0, \quad (6b)$$

$$\begin{vmatrix} \lambda\mu_6-k_6 & \lambda\mu_{67}-k_{67} \\ \lambda\mu_{67}-k_{67} & \lambda\mu_7-k_7 \end{vmatrix} = 0, \quad (6c)$$

$$\begin{vmatrix} \lambda\mu_8-k_8 & \lambda\mu_{89}-k_{89} \\ \lambda\mu_{89}-k_{89} & \lambda\mu_9-k_9 \end{vmatrix} = 0. \quad (6d)$$

In principle, the generalized force constants occurring in Eq. (4) can be evaluated if one substitutes into the secular determinant the values of λ corresponding to the experimentally observed normal frequencies ω corrected for anharmonicity, etc. In this particular case there are 17 generalized force constants occurring in Eq. (5) to be determined from only 9 normal frequencies. It is, therefore, necessary either that additional data be obtained from isotopic molecules or that the 17 generalized force constants be expressed in terms of not more than 9 independent force constants in a physical potential function such as one of the valence or central force type. The number of independent physical force constants can be reduced by (1) arbitrary omission from the physical potential function of certain terms assumed to be small, or (2) assumption that the values of certain physical force constants, such as the CH force constant, are known from previous investigations.

The transformations from the intermediate generalized coordinates defined in Eq. (2) to the normal coordinates Q are given by:

$$\xi_s=\sum_i n_{si}Q_i \ldots s=1, 2, 3, 4; i=1, 2, 3, 4, \quad (7)$$

$$\sigma_s=n_{sj}Q_j \ldots\ldots s=j=5, \quad (8)$$

$$\eta_s=\sum_k n_{sk}Q_k \ldots s=6, 7; k=6, 7, \quad (9)$$

$$\zeta_s=\sum_l n_{sl}Q_l \ldots s=8, 9; l=8, 9. \quad (10)$$

The transformation coefficient n_{sj} is given by:

$$n_{sj}=n_{55}=\mu_5^{-\frac{1}{2}}. \quad (8a)$$

The coefficients n_{sk} are given by:

$$\begin{aligned} n_{6k}&=(\lambda_k\mu_7-k_7)/N_k, \\ n_{7k}&=-(\lambda_k\mu_{67}-k_{67})/N_k, \end{aligned} \quad (9a)$$

where

$$N_k=[(\lambda_k\mu_{67}-k_{67})^2+(\lambda_k\mu_7-k_7)^2]^{\frac{1}{2}},$$

if $k=6, 7$. The coefficients n_{sl} are given by:

$$\begin{aligned} n_{8l}&=(\lambda_l\mu_9-k_9)/N_l, \\ n_{9l}&=(\lambda_l\mu_{89}-k_{89})/N_l, \end{aligned} \quad (10a)$$

where

$$N_l=[(\lambda_l\mu_{89}-k_{89})^2+(\lambda_l\mu_9-k_9)^2]^{\frac{1}{2}},$$

if $l=8, 9$. The coefficients n_{si} are given by:

$$n_{si}=A_{si}/N_i, \quad (7a)$$

where A_{si} is the cofactor of the sth element in the first column of the determinant given in Eq. (6a) with λ set equal to λ_i,

$$N_i=[\mu_1A_{1i}^2+\mu_2A_{2i}^2+\mu_3A_{3i}^2+\mu_4A_{4i}^2+2\mu_{12}A_{1i}A_{2i}]^{\frac{1}{2}}$$

and $s=1, 2, 3, 4$; $i=1, 2, 3, 4$.

In terms of the normal coordinates Q_k the quantities T_v and U_0 are:

$$T_v=(1/2)\sum_{k=1}^{9}\dot{Q}_k^2, \quad (11a)$$

and

$$U_0=(1/2)\sum_{k=1}^{9}\lambda_kQ_k^2=2\pi^2c^2\sum_{k=1}^{9}\omega_k^2Q_k^2. \quad (11b)$$

The approximate forms of the normal modes are illustrated in Fig. 2. Similar pictures of the

modes are given by Wu.[4] The subscripts on the ω's in Fig. 2 follow the notation described above for modes associated with the various symmetry types.

The subsequent discussion can be simplified by the introduction of dimensionless normal coordinates q_h defined by the relation:

$$Q_h=(\hbar/2\pi c\omega_h)^{\frac{1}{2}}q_h, \tag{12}$$

where $\hbar$ is Planck's constant divided by 2π, and c is the velocity of light. In terms of q_h the zero-order vibrational energy is given in the Hamiltonian form by:

$$H=(hc/2)\sum_{h=1}^{9}\omega_h[(p_h^2/\hbar^2)+q_h^2], \tag{13}$$

where $p_h=\partial T/\partial\dot{q}_h=$momentum conjugate to q_h.

5. ANHARMONIC POTENTIAL FUNCTION

Each term in the expression for the total energy must belong to symmetry type A_1. It can be shown by direct multiplication of the characters in Table II that the cubic combinations of normal coordinates occurring in the anharmonic portion of the potential function of a molecule belonging to symmetry group C_{2v} can be A_1^3, $A_2^2A_1$, $B_1^2A_1$, $B_2^2A_1$, and $A_2B_1B_2$. Likewise the quartic combinations occurring are A_1^4, A_2^4, B_1^4, B_2^4, $A_1^2A_2^2$, $A_1^2B_1^2$, $A_1^2B_2^2$, $A_2^2B_1^2$, $A_2^2B_2^2$, $B_1^2B_2^2$, and $A_1A_2B_1B_2$.

The most general cubic portion U_1 of the anharmonic potential function of the tetrahedral X_2YZ_2 model is given by:

$$\begin{aligned}U_1/hc=&\sum_i\beta_{iii}q_i^3+\sum_i\sum_{i'}\beta_{iii'}q_i^2q_{i'}\\&+\sum_i\sum_{i'}\sum_{i''}\beta_{ii'i''}q_iq_{i'}q_{i''}\\&+\sum_i\sum_j\beta_{ijj}q_iq_j^2+\sum_i\sum_k\beta_{ikk}q_iq_k^2\\&+\sum_i\sum_k\sum_{k'}\beta_{ikk'}q_iq_kq_{k'}+\sum_i\sum_l\beta_{ill}q_iq_l^2\\&+\sum_i\sum_l\sum_{l'}\beta_{ill'}q_iq_lq_{l'}\\&+\sum_j\sum_k\sum_l\beta_{jkl}q_jq_kq_l.\end{aligned} \tag{14}$$

The quartic portion U_2 of the anharmonic potential function of the tetrahedral X_2YZ_2 model, which contributes to the allowed energies to

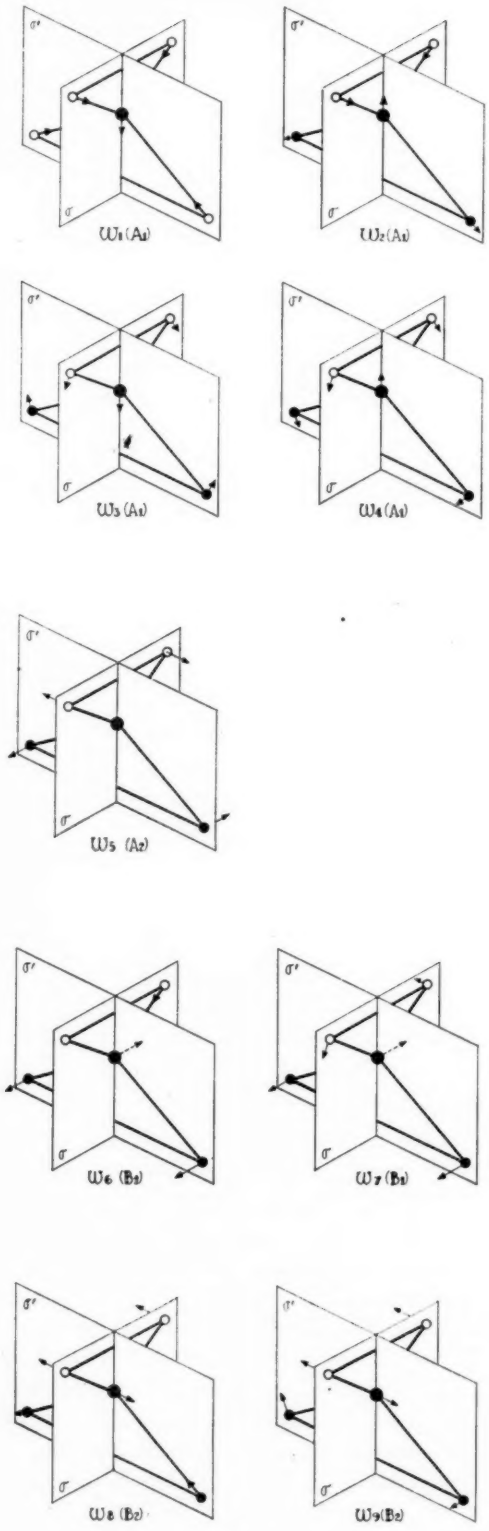

FIG. 2.

second-order approximation,[12] is given by:

$$\begin{aligned}U_2/hc=&\sum_i \gamma_{iiii}q_i^4+\sum_i\sum_{i'}\gamma_{iii'i'}q_i^2q_{i'}^2\\&+\sum_j\gamma_{jjjj}q_j^4+\sum_k\gamma_{kkkk}q_k^4\\&+\sum_k\sum_{k'}\gamma_{kkk'k'}q_k^2q_{k'}^2+\sum_l\gamma_{llll}q_l^4\\&+\sum_l\sum_{l'}\gamma_{lll'l'}q_l^2q_{l'}^2+\sum_i\sum_j\gamma_{iijj}q_i^2q_j^2\\&+\sum_i\sum_k\gamma_{iikk}q_i^2q_k^2+\sum_i\sum_l\gamma_{iill}q_i^2q_l^2\\&+\sum_j\sum_k\gamma_{jjkk}q_j^2q_k^2+\sum_j\sum_l\gamma_{jjll}q_j^2q_l^2\\&+\sum_k\sum_l\gamma_{kkll}q_k^2q_l^2. \quad (15)\end{aligned}$$

In Eqs. (14) and (15) the subscripts i, j, k, l denote coordinates belonging, respectively, to symmetry types A_1, A_2, B_1, and B_2 as specified in Section 4. Primed and unprimed subscripts in a given summation are used to denote different coordinates of the same symmetry type; for example, $\beta_{ii'i''}$ may denote β_{123}, β_{124}, β_{134}, and β_{234}. Each combination of subscripts may occur only once, i.e., permutations of a given combination of subscripts are not allowed; for example, β_{123} is the same as β_{132}, β_{213}, etc. The coefficients β and γ occurring in Eqs. (13) and (14) are expressed in cm^{-1}.

6. VIBRATIONAL ANGULAR MOMENTUM

An internal angular momentum of vibration may arise when two or more normal modes of vibration occur simultaneously. This angular momentum is ordinarily of small magnitude unless the two frequencies involved are nearly or exactly equal. This type of angular momentum is of importance in connection with coriolis interactions between rotations and vibrations discussed in Part II. The components p_x, p_y, and p_z of internal angular momentum are of the same symmetry types as the components of total angular momentum and belong, respectively, to types B_2, B_1, and A_2. These components are defined as:

$$\begin{aligned}p_x&=\textstyle\sum_r m_r(y_r'\dot z_r'-z_r'\dot y_r'),\\p_y&=\textstyle\sum_r m_r(z_r'\dot x_r'-x_r'\dot z_r')\\p_z&=\textstyle\sum_r m_r(x_r'\dot y_r'-y_r'\dot x_r'),\end{aligned}$$

where, p_x may contain combinations of types A_2B_1 and A_1B_2; p_y may contain A_2B_2 and A_1B_1, and p_z may contain A_1A_2 and B_1B_2. The components are expressed in terms of the dimensionless normal coordinates q_h and conjugate momenta p_h as follows:

$$\begin{aligned}p_x&=\textstyle\sum_k \xi_{k5}[(\omega_5/\omega_k)^{\frac12}q_kp_5-(\omega_k/\omega_5)^{\frac12}q_5p_k]\\&\quad+\textstyle\sum_l\sum_i\xi_{li}[(\omega_l/\omega_i)^{\frac12}q_ip_l-(\omega_i/\omega_l)^{\frac12}q_lp_i],\\p_y&=\textstyle\sum_l\eta_{l5}[(\omega_5/\omega_l)^{\frac12}q_lp_5-(\omega_l/\omega_5)^{\frac12}q_5p_l]\\&\quad+\textstyle\sum_k\sum_i\eta_{ki}[(\omega_k/\omega_i)^{\frac12}q_ip_k-(\omega_i/\omega_k)^{\frac12}q_kp_i],\\p_z&=\textstyle\sum_i\zeta_{i5}[(\omega_5/\omega_i)^{\frac12}q_ip_5-(\omega_i/\omega_5)^{\frac12}q_5p_i]\\&\quad+\textstyle\sum_k\sum_l\zeta_{kl}[(\omega_k/\omega_l)^{\frac12}q_lp_k-(\omega_l/\omega_k)^{\frac12}q_kp_l].\end{aligned} \quad (16)$$

The coriolis parameters or moduli of internal angular momentum are defined as follows:

$$\begin{aligned}\xi_{k5}&=(2nd_0/ma_0^2)n_{55}[m(b_0-c_0)n_{6k}-n(e_0+c_0)n_{7k}],\\\xi_{li}&=\{(\mu_1n_{8l}+\mu_{12}n_{9l})n_{1i}+(\mu_2n_{9l}+\mu_{12}n_{8l})n_{2i}\\&\quad+(2/d_0)[m(b_0-c_0)n_{8l}-n(e_0+c_0)n_{9l}]n_{4i}\},\\\eta_{l5}&=(2/d_0)[n(e_0+c_0)n_{9l}-m(b_0-c_0)n_{8l}]n_{55},\\\eta_{ki}&=\{-(\mu_1n_{6k}+\mu_{12}n_{7k})n_{1i}-(\mu_2n_{7k}+\mu_{12}n_{6k})n_{2i}\\&\quad+(2/a_0)[m(b_0-c_0)n_{6k}-n(e_0+c_0)n_{7k}]n_{3i}\},\\\zeta_{i5}&=-[(2nd_0/a_0)n_{3i}+\mu_4n_{4i}]n_{55},\\\zeta_{kl}&=\{(\mu_1n_{6k}+\mu_{12}n_{7k})n_{8l}+(\mu_2n_{7l}+\mu_{12}n_{6k})n_{9l}\},\end{aligned} \quad (17)$$

where i assumes the values 1, 2, 3, 4; k the values 6, 7; and l the values 8, 9.

7. GENERAL VALENCE POTENTIAL FUNCTION

A harmonic potential function suitable for the interpretation of experimental data and the correlation of vibration spectra of related molecules should contain force constants possessing physical significance rather than the generalized algebraic constants occurring in Eq. (5). An appropriate physical potential function is the valence type in which the coordinates used are the valence bonds and their included angles. The valence coordinates suitable for description of infinitesimal vibrations of a group of three atoms (m, n, and a central atom C) are illustrated in

[12] The most general anharmonic potential function contains the following additional quartic terms which are of odd degree in one or more coordinates and do not, therefore, ordinarily contribute to the allowed energies: $q_i^3q_{i'}$, $q_i^2q_{i'}q_{i''}$, $q_iq_{i'}q_{i''}q_{i'''}$, $q_k^3q_{k'}$, $q_i^3q_{l'}$, $q_iq_{i'}q_j^2$, $q_iq_{i'}q_k^2$, $q_iq_{i'}q_kq_{k'}$, $q_i^2q_kq_{k'}$, $q_iq_{i'}q_l^2$, $q_iq_{i'}q_lq_{l'}$, $q_i^3q_lq_{l'}$, $q_j^2q_kq_{k'}$, $q_j^2q_lq_{l'}$, $q_kq_{k'}q_l^2$, $q_kq_{k'}q_lq_{l'}$, $q_k^2q_lq_{l'}$, and $q_iq_jq_kq_l$.

Fig. 3, where $r_m=r_{0m}+\delta r_m$, $r_n=r_{0n}+\delta r_n$, and $\beta_{mn}=\beta_{0mn}+\delta\beta_{mn}$; r_m, r_n, and β_{mn} denote, respectively, the instantaneous values of the two valence bond lengths and the included bond angle, while r_{0m}, r_{0n}, and β_{0mn} denote their equilibrium values and δr_m, δr_n, and $\delta\beta_{mn}$ denote changes occurring during vibration. The quantity $\delta\beta_{mn}$ is given for infinitesimal vibrations by

$$\delta\beta_{mn}=[p_{0mn}\delta p_{mn}-(r_{0m}-r_{0n}\cos\beta_{0mn})\delta r_m - (r_{0n}-r_{0m}\cos\beta_{0mn})\delta r_n]/(r_{0m}r_{0n}\sin\beta_{0mn}) \quad (18)$$

where p_{mn} is the distance between atoms m and n.

In the tetrahedral X_2YZ_2 molecule the relative displacements of the various pairs of atoms during infinitesimal vibrations can be obtained in terms of the intermediate coordinates by the substitution of Eqs. (3) into the expression

$$\delta p_{mn}=[(x_{0m}-x_{0n})(x_m'-x_n') +(y_{0m}-y_{0n})(y_m'-y_n') +(z_{0m}-z_{0n})(z_m'-z_n')]/p_{0mn}.$$

It follows that:

$$\begin{aligned}
&\delta p_{12}=2\xi_3, \quad \delta p_{34}=-2\xi_4,\\
&\delta p_{13}=[f_1-f_2+f_3+f_4]/p_{013},\\
&\delta p_{24}=[f_1-f_2-f_3-f_4]/p_{013},\\
&\delta p_{14}=[f_1+f_2+f_3-f_4]/p_{013},\\
&\delta p_{23}=[f_1+f_2-f_3+f_4]/p_{013},
\end{aligned} \quad (19)$$

where

$$\begin{aligned}
f_1&=(b_0+e_0)(\xi_1-\xi_2)+a_0\xi_3-d_0\xi_4,\\
f_2&=(a_0+d_0\phi_5)\sigma_5,\\
f_3&=[a_0+(b_0+e_0)\phi_6]\eta_6-[a_0+(b_0+e_0)\phi_7]\eta_7,\\
f_4&=[d_0+(b_0+e_0)\phi_8]\zeta_8-[d_0+(b_0+e_0)\phi_9]\zeta_9,\\
p_{013}&=[a_0^2+d_0^2+(b_0+e_0)^2]^{\frac{1}{2}},
\end{aligned}$$

in which ϕ_5, etc. are the quantities defined in Eq. (4a);

$$\begin{aligned}
\delta p_{15}=\delta r_1&=[g_1+g_2]/r_{01},\\
\delta p_{25}=\delta r_2&=[g_1-g_2]/r_{01},
\end{aligned} \quad (20)$$

where

$$\begin{aligned}
g_1&=(b_0-c_0)[(\mu_1\xi_1+\mu_{12}\xi_2)/2m]+a_0\xi_3,\\
g_2&=a_0[(\mu_1/2m)+\phi_6^2]\eta_6+a_0[(\mu_{12}/2m)-\phi_6\phi_7]\eta_7,\\
r_{01}=r_{02}&=p_{015}=[a_0^2+(b_0-c_0^2)]^{\frac{1}{2}};
\end{aligned}$$

and

$$\begin{aligned}
\delta p_{35}=\delta r_3&=[g_3-g_4]/r_{03},\\
\delta p_{45}=\delta r_4&=[g_3+g_4]/r_{03},
\end{aligned} \quad (21)$$

where

$$\begin{aligned}
g_3&=-(e_0+c_0)[(\mu_{12}\xi_1+\mu_2\xi_2)/2n]-d_0\xi_4,\\
g_4&=d_0[(\mu_{12}/2n)-\phi_8\phi_9]\zeta_8+d_0[(\mu_2/2n)+\phi_9^2]\zeta_9,\\
r_{03}&=r_{04}=p_{035}=[d_0^2+(e_0+c_0)^2]^{\frac{1}{2}}.
\end{aligned}$$

Explicit expressions for the $\delta\beta_{mn}$ in terms of the intermediate coordinates can be obtained by substitution of Eqs. (19), (20), and (21) into Eq. (18).

The most general harmonic potential function, which can be set down in terms of the valence coordinates, contains all possible quadratic combinations of these coordinates. In the so-called "valence" potential function it is ordinarily assumed a good approximation to include squared terms in the δr's and $\delta\beta$'s and to omit all or part of the cross products. It has been found in many cases that such an approximation gives a fairly good interpretation of the experimental data; however, the most complete potential function possible should be used to justify analyses of the excellent vibrational data available in many cases. In simple cases, as for example that of H_2O,[13,14] where evaluation of the constants in a complete potential function has been possible, it has been found that none of these constants is negligible. A discussion of the complete valence-type potential function for the tetrahedral X_2YZ_2 model is given below in such a form that approximations can be made simply by dropping the appropriate terms.

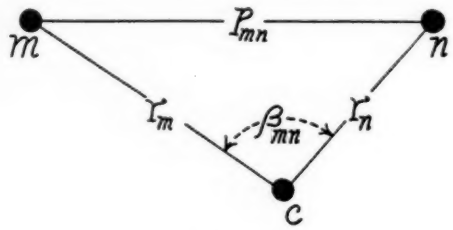

FIG. 3.

The valence coordinates $\delta\beta_{mn}$ and δr_m are not suitable for the description of normal modes because (1) they do not generally fall directly into the required symmetry types and (2) they are usually redundant in the sense that they are more numerous than the degrees of vibrational

[13] B. T. Darling and D. M. Dennison, Phys. Rev. 57, 128 (1940).
[14] W. H. Shaffer and R. R. Newton, J. Chem. Phys. 10, 405 (1942).

freedom. It is possible, however, to set up linear combinations of the valence coordinates which do possess the appropriate symmetry properties and a physical potential function based on such coordinates can be used in the interpretation of data if relations are found between the valence force constants occurring in such a function and the generalized constants occurring in Eq. (5). For the tetrahedral X_2YZ_2 model there are ten possible valence coordinates, namely, four δr's and six $\delta\beta$'s, while there are only nine degrees of freedom. The work of obtaining the expressions relating the k's of Eq. (5) to the valence force constants, which is a formidable task if done by direct substitution, is simplified by the adoption of the following ten combinations of valence coordinates:

$$\begin{aligned}
\Delta_1&=(\delta r_1+\delta r_2)/2,\\
\Delta_2&=(\delta r_3+\delta r_4)/2,\\
\Delta_3&=(r_{01}/2)\delta\beta_{12},\\
\Delta_4&=(r_{03}/2)\delta\beta_{34},\\
\Delta_0&=(r_{01}r_{03})^{\frac{1}{2}}(\delta\beta_{13}+\delta\beta_{24}+\delta\beta_{14}+\delta\beta_{23})/2,\\
\Delta_5&=(r_{01}r_{03})^{\frac{1}{2}}(\delta\beta_{13}+\delta\beta_{24}-\delta\beta_{14}-\delta\beta_{23})/4,\\
\Delta_6&=(\delta r_1-\delta r_2)/2,\\
\Delta_7&=(r_{01}r_{03})^{\frac{1}{2}}(\delta\beta_{13}-\delta\beta_{24}+\delta\beta_{14}-\delta\beta_{23})/4,\\
\Delta_8&=(\delta r_3-\delta r_4)/2,\\
\Delta_9&=(r_{01}r_{03})^{\frac{1}{2}}(\delta\beta_{13}-\delta\beta_{24}-\delta\beta_{14}+\delta\beta_{23})/4.
\end{aligned}\tag{22}$$

The variables Δ_1, Δ_2, Δ_3, and Δ_4 are of symmetry type A_1; Δ_0, of type A_1, is taken to be the redundant combination and can be expressed uniquely as a linear combination of the other four variables of type A_1. Δ_5 is of type A_2; Δ_6 and Δ_7 are of type B_1; and Δ_8 and Δ_9 are of type B_2. The above symmetry combinations can be expressed in terms of the intermediate coordinates as follows:

$$\Delta_i=A_i\xi_1+B_i\xi_2+C_i\xi_3+D_i\xi_4 \quad (i=1,2,3,4,0) \tag{23}$$

where

$$\begin{aligned}
&A_1/\cos\alpha_{012}=-A_3/\sin\alpha_{012}=\mu_1/2m,\\
&-A_2/\cos\alpha_{034}=A_4/\sin\alpha_{034}=\mu_{12}/2n,\\
&B_1/\cos\alpha_{012}=-B_3/\sin\alpha_{012}=\mu_{12}/2m,\\
&-B_2/\cos\alpha_{034}=B_4/\sin\alpha_{034}=\mu_2/2n,\\
&C_1=\sin\alpha_{012},\quad C_2=C_4=0,\quad C_3=\cos\alpha_{012},\\
&D_1=D_3=0,\quad D_2=-\sin\alpha_{034},\quad D_4=-\cos\alpha_{034},
\end{aligned}\tag{23a}$$

$$\begin{aligned}
A_0&=[(b_0+e_0)+\cos\beta_{013}(r_{013}A_1+r_{01}A_2)\\
&\quad-(r_{01}A_1+r_{03}A_2)]/\delta_0,\\
B_0&=[-(b_0+e_0)+\cos\beta_{013}(r_{03}B_1-r_{01}B_2)\\
&\quad-(r_{01}B_1-r_{03}B_3)]/\delta_0,\\
C_0&=[\sin\alpha_{012}(r_{03}\cos\beta_{013}-r_{01})+\alpha_0]/\delta_0,\\
D_0&=[-\sin\alpha_{034}(r_{01}\cos\beta_{013}-r_{03})-d_0]/\delta_0,
\end{aligned}$$

if $\alpha_{0mn}=\beta_{0mn}/2$, $\delta_0=(r_{01}r_{03})^{\frac{1}{2}}\sin\beta_{013}$;

$$\Delta_5=A_5\sigma_5, \tag{24}$$

where

$$A_5=-(\mu_5/2n)(\alpha_0/\delta_0); \tag{24a}$$

$$\Delta_6=A_6\eta_6+B_6\eta_7,\quad \Delta_7=A_7\eta_6+B_7\eta_7, \tag{25}$$

where

$$\begin{aligned}
&(A_6/\mu_6)=(B_6/\mu_{67})=(\sin\alpha_{012}/2m),\\
A_7&=[\alpha_0+\phi_6(b_0+e_0)\\
&\quad+(\mu_6/2m)(r_{03}\cos\beta_{013}-r_{01})\sin\alpha_{012}]/\delta_0,\\
B_7&=[-\alpha_0-\phi_7(b_0+e_0)\\
&\quad+(\mu_{67}/2m)(r_{03}\cos\beta_{013}-r_{01})\sin\alpha_{012}]/\delta_0;
\end{aligned}\tag{25a}$$

$$\Delta_8=A_8\zeta_8+B_8\zeta_9,\quad \Delta_9=A_9\zeta_8+B_9\zeta_9, \tag{26}$$

where

$$\begin{aligned}
&(A_8/\mu_{89})=(B_8/\mu_9)=-\sin\alpha_{034}/2n,\\
A_9&=[d_0+\phi_8(b_0+e_0)+(\mu_{89}/2n)\\
&\quad\times(r_{03}-r_{01}\cos\beta_{013})\sin\alpha_{034}]/\delta_0,\\
B_9&=[-d_0-\phi_9(b_0+e_0)+(\mu_9/2n)\\
&\quad\times(r_{03}-r_{01}\cos\beta_{013})\sin\alpha_{034}]/\delta_0.
\end{aligned}\tag{26a}$$

The most general harmonic potential function U_0 is given in terms of the symmetry combinations by:

$$\begin{aligned}
2_0U=&K_1\Delta_1^2+K_2\Delta_2^2+K_3\Delta_3^2+K_4\Delta_4^2+K_0\Delta_0^2\\
&+2K_{12}\Delta_1\Delta_2+2K_{13}\Delta_1\Delta_3+2K_{14}\Delta_1\Delta_4\\
&+2K_{23}\Delta_2\Delta_3+2K_{24}\Delta_2\Delta_4+2K_{34}\Delta_3\Delta_4\\
&+2K_{01}\Delta_0\Delta_1+2K_{02}\Delta_0\Delta_2+2K_{03}\Delta_0\Delta_3\\
&+2K_{04}\Delta_0\Delta_4+K_5\Delta_5^2+K_6\Delta_6^2+K_7\Delta_7^2\\
&+2K_{67}\Delta_6\Delta_7+K_8\Delta_8^2\\
&+K_9\Delta_9^2+2K_{89}\Delta_8\Delta_9,
\end{aligned}\tag{27}$$

in which cross products occur only among variables of the same symmetry type. The complete valence-type potential function U_0 for the tetrahedral X_2YZ_2 model can be written in terms of

the valence coordinates as:

$$2U_0 = c_1[(\delta r_1)^2+(\delta r_2)^2]+c_1'[(\delta r_3)^2+(\delta r_4)^2]+c_2 r_{01}^2(\delta\beta_{12})^2+c_2' r_{03}^2(\delta\beta_{34})^2+c_2'' r_{01}r_{03}[(\delta\beta_{13})^2+(\delta\beta_{24})^2$$
$$+(\delta\beta_{14})^2+(\delta\beta_{23})^2]+c_3\delta r_1\delta r_2+c_3'\delta r_3\delta r_4+c_3''(\delta r_1+\delta r_2)(\delta r_3+\delta r_4)+c_4 r_{01}(\delta r_1+\delta r_2)\delta\beta_{12}$$
$$+c_4' r_{03}(\delta r_3+\delta r_4)\delta\beta_{34}+r_{01}^{\frac{1}{2}}r_{03}^{\frac{1}{2}}\{c_4''[\delta r_1(\delta\beta_{13}+\delta\beta_{14})+\delta r_2(\delta\beta_{23}+\delta\beta_{24})]+c_4'''[\delta r_3(\delta\beta_{13}+\delta\beta_{23})$$
$$+\delta r_4(\delta\beta_{14}+\delta\beta_{24})]\}+c_5 r_{03}(\delta r_1+\delta r_2)\delta\beta_{34}+c_5' r_{01}(\delta r_3+\delta r_4)\delta\beta_{12}$$
$$+r_{01}^{\frac{1}{2}}r_{03}^{\frac{1}{2}}\{c_5''[\delta r_1(\delta\beta_{24}+\delta\beta_{23})+\delta r_2(\delta\beta_{13}+\delta\beta_{14})]+c_5'''[\delta r_3(\delta\beta_{14}+\delta\beta_{24})+\delta r_4(\delta\beta_{13}+\delta\beta_{23})]\}$$
$$+r_{01}r_{03}\{c_6\delta\beta_{12}\delta\beta_{34}+c_6'(\delta\beta_{13}\delta\beta_{24}+\delta\beta_{14}\delta\beta_{23})+c_7(\delta\beta_{13}\delta\beta_{14}+\delta\beta_{23}\delta\beta_{24})+c_7'(\delta\beta_{13}\delta\beta_{23}+\delta\beta_{14}\delta\beta_{24})\}$$
$$+r_{01}^{\frac{1}{2}}r_{03}^{\frac{1}{2}}[c_7'' r_{01}\delta\beta_{12}+c_7''' r_{03}\delta\beta_{34}](\delta\beta_{13}+\delta\beta_{24}+\delta\beta_{14}+\delta\beta_{23}) \quad (28)$$

where

$$K_0=2(2c_2''+c_6'+c_7+c_7'); \quad K_1=2c_1+c_3;$$
$$K_2=2c_1'+c_3'; \quad K_3=4c_2; \quad K_4=4c_2';$$
$$K_5=2(2c_2''+c_6'-c_7-c_7'); \quad K_6=2c_1-c_3;$$
$$K_7=2(2c_2''-c_6'+c_7-c_7'); \quad K_8=2c_1'-c_3';$$
$$K_9=2(2c_2''-c_6'-c_7+c_7'); \quad K_{01}=2(c_4''+c_5''); \quad (29)$$
$$K_{02}=2(c_4'''+c_5'''); \quad K_{03}=4c_7''; \quad K_{04}=4c_7''';$$
$$K_{12}=2c_3''; \quad K_{13}=2c_4; \quad K_{14}=2c_5;$$
$$K_{23}=2c_5'; \quad K_{24}=2c_4'; \quad K_{34}=2c_6;$$
$$K_{67}=2(c_4''-c_5''); \quad K_{89}=2(c_4'''-c_5''').$$

Substitution of Eqs. (23)–(26) into Eq. (27) and comparison of the resulting expression with Eq. (5) lead to the relations between the K's of Eq. (27) and the generalized force constants $k_{ss'}$ of Eq. (5); substitution of Eq. (29) into the latter relations yields the expressions for the $k_{ss'}$ in terms of the valence force constants.

8. VALENCE POTENTIAL FUNCTION FOR CH_2D_2

The CH_2D_2 molecule is the special case of the tetrahedral X_2YZ_2 model for which, in the equilibrium configuration, all the valence bonds have the same length r_0 as in CH_4, and all the bond angles have the tetrahedral value $\beta_0 = 109°27'$. It follows for CH_2D_2 that the equilibrium dimensions defined in Section 2 have the values:

$$a_0=d_0=r_0(2/3)^{\frac{1}{2}},$$
$$b_0=[(4n+M)/\textstyle\sum](r_0/3^{\frac{1}{2}}),$$
$$c_0=[2(n-m)/\textstyle\sum](r_0/3^{\frac{1}{2}}), \quad (30)$$
$$e_0=[(4m+M)/\textstyle\sum](r_0/3^{\frac{1}{2}}),$$
$$\sin\alpha_0=(2/3)^{\frac{1}{2}}; \quad \cos\alpha_0=3^{-\frac{1}{2}};$$
$$\sin\beta_0=2^{\frac{1}{2}}/3; \quad \cos\beta_0=-1/3,$$

where $\sum$ denotes the total mass, $\sum=2m+2n+M$, of the molecule if m is the mass of H, n the mass of D, and M the mass of C. The kinetic energy coefficients defined in Eq. (4a) become:

$$\mu_1=(2m+M)(2m/M); \quad \mu_2=(2n+M)(2n/M);$$
$$\mu_{12}=(4nm/M); \quad \mu_3=2m; \quad \mu_4=2n;$$
$$\mu_5=(m+n)(2n/m); \quad \mu_6=\mu_1+m; \quad (31)$$
$$\mu_7=\mu_2+(n^2/m); \quad \mu_{67}=\mu_{12}-n;$$
$$\mu_8=\mu_1+(m^2/n); \quad \mu_9=\mu_2+n; \quad \mu_{89}=\mu_{12}-m.$$

The coefficients defined in Eqs. (23a), (24a), (25a), and (26) become:

$$A_1=-2^{-\frac{1}{2}}A_3=3^{-\frac{1}{2}}(M+2m)/M;$$
$$A_2=-2^{-\frac{1}{2}}A_4=-3^{-\frac{1}{2}}(2m/M);$$
$$A_0=-B_0=6^{-\frac{1}{2}};$$
$$B_1=-2^{-\frac{1}{2}}B_3=3^{-\frac{1}{2}}(2n/M);$$
$$B_2=-2^{-\frac{1}{2}}B_4=-3^{-\frac{1}{2}}(M+2n/M;$$
$$C_1=-D_2=-(2/3)^{\frac{1}{2}};$$
$$C_3=-D_4=-3^{-\frac{1}{2}};$$
$$C_2=D_1=C_4=D_3=0; \quad (32)$$
$$C_0=-D_0=-3^{-\frac{1}{2}}/2;$$
$$A_5=-3^{\frac{1}{2}}(m+n)/2m;$$
$$(A_6/\mu_6)=(B_6/\mu_{67})=(2/3)^{\frac{1}{2}}/2m;$$
$$A_7=3^{\frac{1}{2}}[1-(\mu_6/3m)];$$
$$B_7=-3^{\frac{1}{2}}[1+(n/m)+(2\mu_{67}/3m)]/2;$$
$$(A_8/\mu_{89})=(B_8/\mu_9)=-(2/3)^{\frac{1}{2}}/2n;$$
$$A_9=3^{\frac{1}{2}}[1+(m/n)+(2\mu_{89}/3n)]/2;$$
$$B_9=-3^{\frac{1}{2}}[1-(\mu_9/3n)].$$

For CH_2D_2 all the valence force constants c_i carrying a given subscript in Eq. (28) become equal and the general valence potential function

U_0 is given by:

$$\begin{aligned}2U_0 = c_1 \sum_m (\delta r_m)^2 + c_2 r_0^2 \sum_{m,n} (\delta\beta_{mn})^2 \\ + c_3 \sum_{m>n} \delta r_n \delta r_m + c_4 r_0 \sum_{m,n} \delta\beta_{mn}(\delta r_m + \delta r_n) \\ + c_5 r_0 \sum \delta\beta_{mn}(\delta r_{m'} + \delta r_{n'}) \\ + c_6 r_0^2 \sum \delta\beta_{mn}\delta\beta_{m'n'} \\ + c_7 r_0^2 \sum \delta\beta_{mn}\delta\beta_{mn'}. \quad (33)\end{aligned}$$

Relations between the valence force constants of Eq. (33) and the K's of Eq. (27) are obtained from Eq. (29) simply by removing the primes on the c's.

It can be shown that the generalized force constants of Eq. (5) are the following functions of the valence force constants, for the case of CH_2D_2:

$$\begin{aligned}k_1 &= [A + (2\mu_1/M)B]/3, \\ k_2 &= [A + (2\mu_2/M)B]/3, \\ k_{12} &= [C + 2(M+n+\mu_{12})(B/M)]/3, \\ k_3 = k_4 &= [4c_1 + 5c_2 + 2c_3 + 2^{\frac{1}{2}}(c_4 - c_5) \\ &\qquad + (c_6/2) - 3c_7]/3, \\ k_{34} &= [-c_2 - 4c_3 + 2^{\frac{1}{2}}(c_4 - c_5) - (5c_6/2) + 3c_7]/3, \\ k_{13} &= 2^{\frac{1}{2}}[D + (2m/M)E]/3, \\ k_{14} &= 2^{\frac{1}{2}}[F + (2m/M)E]/3, \\ k_{23} &= 2^{\frac{1}{2}}[F + (2n/M)E]/3, \\ k_{24} &= 2^{\frac{1}{2}}[D + (2n/M)E]/3,\end{aligned} \quad (34)$$

where

$$\begin{aligned}A &= 2c_1 + 10c_2 + c_3 - 2\cdot 2^{\frac{1}{2}}(c_4 - c_5) + c_6 - 6c_7, \\ B &= 2c_1 + 8c_2 - c_3 - 4\cdot 2^{\frac{1}{2}}(c_4 - c_5) - 4c_6, \\ C &= -2c_2 - 2c_3 - 2\cdot 2^{\frac{1}{2}}(c_4 - c_5) - 5c_6 + 6c_7, \\ D &= 2c_1 - 5c_2 + c_3 - 2^{-\frac{1}{2}}(c_4 - c_5) - (c_6/2) + 3c_7, \\ E &= 2c_1 - 4c_2 - c_3 - 2^{-\frac{1}{2}}(c_4 - c_5) + 2c_6, \\ F &= c_2 - 2c_3 - 2^{-\frac{1}{2}}(c_4 - c_5) + (5c_6/2) - 3c_7;\end{aligned}$$

and

$$k_5 = 6[(m+n)/2m]^2(2c_2 + c_6 - 2c_7), \quad (35)$$

$$\begin{aligned}k_6 &= A_6^2(2c_1 - c_3) + 2A_7^2(2c_2 - c_6) \\ &\qquad + 4A_6A_7(c_4 - c_5), \\ k_7 &= B_6^2(2c_1 - c_3) + 2B_7^2(2c_2 - c_6) \\ &\qquad + 4B_6B_7(c_4 - c_5), \\ k_{67} &= A_6B_6(2c_1 - c_3) + 2A_7B_7(2c_2 - c_6) \\ &\qquad + 2(A_6B_7 + A_7B_6)(c_4 - c_5),\end{aligned} \quad (36)$$

$$\begin{aligned}k_8 &= A_8^2(2c_1 - c_3) + 2A_9^2(2c_2 - c_6) \\ &\qquad + 4A_8A_9(c_4 - c_5), \\ k_9 &= B_8^2(2c_1 - c_3) + 2B_9^2(2c_2 - c_6) \\ &\qquad + 4B_8B_9(c_4 = c_5), \\ k_{89} &= A_8B_8(2c_1 - c_3) + 2A_9B_9(2c_2 - c_6) \\ &\qquad + 2(A_8B_9 + A_9B_8)(c_4 - c_5),\end{aligned} \quad (37)$$

where A_6, A_7, etc., are quantities defined in Eq. (32). It is obvious from Eqs. (34)–(37) that the 17 generalized force constants of Eq. (5) can be expressed for the case of CH_2D_2 as functions of 6 independent valence force constants,[15] namely, c_1, c_2, c_3, $c_4 - c_5$, c_6, and c_7, which occur in the most general physical potential function of the valence type. It follows that it should be possible to determine all six of the valence force constants from the infra-red and Raman spectra of CH_2D_2 since this molecule has nine different vibration frequencies of which all are Raman active and all except one are infra-red active.

[15] As a check on the expressions (34)–(37), the secular determinant (6) has been set up for the case in which $m = n$ and it was found to yield correctly the expressions for the CH_4 frequencies.

THE JOURNAL OF CHEMICAL PHYSICS VOLUME 12, NUMBER 12 DECEMBER, 1944

The Infra-Red Spectra of Bent XYZ Molecules

Part I. Vibration-Rotation Energies

W. H. SHAFFER AND R. P. SCHUMAN
Mendenhall Laboratory of Physics, The Ohio State University, Columbus, Ohio

(Received October 12, 1944)

The rotation-vibration Hamiltonian, complete to second order of approximation, is set up for the bent XYZ molecular model. The allowed energies are calculated and expressed in term-value form, $E=hc(G+F)$; the vibrational term G is given explicitly and the elements of the secular determinant are given for evaluation of the rotational term F. The valence-force form of harmonic potential function is discussed for the bent XYY′ model and normal frequencies of HDO are calculated.

I. INTRODUCTION

THE rotation-vibration spectra of many polyatomic molecules, when observed with the excellent prism-grating spectrometers now available, exhibit fine structure and other features which cannot be adequately interpreted on the basis of the simple theory in which it is assumed that the vibrations of a molecule are simple harmonic and independent of the rotations. In order that the spectroscopist may obtain the maximum amount of information concerning molecular structure from the spectral data, it is necessary that an adequate theoretical study be made of the dependence of the rotation-vibration energies on molecular configuration, force constants, interactions between rotations and vibrations, etc. Such studies[1–11] have already been made for several types of molecules and the general methods involved have been discussed by Dennison,[12] Nielsen,[13] Wilson and Howard,[14] and Wilson.[15]

Triatomic molecules, particularly those containing H or D atoms, afford a good field of study on account of the relative simplicity of the molecular configuration, small number of modes of vibration, possibility of resolving the fine structure of the bands, etc. The bent symmetrical XY_2 or H_2O type molecular model has been treated quite completely by Shaffer and Nielsen[3] (SN) and subsequently Nielsen[16] has interpreted the fine structure of several H_2O bands. The linear symmetrical XY_2 or CO_2 type molecule has been treated by Adel and Dennison[2] and the linear XYZ or HCN type by Nielsen.[11] A complete study of the bent XYZ molecule, to the order of approximation required for analysis of the fine structure of infra-red spectra, has not been reported in the literature. Studies of the normal modes and force constants have been made by Salant and Rosenthal,[17] Van Vleck and Cross,[18] and others; Libby[19] has studied the purely vibrational part of the problem including anharmonic terms. It has seemed advisable, therefore, to make for the bent XYZ model the same type of calculation as that made by SN[3] for the bent XY_2 model in order that the basis may be laid for adequate analysis of the spectral data available on such molecules as HDO, HDS, HDSe, and the like. In this paper the vibration-rotation energy expressions are obtained, to second order of approximation, for the general

[1] E. Fues, Zeits. f. Physik **44**, 91, 110 (1927).
[2] A. Adel and D. M. Dennison, Phys. Rev. **43**, 716 (1933); **44**, 99 (1933).
[3] W. H. Shaffer and H. H. Nielsen, Phys. Rev. **56**, 188 (1939).
[4] W. H. Shaffer, H. H. Nielsen, and L. H. Thomas, Phys. Rev. **56**, 895 (1939); **56**, 1051 (1939).
[5] W. H. Shaffer and S. Silver, J. Chem. Phys. **9**, 599 (1941).
[6] W. H. Shaffer, J. Chem. Phys. **9**, 607 (1941).
[7] W. H. Shaffer and A. H. Nielsen, J. Chem. Phys. **9**, 847 (1941).
[8] W. H. Shaffer, J. Chem. Phys. **10**, 1 (1942).
[9] S. Silver and E. S. Ebers, J. Chem. Phys. **10**, 559 (1942).
[10] S. Silver, J. Chem. Phys. **10**, 565 (1942).
[11] A. H. Nielsen, J. Chem. Phys. **11**, 160 (1943).
[12] D. M. Dennison, Rev. Mod. Phys. **3**, 280 (1931).
[13] H. H. Nielsen, Phys. Rev. **60**, 794 (1941).
[14] E. Bright Wilson, Jr., and J. B. Howard, J. Chem. Phys. **4**, 262 (1936).
[15] E. B. Wilson, Jr., J. Chem. Phys. **4**, 313, 526 (1936); **5**, 617 (1937).
[16] H. H. Nielsen, Phys. Rev. **59**, 565 (1941); **62**, 422 (1942).
[17] E. O. Salant and J. E. Rosenthal, Phys. Rev. **42**, 812 (1932).
[18] J. H. Van Vleck and P. C. Cross, J. Chem. Phys. **1**, 357 (1933).
[19] W. F. Libby, J. Chem. Phys. **11**, 101 (1943).

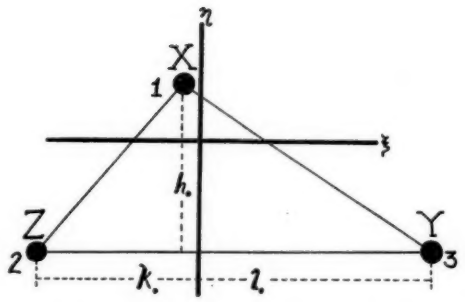

FIG. 1. *Note:* The numerals *2* and *3* in the above cut should be interchanged.

bent XYZ molecular model of which HDO type molecules form a special case.

II. EQUILIBRIUM CONFIGURATION AND COORDINATES

The assumed equilibrium configuration of the general bent XYZ model, shown in Fig. 1, is a triangle of height h_0 and base k_0+l_0. The X atom of mass m_1 is situated at the apex of the triangle, and the Y and Z atoms of masses m_2 and m_3, respectively, are situated at the base corners. In order to specify the equilibrium (vibrationless) positions of the atomic nuclei, a preliminary right-handed body-fixed rectangular coordinate system $\xi\eta\zeta$ is adopted with the molecule lying in the $\xi\eta$ plane, the coordinate origin at the center of mass of the molecule and the ξ axis parallel to the base of the triangle as shown in Fig. 1. The equilibrium coordinates of the various atoms are shown in Table I, where $M=m_1+m_2+m_3$.

A set of principal axes of inertia xyz is adopted for the equilibrium configuration in order to facilitate the investigation of interactions between rotation and vibration. The xyz coordinate system, shown in Fig. 2, has its origin at the center of mass, its z axis coincident with the ζ axis, and its xy axes in the plane of the molecule and making an angle ϵ with the $\xi\eta$ axes. The equilibrium x and y coordinates are given by

$$\begin{aligned} x_{0i} &= \xi_{0i}\cos\epsilon+\eta_{0i}\sin\epsilon, \\ y_{0i} &= -\xi_{0i}\sin\epsilon+\eta_{0i}\cos\epsilon, \end{aligned} \tag{1}$$

where ϵ is so determined that the equilibrium value of the product of inertia,

$$I_{exy}=\sum_i m_i x_{0i}y_{0i},$$

vanishes ($I_{eyz}=I_{ezx}=0$, because $z_{0i}=\zeta_{0i}=0$). It

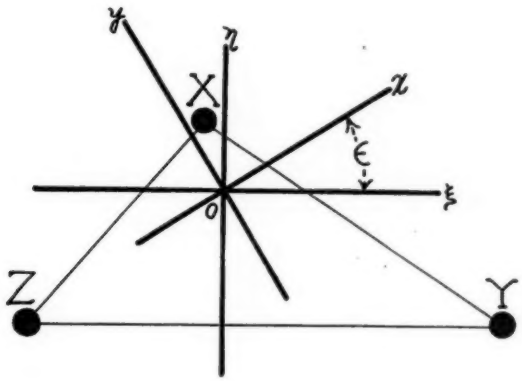

FIG. 2.

follows that

$$\tan 2\epsilon=(A/B), \tag{2}$$

where

$$A=2m_1h_0(m_3k_0-m_2l_0), \tag{2a}$$

$$B=m_3(m_1+m_2)k_0^2+m_2(m_1+m_3)l_0^2 +2m_2m_3k_0l_0-m_1(m_2+m_3)h_0^2. \tag{2b}$$

The equilibrium values of the principal moments of inertia are

$$\begin{aligned} I_{ex} &= (I_{ez}-I')/2, \\ I_{ey} &= (I_{ez}+I')/2, \\ I_{ez} &= [B+2m_1(m_2+m_3)h_0^2]/M \end{aligned} \tag{3}$$

where $I'=\pm(A^2+B^2)^{\frac{1}{2}}/M$.

The principal moments of inertia of the HDO type molecule can be obtained from the above general expressions if one sets $k_0=l_0$.

III. THE NORMAL COORDINATES

The instantaneous positions of the respective atoms during vibration are referred to a body-fixed right-handed rectangular coordinate system xyz, whose origin remains at the center of gravity of the molecule, whose xy plane is the plane of the molecule, and which coincides with the principal axes when the atoms are in their equilibrium positions. The instantaneous position of the ith atom is given by $(x_i, y_i, z_i)=(x_{0i}+x_i', y_{0i}+y_i', z_{0i}+z_i')$, where the primed quantities are rectangular components of displacement from the equilibrium position and where $z_{0i}=z_i'=0$. One can readily choose a set of $3N-6=3$ generalized coordinates, suitable for the study of both the purely vibrational problem and the interactions between rotation and vibration, with

the aid of the Eckart conditions:[14,20]

$$\text{and} \quad \sum_i m_i x_i' = 0, \quad \sum_i m_i y_i' = 0,$$
$$\sum_i m_i (x_{0i} y_i' - y_{0i} y_i' - y_{0i} x_i') = 0.$$

An appropriate set of generalized coordinates, which reduce in the limiting case to those employed in the XY_2 problem,[3,17,21] is

$$\begin{aligned} u_1 &= x_1' - [(m_2 x_2' + m_3 x_3')/(m_2+m_3)], \\ u_2 &= y_1' - [(m_2 y_2' + m_3 y_3')/(m_2+m_3)], \\ u_3 &= x_2' - x_3'. \end{aligned} \tag{4}$$

It follows from the Eckart conditions and Eqs. (4) that

$$\begin{aligned} x_1' &= (\mu/m_1)u_1, \\ x_2' &= -(\mu/(m_2+m_3))u_1 + (\mu'/m_2)u_3, \\ x_3' &= -(\mu/(m_2+m_3))u_1 - (\mu'/m_3)u_3, \\ y_1' &= (\mu/m_1)u_2, \\ y_2' &= (\mu\alpha/m_2)u_2 + (\mu''/m_2)u_1 + (\mu'\gamma/m_2)u_3, \\ y_3' &= (\mu\beta/m_3)u_2 - (\mu''/m_3)u_1 - (\mu'\gamma/m_3)u_3, \end{aligned}$$

TABLE I.

	m_i	i	ξ_{0i}	η_{0i}	ζ_{0i}
X	m_1	1	$(m_3k_0 - m_2l_0)/M$	$(m_2+m_3)h_0/M$	0
Y	m_2	2	$(m_3k_0 + (m_1+m_3)l_0)/M$	$-m_1h_0/M$	0
Z	m_3	3	$(-m_2l_0 + (m_1+m_2)k_0)/M$	$-m_1h_0/M$	0

where

$$\begin{aligned} \mu &= (m_2+m_3)m_1/M, \\ \mu' &= m_2m_3/(m_2+m_3), \\ \mu'' &= m_1y_{01}/(x_{02}-x_{03}), \\ \alpha &= (x_{03}-x_{01})/(x_{02}-x_{03}), \\ \beta &= (x_{02}-x_{01})/(x_{02}-x_{03}), \\ \gamma &= (y_{02}-y_{03})/(x_{02}-x_{03}). \end{aligned}$$

The kinetic energy of vibration of the XYZ molecule is

$$\begin{aligned} T = (1/2)[&\mu_{11}\dot{u}_1^2 + \mu_{22}\dot{u}_2^2 + \mu_{33}\dot{u}_3^2 + 2\mu_{12}\dot{u}_1\dot{u}_2 \\ &+ 2\mu_{13}\dot{u}_1\dot{u}_3 + 2\mu_{23}\dot{u}_2\dot{u}_3], \end{aligned} \tag{6}$$

where

$$\begin{aligned} \mu_{11} &= \mu + (\mu''^2/\mu'), \\ \mu_{22} &= (\mu^2/m_1) + (\mu^2\alpha^2/m_2) - (\mu^2\beta^2/m_3), \\ \mu_{33} &= \mu'(1+\gamma^2), \\ (\mu_{12}/\mu'') &= (\mu_{23}/\mu'\gamma) = (\mu\alpha/m_2) - (\mu\beta/m_3), \\ \mu_{13} &= \mu''\gamma. \end{aligned}$$

The harmonic (quadratic) potential energy function is

$$\begin{aligned} U_0 = (1/2)[&k_{11}u_1^2 + k_{22}u_2^2 + k_{33}u_3^2 \\ &+ 2k_{12}u_1u_2 + 2k_{13}u_1u_3 + 2k_{23}u_2u_3], \end{aligned} \tag{7}$$

where the coefficients k_{11}, etc., are generalized force constants; the special valence form of harmonic potential function is discussed in Section IV for the case of HDO.

The characteristic frequencies ω_k of the normal modes of oscillation are given in wave numbers by

$$\omega_k = (2\pi c)^{-1}\lambda_k^{\frac{1}{2}}; \quad k = 1, 2, 3, \tag{8}$$

where the λ_k are roots of Lagrange's secular determinant,

$$\begin{vmatrix} \mu_{11}\lambda - k_{11} & \mu_{12}\lambda - k_{12} & \mu_{13}\lambda - k_{13} \\ \mu_{12}\lambda - k_{12} & \mu_{22}\lambda - k_{22} & \mu_{23}\lambda - k_{23} \\ \mu_{13}\lambda - k_{13} & \mu_{23}\lambda - k_{23} & \mu_{33}\lambda - k_{33} \end{vmatrix} = 0. \tag{9}$$

The intermediate coordinates, u_1, u_2, and u_3, are given in terms of the normal coordinates Q_k by the relations,

$$\begin{aligned} u_1 &= n_{11}Q_1 + n_{12}Q_2 + n_{13}Q_3, \\ u_2 &= n_{21}Q_1 + n_{22}Q_2 + n_{23}Q_3, \\ u_3 &= n_{31}Q_1 + n_{32}Q_2 + n_{33}Q_3, \end{aligned} \tag{10}$$

in which the coefficients n_{jk} are

$$n_{jk} = N_{jk}/N_k, \tag{11}$$

if N_{jk} is the cofactor of the jk element in Lagrange's determinant (9) with $\lambda = \lambda_k$, ($k = 1, 2, 3$), and

$$N_k = \left\{ \sum_{j=1}^{3} \left[\mu_{jj} N_{jk}^2 + \sum_{j'} \mu_{jj'} N_{jk} N_{j'k} \right] \right\}^{\frac{1}{2}}, \text{ if } j' \neq j.$$

The coefficients n_{jk} can be determined for a particular molecule from the experimental values of λ_k, if there is reason for assuming a potential function U_0 which involves only three force constants or if six force constants can be evaluated from additional data supplied by an isotopic

[20] C. Eckart, Phys. Rev. **47**, 552 (1935).
[21] W. H. Shaffer and R. R. Newton, J. Chem. Phys. **10**, 405 (1942).

molecule; the exact form of the normal modes can be found by combination of Eqs. (5) and (10), in a manner similar to that[21] employed for H_2O and D_2O.

Dimensionless coordinates q_k defined by the relation $q_k=(2\pi c\omega_k/\hbar)^{\frac{1}{2}}Q_k$ are convenient for the quantum-mechanical part of the problem. The energy associated with the normal modes of vibration has the Hamiltonian form

$$H_{0v}=(hc/2)\sum_{k=1}^{3}\omega_k[(p_k^2/h^2)+q_k^2], \quad (12)$$

where $p_k=\partial T/\partial\dot{q}_k$ is the momentum conjugate to q_k.

The cubic and quartic portions of the potential function contain the following terms contributing to the first- and second-order energies:

$$U_1=hc[\beta_{111}q_1^3+\beta_{222}q_2^3+\beta_{333}q_3^3+\beta_{112}q_1^2q_2+\beta_{113}q_1^2q_3+\beta_{221}q_2^2q_1+\beta_{223}q_2^2q_3 +\beta_{331}q_3^2q_1+\beta_{332}q_3^2q_2+\beta_{123}q_1q_2q_3], \quad (13)$$

$$U_2=hc[\gamma_{1111}q_1^4+\gamma_{2222}q_2^4+\gamma_{3333}q_3^4+\gamma_{1122}q_1^2q_2^2+\gamma_{1133}q_1^2q_3^2+\gamma_{2233}q_2^2q_3^2]. \quad (14)$$

IV. VALENCE POTENTIAL FUNCTION FOR HDO

The HDO-type molecule is the special case of the bent XYZ model in which X becomes O, Y becomes H, and Z becomes D. It is reasonable to assume that HDO has the same equilibrium geometrical configuration as H_2O and D_2O, *viz.*, an isosceles triangle with O at the apex. If $\beta_0=2\alpha_0$ and r_0 denote, respectively, the equilibrium values of the apex angle and OH (or OD) distance, it follows that $k_0=l_0=p_0/2=r_0\sin\alpha_0$ and $h_0=r_0\cos\alpha_0$. If $r_2=r_0+\delta r_2$, $r_3=r_0+\delta r_3$, and $p=p_0+\delta p$ denote, respectively, the instantaneous values of the OH, OD, and HD distances, appropriate displacement coordinates for setting up a harmonic potential function of the central-force type are δr_2, δr_3, and δp. If $\beta=\beta_0+\delta\beta$ denotes the instantaneous value of the apex angle, appropriate coordinates for a valence-force potential function are δr_2, δr_3, and $\delta\beta$. The displacement coordinates defined above are, for infinitesimal vibrations, the following functions of the coordinates u_1, u_2, and u_3:

$$\begin{aligned}\delta r_2&=A_1u_1+A_2u_2+A_3u_3,\\ \delta r_3&=B_1u_1+B_2u_2+B_3u_3,\\ \delta\beta&=[C_1u_1+C_2u_2+C_3u_3]/r_0,\\ \delta p&=D_1u_1+D_2u_2+D_3u_3,\end{aligned} \quad (15)$$

where

$$\begin{aligned}A_1&=[(x_{01}-x_{02})-(\mu''/m_2)(y_{01}-y_{02})]/r_0,\\ B_1&=[(x_{01}-x_{03})+(\mu''/m_3)(y_{01}-y_{03})]/r_0,\\ D_1&=(\mu''/\mu')(y_{02}-y_{03})/p_0,\\ C_1&=(r_0/h_0)D_1-(p_0/2h_0)(A_1+B_1),\\ A_2&=\mu(y_{01}-y_{02})[(1/m_1)-(\alpha/m_2)]/r_0,\\ B_2&=\mu(y_{01}-y_{03})[(1/m_1)+(\beta/m_3)]/r_0,\\ D_2&=\mu(y_{02}-y_{03})[(\alpha/m_2)+(\beta/m_3)]/p_0,\\ C_2&=(r_0/h_0)D_2-(p_0/2h_0)(A_2+B_2),\\ A_3&=-(\mu'/m_2)[(x_{01}-x_{02})+\gamma(y_{01}-y_{02})]/r_0,\\ B_3&=(\mu'/m_3)[(x_{01}-x_{03})+\gamma(y_{01}-y_{03})]/r_0,\\ D_3&=[(x_{02}-x_{03})+\gamma(y_{02}-y_{03})]/p_0,\\ C_3&=(r_0/h_0)D_3-(p_0/2h_0)(A_3+B_3).\end{aligned}$$

The complete valence-force potential function U_0 for HDO is

$$U_0=(1/2)[c_1(\langle\delta r_2\rangle^2+\langle\delta r_3\rangle^2)+c_2r_0^2\cos^2\alpha_0\langle\delta\beta\rangle^2+2c_3r_0\cos\alpha_0\delta\beta(\delta r_2+\delta r_3)+2c_4\delta r_2\delta r_3]. \quad (16)$$

The generalized force constants in Eq. (7) are given in terms of the constants in Eq. (16) by the following relations, in which the indices k and k' independently assume the values 1, 2, and 3:

$$k_{kk'}=\{(A_kA_{k'}+B_kB_{k'})c_1+C_kC_{k'}c_2\cos^2\alpha_0+[(A_k+B_k)C_{k'}+(A_{k'}+B_{k'})C_k]c_3\cos\alpha_0 +(A_kB_{k'}+A_{k'}B_k)c_4\}. \quad (17)$$

The constants in the valence potential function and the normal frequencies of HDO can readily be calculated with the aid of Eqs. (9) and (17) if one uses the force constants computed by Shaffer and Newton[21] and molecular dimensions found by Darling and Dennison[22] from the spectra of H_2O and D_2O. The force constants, in units of 10^5 dynes per cm, are $c_1=8.423$, $c_2=2.049$, $c_3=0.4047$ and $c_4=-0.1015$. The molecular dimensions are $r_0=0.9580$A and $\beta_0=2\alpha_0=104°\,31'$. It follows that the angle ϵ defined in Eq. (1) has the value $\epsilon=21°\,5.5'$ for HDO, and $x_{01}=0.07093$A, $x_{02}=0.5667$A, $x_{03}=-0.8469$A, $y_{01}=0.07251$A, $y_{02}=-0.7472$A, $y_{03}=-0.2020$A. The kinetic energy constants defined in Eq. (6) have the following values for HDO (H=1.00813, D=2.01473, O=16.00000) in units of 10^{-24} gram: $\mu_{11}=5.886$, $\mu_{22}=5.814$, $\mu_{33}=1.282$, $\mu_{12}=-1.628$, $\mu_{13}=-0.5256$, and $\mu_{23}=0.5142$. The potential energy constants defined in Eq. (7) have the following values for HDO, in units of 10^5 dynes per cm: $k_{11}=22.67$, $k_{22}=20.56$, $k_{33}=3.934$, $k_{12}=-13.86$, $k_{13}=-3.652$, and $k_{23}=6.873$. Substitution of the above values of constants into Eq. (9) leads to the following values of λ_k, in units of 10^{29} sec.$^{-1}$: $\lambda_1=5.3470$, $\lambda_2=2.8175$, $\lambda_3=0.77551$. The calculated values of the normal frequencies of HDO, $\omega_k=\lambda_k^{\frac{1}{2}}/2\pi c$, are $\omega_1=3882.(2)$ cm^{-1}, $\omega_2=2818.(1)$ cm^{-1}, and $\omega_3=1449.(6)$ cm^{-1}. Libby,[19] using slightly different values of the valence force constants given by Darling and Dennison,[22] has computed $\omega_1=3883.8$ cm^{-1}, $\omega_2=2820.3$ cm^{-1}, and $\omega_3=1449.4$ cm^{-1}. Two observed infra-red bands assigned[23] to HDO have centers at 2720 cm^{-1} and 1403 cm^{-1}.

The constants computed above enable one to compute the following values of the principal equilibrium moments of inertia of HDO, in units of 10^{-40} g-cm^2: $I_{ex}=1.210$, $I_{ey}=3.070$, $I_{ez}=4.280$.

V. THE CLASSICAL ROTATION PROBLEM

The principal axes of inertia for the equilibrium configuration of the bent XYZ model were specified by Eqs. (1) and (2), and the equilibrium values I_{ex}, I_{ey}, and I_{ez}, of the principal moments of inertia were given in Eq. (3). The instantaneous values, during vibration, of the moments and products of inertia are:

$$\begin{aligned}
I_x&=I_{ex}\left\{1+\sum_{k=1}^{3}\left[a_k'q_k+a_{kk}'q_k^2+\sum_{k<k'=2}^{3}a_{kk'}'q_kq_{k'}\right]\right\},\\
I_y&=I_{ey}\left\{1+\sum_{k=1}^{3}\left[b_k'q_k+b_{kk}'q_k^2+\sum_{k<k'=2}^{3}b_{kk'}'q_kq_{k'}\right]\right\},\\
I_z&=I_{ez}\left\{1+\sum_{k=1}^{3}\left[c_k'q_k+c_{kk}'q_k^2+\sum_{k<k'=2}^{3}c_{kk'}'q_kq_{k'}\right]\right\},\\
I_{xy}&=I_{ex}^{\frac{1}{2}}I_{ey}^{\frac{1}{2}}\left\{\sum_{k=1}^{3}\left[d_k'q_k+d_{kk}'q_k^2+\sum_{k<k'=2}^{3}d_{kk'}'q_kq_{k'}\right]\right\},
\end{aligned} \quad (18)$$

in which, if $\tau=(h/2\pi c)$,

$$a_k=\omega_k^{\frac{1}{2}}a_k'=4\tau^{-\frac{1}{2}}A_e[8m_1y_{01}n_{1k}+\mu(y_{01}+\alpha y_{02}-\beta y_{03})+2\mu'\gamma(y_{01}-y_{03})n_{3k}],$$

$$b_k=\omega_k^{\frac{1}{2}}b_k'=4\tau^{-\frac{1}{2}}B_e[m_1x_{01}n_{1k}+\mu'(x_{02}-x_{03})n_{3k}],$$

$$c_k=\omega_k^{\frac{1}{2}}c_k'=C_e[(a_k/A_e)+(b_k/B_e)],$$

$$d_k=\omega_k^{\frac{1}{2}}d_k'=4\tau^{-\frac{1}{2}}A_e^{\frac{1}{2}}B_e^{\frac{1}{2}}[m_1y_{01}n_{1k}+\mu'(y_{02}-y_{03})n_{3k}],$$

[22] B. T. Darling and D. M. Dennison, Phys. Rev. **57**, 128 (1940).
[23] Ta-You Wu, *Vibrational Spectra and Structure of Polyatomic Molecules* (Prentice-Hall, Inc., New York, 1940).

$$a_{kk'}=\omega_k^{\frac{1}{2}}\omega_{k'}^{\frac{1}{2}}a'_{kk'}=2A_e[(\mu''^2/\mu')n_{1k}n_{1k'}+\mu_{22}n_{2k}n_{2k'}+\mu'\gamma^2n_{3k}n_{3k'}$$
$$+\mu_{12}(n_{1k}n_{2k'}+n_{2k}n_{1k'})+\mu_{23}(n_{2k}n_{3k'}+n_{3k}n_{2k'})+\mu_{13}(n_{1k}n_{3k'}+n_{3k}n_{1k'})],$$

$$b_{kk'}=\omega_k^{\frac{1}{2}}\omega_{k'}^{\frac{1}{2}}b'_{kk'}=2B_e[\mu n_{1k}n_{1k'}+\mu' n_{3k}n_{3k'}],$$

$$c_{kk}=\omega_k c'_{kk'}-2C_e\sum_{k'\neq k}\zeta^2_{kk'}=C_e[(a_{kk}/A_e)+(b_{kk}/B_e)],$$

$$c_{kk'}=\omega_k^{\frac{1}{2}}\omega_{k'}^{\frac{1}{2}}c'_{kk'}+4C_e\sum_{k''}\zeta_{kk''}\zeta_{k'k''}=C_e[(a_{kk'}/A_e)+(b_{kk'}/B_e)],$$

if
$$d_{kk'}=2A_e^{\frac{1}{2}}B_e^{\frac{1}{2}}[\mu(n_{1k}n_{2k'}+n_{2k}n_{1k'})+\mu''(n_{1k}n_{3k'}+n_{3k}n_{1k'})+\mu'''(n_{2k}n_{3k'}+n_{3k}n_{2k'})+2\mu'\gamma n_{3k}n_{3k}],$$
$$\zeta_{kk'}=-\zeta_{k'k}=\mu(n_{1k}n_{2k'}-n_{2k}n_{1k'})+\mu''(n_{3k}n_{1k'}-n_{1k}n_{3k'})+\mu'''(n_{3k}n_{2k'}-n_{2k}n_{3k'}),$$
$$\mu'''=m_1x_{01}/(x_{03}-x_{02}),$$

and the equilibrium values of the rotational constants are

$$A_e=(h/8\pi^2cI_{ex}),\quad B_e=(h/8\pi^2cI_{ey}),\quad C_e=(h/8\pi^2cI_{ez}).$$

The quantities a_{kk}, b_{kk}, and d_{kk} are obtained, respectively, from $a_{kk'}$, $b_{kk'}$, and $d_{kk'}$ by setting $k'=k$. It follows from the definitions of c_k and $c_{kk'}$, that

$$(c_k/C_e)-(a_k/A_e)-(b_k/B_e)=0\quad\text{and}\quad(c_{kk'}/C_e)-(a_{kk'}/A_e)-(b_{kk'}/B_e)=0. \tag{20}$$

The vibrational angular momentum of the bent XYZ model has only a z component, different from zero,

$$p_z=\sum\zeta_{kk'}[(\omega_{k'}/\omega_k)^{\frac{1}{2}}q_kp_{k'}-(\omega_k/\omega_{k'})^{\frac{1}{2}}q_{k'}p_k]. \tag{21}$$

If the rotating vibrating XYZ molecular model is considered as a semirigid rotator with an internal flywheel, its rotational energy is given in the classical Hamiltonian form by

$$H_{\text{rot}}=(1/2)\{\mu_{xx}P_x^2+\mu_{yy}P_y^2+\mu_{zz}(P_z-p_z)^2+2\mu_{xy}P_xP_y\}, \tag{22}$$

where P_x, P_y, and P_z are components of total angular momentum, p_z is the internal angular momentum, and, to second order of approximation,

$$\mu_{xx}=I_{ex}^{-1}\{1-\sum_k[a_k'q_k-(a_k'^2-a'_{kk}+d_k'^2)q_k^2]\},$$
$$\mu_{yy}=I_{ey}^{-1}\{1-\sum_k[b_k'q_k-(b_k'^2-b'_{kk}+d_k'^2)q_k^2]\},$$
$$\mu_{zz}=I_{ez}^{-1}\{1-\sum_k[c_k'q_k-(c_k'^2-c'_{kk})q_k^2]\},$$
$$\mu_{xy}=I_{ex}^{-\frac{1}{2}}I_{ey}^{-\frac{1}{2}}\{\sum_k[d_k'q_k+(d'_{kk}-a_k'd_k'-b_k'd_k')q_k^2]\}.$$

(Quadratic cross-product terms have been omitted from the above expressions because they do not ordinarily contribute to the first- or second-order energies.)

VI. THE QUANTUM-MECHANICAL HAMILTONIAN

The appropriate quantum-mechanical Hamiltonian for investigation of the rotation-vibration problem of the bent XYZ molecular model can be set up according to the method of Wilson and Howard[14] and has the following zero-, first-, and second-order parts which can contribute to the allowed energy expressions to second order of approximation:

$$H_0=(hc/2)\sum_{k=1}^{3}\omega_k[(p_k^2/\hbar^2)+q_k^2]+(hc/\hbar^2)[A_eP_x^2+B_eP_y^2+C_eP_z^2], \tag{23}$$

$$H_1 = U_1 - (p_z P_z / I_{ez}) - (hc/\hbar^2) \sum_{k=1}^{3} \{q_k[a_k' A_e P_x^2 + b_k' B_e P_y^2 + c_k' C_e P_z^2 - d_k' A_e^{\frac{1}{2}} B_e^{\frac{1}{2}} (P_x P_y + P_y P_x)]\}, \quad (24)$$

$$H_2 = U_2 + (hc/\hbar^2)[C_e p_z^2] + (hc/\hbar^2) \sum_{k=1}^{3} \{q_k^2[(a_k'^2 - a_{kk}' + d_k'^2) A_e P_x^2 + (b_k'^2 - b_{kk}' + d_k'^2) B_e P_y^2 + (c_k'^2 - c_{kk}') C_e P_z^2 + (d_{kk}' - a_k' d_k' - b_k' d_k') A_e^{\frac{1}{2}} B_e^{\frac{1}{2}} (P_x P_y + P_y P_x)]\}. \quad (25)$$

Certain lengthy terms, which usually occur in H_1 and H_2, have been omitted from Eqs. (24) and (25) because they either have no effect on the energies to second order of approximation or affect only the constant term hcG_0 in the final energy expression (28).

The perturbation calculation required for the evaluation of the eigenvalues of the Hamiltonian is simplified by a contact transformation, $H' = THT^{-1}$, of the type described by Thomas[24] and others,[4–10,12] where $T = e^{i\lambda S}$ $(i = \sqrt{-1})$ and $H_0' = H_0$, $H_1' = H_1 + i(SH_0 - H_0 S)$, and $H_2' = H_2 + (i/2)[S(H_1 + H_1') - (H_1 + H_1')S]$. In the cases where there are no vibrational degeneracies, real or accidental, it is possible to set up a function S which reduces H_1' to zero and the perturbation calculation involves only the evaluation of the eigenvalues of H_0' and H_2'. For the bent XYZ model, H_2' has the following form (each of the subscripts k, k', and k'' can assume the values 1, 2, and 3, but in a given coefficient $k \neq k'$, $k' \neq k''$, $k'' \neq k$):

$$H_2' = hc\left\{\sum_k \left[\gamma'_{kkk'k'} q_k^4 + \sum_{k'} \gamma'_{kkk'k'} q_k^2 q_{k'}^2\right] + \sum_k (q_k^2/\hbar^2)[\alpha_k A_e P_x^2 + \beta_k B_e P_y^2 + \gamma_k C_e P_z^2 + \delta_k A_e^{\frac{1}{2}} B_e^{\frac{1}{2}} (P_x P_y + P_y P_x)] + (1/\hbar^2)[C_e p_z^2]\right\} + H_{2c}' \quad (26)$$

where H_{2c}', the second-order energy correction associated with centrifugal stretching, has the form

$$H_{2c}' = -(hc/\hbar^4)[\tau_{xxxx} P_x^4 + \tau_{yyyy} P_y^4 + \tau_{zzzz} P_z^4 + \tau_{xxyy}(P_x^2 P_y^2 + P_y^2 P_x^2) + \tau_{xxzz}(P_x^2 P_z^2 + P_z^2 P_x^2) + \tau_{yyzz}(P_y^2 P_z^2 + P_z^2 P_y^2) + \tau_{xyxy}(P_x P_y + P_y P_x)^2 - (\tau_{xxxy} P_x^2 + \tau_{yyyx} P_y^2 + \tau_{zzzy} P_z^2)(P_x P_y + P_y P_x) - (P_x P_y + P_y P_x)(\tau_{xxxy} P_x^2 + \tau_{yyyx} P_y^2 + \tau_{zzzy} P^2)], \quad (27)$$

if

$$\gamma'_{kkkk} = \left[\gamma_{kkkk} - (5\beta_{kkk}^2/2\omega_k) - \sum_{k'} (8\omega_k^2 - 3\omega_{k'}^2)(\beta_{kkk'}^2/2\omega_{k'})/(4\omega_k^2 - \omega_{k'}^2)\right],$$

$$\gamma'_{kkk'k'} = [\gamma_{kkk'k'} - (2\omega_k \beta_{kkk'}^2/(4\omega_k^2 - \omega_{k'}^2)) - (2\omega_{k'} \beta_{k'k'k}/(4\omega_{k'}^2 - \omega_k^2)) - (3\beta_{kkk}\beta_{kkk'}/\omega_k) - (3\beta_{k'k'k'}\beta_{k'k'k}/\omega_{k'}) - (\beta_{kkk''}\beta_{k'k'k''}/\omega_{k''}) - (\omega_{k''}^2 - \omega_k^2 - \omega_{k'}^2)(\omega_{k''}\beta_{123}^2/2D_{123})],$$

$$D_{123} = (\omega_1 + \omega_2 + \omega_3)(\omega_1 - \omega_2 - \omega_3)(\omega_1 - \omega_2 + \omega_3)(\omega_1 + \omega_2 - \omega_3),$$

$$\alpha_k = [(a_k^2 - a_{kk} + d_k^2)/\omega_k) + (3a_k\beta_{kkk}/\omega_k^{\frac{1}{2}}) + \sum_{k'} (a_{k'}\beta_{kkk'}/\omega_{k'}^{\frac{1}{2}})],$$

$$\beta_k = [((b_k^2 - b_{kk} + d_k^2)/\omega_k) + (3b_k\beta_{kkk}/\omega_k^{\frac{1}{2}}) + \sum_{k'} (b_{k'}\beta_{kkk'}/\omega_{k'}^{\frac{1}{2}})],$$

$$\gamma_k = [((c_k^2 - c_{kk})/\omega_k) + (3c_k\beta_{kkk}/\omega_k^{\frac{1}{2}}) + \sum_{k'} (c_{k'}\beta_{kkk'}/\omega_{k'}^{\frac{1}{2}}) + 2C_e \sum_{k'} (3\omega_k^2 + \omega_{k'}^2)(\zeta_{kk'}^2/\omega_k)/(\omega_k^2 - \omega_{k'}^2)],$$

$$\delta_k = [(d_{kk} - a_k d_k - b_k d_k)/\omega_k],$$

$$\tau_{xxxx} = A_e^2 \sum_k (a_k^2/2\omega_k^2), \qquad \tau_{yyyy} = B_e^2 \sum_k (b_k^2/2\omega_k^2),$$

$$\tau_{zzzz} = C_e^2 \sum_k (c_k^2/2\omega_k^2), \qquad \tau_{xxyy} = A_e B_e \sum_k (a_k b_k/2\omega_k^2),$$

$$\tau_{xxzz} = A_e C_e \sum_k (a_k c_k/2\omega_k^2), \qquad \tau_{yyzz} = B_e C_e \sum_k (b_k c_k/2\omega_k^2),$$

$$\tau_{xyxy} = A_e B_e \sum_k (d_k^2/2\omega_k^2), \qquad \tau_{xxxy} = A_e^{\frac{1}{2}} B_e^{\frac{1}{2}} \sum_k (a_k d_k/2\omega_k^2),$$

$$\tau_{yyyx} = A_e^{\frac{1}{2}} B_e^{\frac{1}{2}} \sum_k (b_k d_k/2\omega_k^2), \qquad \tau_{zzzy} = A_e^{\frac{1}{2}} B_e^{\frac{1}{2}} C_e \sum_k (c_k d_k/2\omega_k^2).$$

Inspection of Eq. (26) shows that resonance degeneracy can occur in any of the following cases: $2\omega_k \cong \omega_{k'}$, $\omega_k \cong \omega_{k'} + \omega_{k''}$ or $\omega_k \cong \omega_{k'}$. In such a case, the term from which it arises cannot be removed

[24] L. H. Thomas, J. Chem. Phys. **10**, 532, 538 (1942).

from H_1' by the contact transformation and a degenerate perturbation calculation is required to evaluate its effect on the energy.

VII. THE ALLOWED ENERGIES

The allowed values of H_0 and H_2 have been determined by a method similar to that employed by SN[3] for the bent XY_2 model. The first step in the procedure is the evaluation of the general matrix element of $H_0'+H_2'$ which is diagonal in all the vibrational quantum numbers, while the angular momentum operators are considered as constants. The result can be written in the form $E_{\text{vib}}+H_R$, where $E_{\text{vib}}=hcG$ contains all the terms in the energy which are independent of rotational quantum numbers and H_R is a form of the Hamiltonian for an asymmetric rotator with the equilibrium rotational constants replaced by values effective in the respective vibrational states and with the addition of centrifugal stretching terms.

The vibrational term G is given by

$$G=G_0+\sum_k\left[\omega_k(v_k+\tfrac{1}{2})+G_{kk}(v_k+\tfrac{1}{2})^2+\sum_{k'>k}G_{kk'}(v_k+\tfrac{1}{2})(v_{k'}+\tfrac{1}{2})\right] \tag{28}$$

where

$$G_0=(1/16)\sum_k\left[6\gamma_{kkkk}-(7\beta_{kkk}^2/\omega_k)+(3\omega_{k'}\beta_{kkk'}^2/(4\omega_k^2-\omega_{k'}^2))-(4\omega_1\omega_2\omega_3\beta_{123}^2/D_{123})\right]$$

$$+(1/4)\sum_k\left[a_{kk}+b_{kk}+c_{kk}+a_kb_k+b_kc_k+c_ka_k-d_k^2-(3/8)(a_k+b_k+c_k)^2-2C_e\sum_{k'>k}\zeta_{kk'}^2\right],$$

$$G_{11}=(1/4)[6\gamma_{1111}-15(\beta_{111}^2/\omega_1)-E_{12}(\beta_{112}^2/\omega_2)-E_{13}(\beta_{113}^2/\omega_3)],$$

$$G_{22}=(1/4)[6\gamma_{2222}-15(\beta_{222}^2/\omega_2)-E_{21}(\beta_{221}^2/\omega_1)-E_{23}(\beta_{223}^2/\omega_3)],$$

$$G_{33}=(1/4)[6\gamma_{3333}-15(\beta_{333}^2/\omega_3)-E_{31}(\beta_{331}^2/\omega_1)-E_{32}(\beta_{332}^2/\omega_2)],$$

$$G_{12}=\gamma_{1122}-3(\beta_{111}\beta_{221}/\omega_1)-3(\beta_{222}\beta_{112}/\omega_2)-(\beta_{113}\beta_{223}/\omega_3)$$
$$-F_{12}(\beta_{112}^2/\omega_1)-F_{21}(\beta_{221}^2/\omega_2)-C_{312}(\beta_{123}^2/\omega_3)+K_{12}\zeta_{12}^2C_e,$$

$$G_{23}=\gamma_{2233}-3(\beta_{222}\beta_{332}/\omega_2)-3(\beta_{333}\beta_{223}/\omega_3)-(\beta_{331}\beta_{221}/\omega_1)$$
$$-F_{23}(\beta_{223}^2/\omega_2)-F_{32}(\beta_{332}^2/\omega_3)-C_{123}(\beta_{123}^2/\omega_1)+K_{23}\zeta_{23}^2C_e,$$

$$G_{31}=\gamma_{3311}-3(\beta_{333}\beta_{331}/\omega_3)-3(\beta_{111}\beta_{113}/\omega_1)-(\beta_{112}\beta_{332}/\omega_2)$$
$$-F_{13}(\beta_{113}^2/\omega_1)-F_{31}(\beta_{331}^2/\omega_3)-C_{231}(\beta_{123}^2/\omega_2)+K_{31}\zeta_{31}^2C_e,$$

if

$$E_{kk'}=[(8\omega_k^2-3\omega_{k'}^2)/(4\omega_k^2-\omega_{k'}^2)],$$
$$F_{kk'}=[2\omega_k^2/(4\omega_k^2-\omega_{k'}^2)],$$
$$C_{kk'k''}=[\omega_k^2(\omega_k^2-\omega_{k'}^2-\omega_{k''}^2/2D_{123}],$$
$$K_{kk'}=[(\omega_k^2+\omega_{k'}^2)/\omega_k\omega_{k'}].$$

The effective rotational Hamiltonian H_R is

$$H_R=(hc/h^2)\{A_VP_x^2+B_VP_y^2+C_VP_z^2+D_V(P_xP_y+P_yP_x)\}+H_{2c}', \tag{29}$$

where H_{2c}' is the term defined in Eq. (27) and

$$\begin{aligned}A_V&=A_e[1+\textstyle\sum_k\alpha_k(v_k+\tfrac{1}{2})],\\ B_V&=B_e[1+\textstyle\sum_k\beta_k(v_k+\tfrac{1}{2})],\\ C_V&=C_e[1+\textstyle\sum_k\gamma_k(v_k+\tfrac{1}{2})],\\ D_V&=A_e^{\frac{1}{2}}B_e^{\frac{1}{2}}\textstyle\sum_k\delta_k(v_k+\tfrac{1}{2}),\end{aligned} \tag{29a}$$

if α_k, β_k, γ_k, δ_k, τ_{zzzz}, etc., are quantities in connection with Eqs. (26) and (27).

It follows from Eqs. (29a) and (20) that the quantity $\Delta=[(1/C_V)-(1/A_V)-(1/B_V)]$ is independent of the anharmonic constants, to second order of approximation, and has the value

$$\Delta=\sum_k \omega_k^{-1}[c_k^2 I_{ez}-(b_k^2+d_k^2)I_{ey}-(a_k^2+d_k^2)I_{ex}]. \tag{30}$$

A similar relation has been found to hold for the bent XY_2 model by Darling and Dennison[21] and for the planar XY_3 model by Shaffer and Silver;[5] such a relation does not appear to hold for non-planar molecules.[6]

The secular determinant for evaluation of the allowed values of H_R is similar to the Wang[25] secular determinant for the asymmetric rigid rotator, and like that proposed by SN[3] for the semirigid bent XY_2 model. If the wave functions for the symmetric rigid rotator are used as basic functions for the expansion of the rotational wave functions of the bent XYZ model, the secular determinant is

$$|(JKM|H_R|JK'M)-E_R\delta_{kk'}|=0, \tag{31}$$

where J, K, and M are the usual quantum numbers associated, respectively, with total angular momentum $[P^2=J(J+1)\hbar^2]$, component of angular momentum along the rotator's symmetry axis $[P_z=K\hbar]$, and component along the direction of a magnetic field $[P_F=M\hbar]$; J is a positive integer, $K=0, \pm1, \cdots, \pm J$, and $M=0, \pm1, \pm2, \cdots, \pm J$. The appropriate matrix elements for setting up the secular determinant (31) have been given by SN[3], are all diagonal in J and M, and have values independent of M. It is necessary to solve a $2J+1$-fold determinant for each value of J with the elements,

$$(K|H_R|K)-E_R=hc\{R_1+R_2K^2+R_3K^4\}-E_R, \tag{31a}$$

$$(K|H_R|K\pm2)=hc\{(R_4\pm iR_4')+2(R_5\pm iR_5')(K^2\pm2K+2)\}[f-K(K\pm1)]^{\frac{1}{2}}[f-(K\pm1)(K\pm2)]^{\frac{1}{2}}, \tag{31b}$$

$$(K|H_R|K\pm4)=hc(R_6\pm iR_6')[f-K(K\pm1)]^{\frac{1}{2}}[f-(K\pm1)(K\pm2)]^{\frac{1}{2}}[f-(K\pm2)(K\pm3)]^{\frac{1}{2}}\times[f-(K\pm3)(K\pm4)]^{\frac{1}{2}}, \tag{31c}$$

where

$$i=(-1)^{\frac{1}{2}}, \quad f=J(J+1),$$

$$R_1=(f/2)(A_V+B_V)+(f/4)(\tau_{xxxx}+\tau_{yyyy}-2\tau_{xxyy}+4\tau_{xyxy}]-(f^2/8)[3\tau_{xxxx}+3\tau_{yyyy}+2\tau_{xxyy}+4\tau_{xyxy}],$$

$$R_2=(1/2)(2C_V-B_V-A_V)-(5/8)[\tau_{xxxx}+\tau_{yyyy}-2\tau_{xxyy}+4\tau_{xyxy}]+(f/4)[3\tau_{xxxx}+3\tau_{yyyy}+2\tau_{xxyy}-4\tau_{xxxz}-4\tau_{yyyz}+4\tau_{xyxy}],$$

$$R_3=(1/8)[-3\tau_{xxxx}-3\tau_{yyyy}-8\tau_{zzzz}-2\tau_{xxyy}+8\tau_{xxzz}+8\tau_{yyzz}-4\tau_{xyxy}],$$

$$R_4=(1/4)(A_V-B_V)-(f/4)(\tau_{xxxx}-\tau_{yyyy}),$$

$$R_4'=(1/2)[D_V+f(\tau_{xxzy}+\tau_{yyyz})],$$

$$R_5=(1/8)[\tau_{xxxx}-\tau_{yyyy}-2\tau_{xxzz}+2\tau_{yyzz}],$$

$$R_5'=(1/4)[2\tau_{zzzy}-\tau_{xxzy}-\tau_{yyyz}],$$

$$R_6=(1/16)[-\tau_{xxxx}-\tau_{yyyy}+2\tau_{xxyy}+4\tau_{xyxy}],$$

$$R_6'=(1/4)[\tau_{xxxy}-\tau_{yyyz}].$$

The complex character of the off-diagonal elements defined in Eqs. (31b) and (31c) is associated with the complete lack of point symmetry in the configuration of the bent XYZ model. The secular determinant for each value of J can be factored into four parts, in general, and expanded in the manner discussed by SN[3] and Nielsen[15] for the bent XY_2 model.

The total rotation-vibration energy of the bent XYZ model can be written in term-value form, to second order of approximation, as

$$E=hc(G+F), \tag{32}$$

[25] S. C. Wang, Phys. Rev. **34**, 243 (1929).

where $G=E_V/hc$ is the vibrational term given in Eq. (28) and $F=E_R/hc$, if E_R is a root of the secular determinant (31). The selection rules allow all possible vibrational transitions because of the asymmetry of the molecular configuration. The selection rules for the rotational transitions and the calculations of the intensities of the rotational lines in the bands of asymmetric molecules have been discussed by Dennison,[11] Nielsen,[15] and others.

THE JOURNAL OF CHEMICAL PHYSICS VOLUME 12, NUMBER 12 DECEMBER, 1944

Electrical Anisotropy of Xerogels of Hydrophile Colloids. Part II*†

S. E. SHEPPARD AND P. T. NEWSOME
Eastman Kodak Company, Rochester, New York

(Received October 5, 1944)

An improved, though still relative, quantitative expression has been derived for the electrical anisotropy E. A. The E. A. is a linear function of the elongation up to a certain limit, as is also the optical birefringence. The relation of electrical to optical anisotropy has been studied in greater detail. A more critical discussion in terms of atomic model structures is given of the hypothesis that E. A. in the compounds studied is due to the formation of continuous parallel chains of hydrogen bridges, having electronically conducting character. The materials studied were: polyvinyl acetate and its hydrolyzed stages down to polyvinyl alcohol, cellulose acetate and its hydrolyzed stages down to (hydrate) cellulose.

IN Part I the electrical anisotropy was expressed quantitatively in a quite relative form as ϕ/V^2h, where ϕ is the angle of rotation (from 45° as rest) by a field V, for a cylinder of unit radius and thickness h.**

MODIFICATION OF THE QUANTITATIVE EXPRESSION

It has been observed that the effect, for a disk not too large compared with the electrode, or pole-piece diameters, is an inverse linear function of the square of the distance between them, confirming the proportionality to V^2. Further, it is found that the effect, other things being equal, is proportional to r^3 where r is the radius (cf. Fig. 1). Thus, it is proportional to the volume hr^2, of the cylinder or disk, and again to the radius r, as defining the torque on the dipole of effective charge separation $2r$. To compare substances of different (monomeric) molecular weight, we can advance to the expression:

$$\text{E. A.}=K\cdot f(\Delta l/l)hr^3V^2d/M_m,$$

where K is an apparatus constant which can also include Avogadro's constant, r = radius in cm, h = thickness, $f(\Delta l/l)$ is a function of the *elongation*, which reduces to proportionality for a certain range, V = voltage, d = specific gravity, and M_m = "equivalent" monomeric molecular weight.*

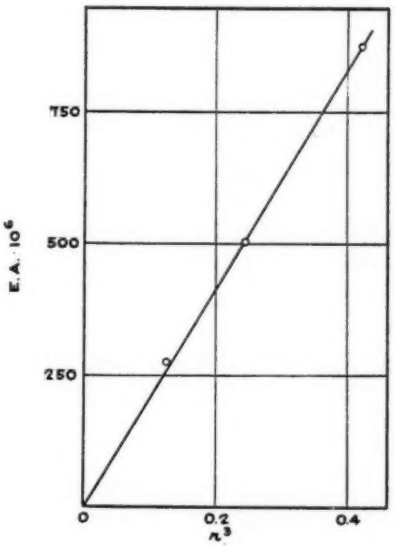

FIG. 1. Variation of electrical anisotropy of polyvinyl alcohol with the radius of the disk (200 percent elongation).

* Presented in the inaugural program of the Division of High-Polymer Physics, American Physical Society, Rochester, New York, June 23–24, 1944. For Part I, see J. Chem. Phys. 12, 244 (1944).

† Communication No. 997 from the Kodak Research Laboratories.

** Instead of t, used in Part I.

* E.g., $C_2(OH)$ for polyvinyl alcohol, $C_6(OH)_3$ for cellulose.

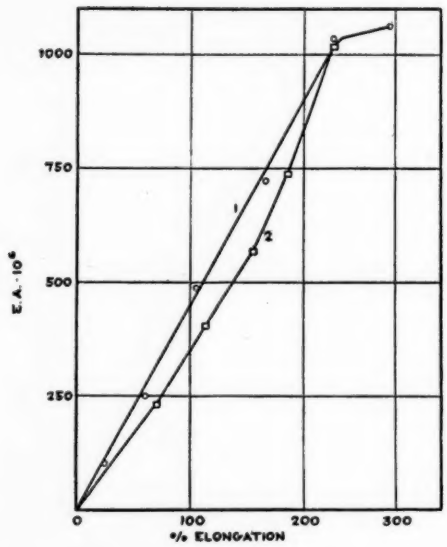

FIG. 2. Effect of elongation on electrical orientation of polyvinyl alcohol. 1. High viscosity. 2. Low viscosity.

ELONGATION

Since, usually, internal orientation or "fibering" has been produced by stretching, the relation of E. A. to the amount of elongation to which the material has been subjected is important. This will be discussed in greater detail later; at this point it suffices to state that over a certain range, and with certain conditions maintained constant, the E. A. appears proportional to the actual elongation $\Delta l/l$, which, usually, will be expressed as a percentage. This is illustrated in Fig. 2. Fuller confirmation of the proportionality, up to some kind of elastic limit, is shown by the relation of the optical birefringence to the E. A.

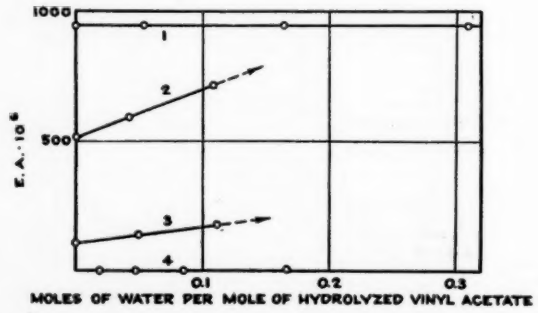

FIG. 3. Effect of water content on the electrical anisotropy of polyvinyl acetates at 225 percent elongation. 1. Polyvinyl alcohol. 2. Hydrolyzed polyvinyl acetate (73 percent polyvinyl alcohol). 3. Hydrolyzed polyvinyl acetate (35 percent polyvinyl alcohol). 4. Polyvinyl acetate.

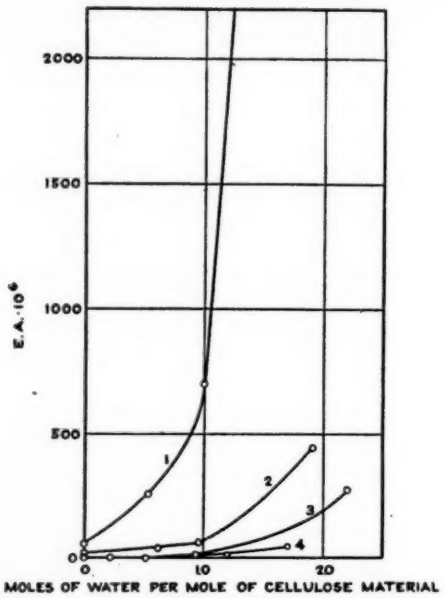

FIG. 4. Effect of water content on the electrical anisotropy of cellulose materials. 1. Cellulose, 0. 2. Cellulose acetate, 24.5 percent acetyl. 3. Cellulose acetate, 40.0 percent acetyl. 4. Cellulose acetate, 44.5 percent acetyl.

on the one hand, and to the elongation on the other (*vide supra*). These relations—of the linear regime to that beyond—are undoubtedly of great interest for the problems of structure and elasticity, but for the present we shall disregard them and confine ourselves to comparison of materials at corresponding stages of elongation —and in which, for the present, only "frozen in" states are considered.

MATERIALS

Previously, it was found that only colloids containing autonomic hydroxyl, or perhaps an equivalent amino-group, as in proteins, were reactive. It was further observed that polyvinyl alcohol was reactive independently of moisture content, within measurable limits. At this stage, therefore, attention was largely concentrated on materials of the two macromolecular series:

1. Polyvinyl acetate↔polyvinyl alcohol.
2. Cellulose triacetate↔cellulose.

INFLUENCE OF ADSORBED WATER (MOISTURE REGAIN)

Neither fully acetylated polyvinyl acetate, nor "cellulose triacetate," shows more than a trace of

response at any humidity. Very slight residual effects at high humidity might be due to "spots" of incomplete esterification. With polyvinyl acetate there is practically no effect of moisture at either extreme of composition, but there is a definite sensitivity for intermediate, partly acetylated or deacetylated materials (cf. Fig. 3). With cellulose, while there is practically no effect of water upon the "triacetate," there is a steadily increasing effect on deacetylating, no maximum being reached, but the greatest effect occurring with cellulose itself (cf. Fig. 4).

Actually, the range of water adsorption—in terms of vapor pressure or relative humidity—which could be studied was limited by the rigidity of the sample. Above a certain value the disk becomes flabby and badly distorted. Even before this, the adsorption of water tends to a deformation, and there occurs swelling and dilation principally transverse to the direction of stretch, as shown in previous studies on gelatin.[1] The over-all behavior is therefore represented by that shown in Fig. 5 (for gelatin). The transverse expansion introduces a "form" anisotropy which first counteracts and then surpasses the internal anisotropy.

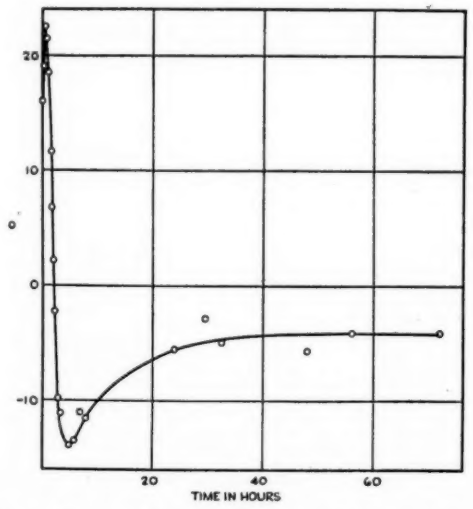

FIG. 5. Change of E. A. of gelatin with time at 95 percent R. H. due to unequal swelling along and across direction of elongation. *Note:* The open circle shown to the left of the above figure should be ϕ.

[1] S. E. Sheppard and J. G. McNally, *Colloid Symposium Annual* (John Wiley & Sons Inc., New York, 1930), Vol. VII, p. 17.

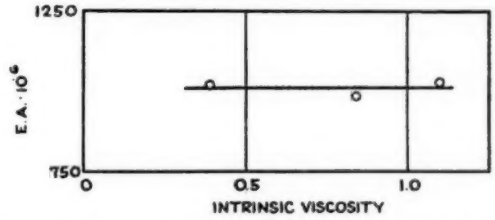

FIG. 6. Relation of E. A. to intrinsic viscosity (chain length) of polyvinyl alcohol samples.

EFFECT OF MOLECULAR WEIGHT OR CHAIN LENGTH

A number of polyvinyl alcohol samples having, according to measurements of their specific viscosities, considerably different average molecular weights, was examined. It appeared (cf. Fig. 6) that the E. A. is independent of the mean molecular weight and chain length, at any rate over a considerable range.

CORRELATION OF ELECTRICAL ANISOTROPY WITH OPTICAL BIREFRINGENCE

In Part I definite birefringence measurements were educed as evidence of "fibering," of macromolecular orientation, for the sheets examined. This relation has been studied in greater detail.

As noted, with increasing elongation, the E. A. of polyvinyl alcohol increases regularly—and approximately linearly—up to about 250 percent, when the rate of increase of E. A. appears to decrease rather sharply (cf. Fig. 2). The optical birefringence was also observed to increase at first linearly with the elongation, but then a nonlinear region, with indications of approach to a limit, supervened (cf. Fig. 7). For the primary linear relation between the E. A. and the optical birefringence for the same material, see Fig. 8.

What has just been said applies only to the hydrophile colloids which manifest the property of electrical anisotropy, and not to the purely organophile ones, such as cellulose triacetate, or polyvinyl chloride which become birefringent on elongation, but not electrically anisotropic. Moreover, while in most cases the optical birefringence is *positive*, in the sense that $n_\gamma > n_\beta$, where the maximum index n_γ is in the direction of the elongation, this is not necessarily the case. Examples were noted in Part I where n_γ could be perpendicular to the plane of the sheet, and

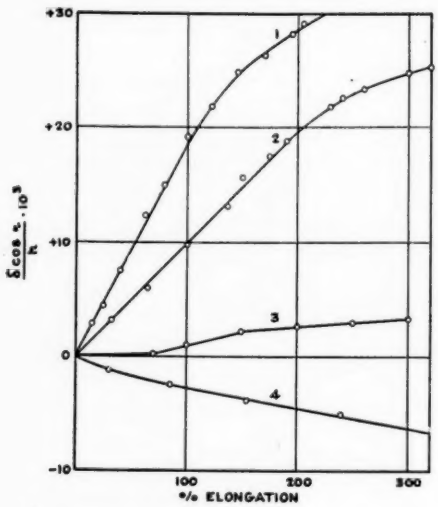

FIG. 7. Influence of elongation on the birefringence of polyvinyl alcohol and polyvinyl acetates. 1. Polyvinyl alcohol. 2. Hydrolyzed polyvinyl acetate (73 percent polyvinyl alcohol). 3. Hydrolyzed polyvinyl acetate (35 percent polyvinyl alcohol). 4. Polyvinyl acetate.

it could happen that it would be in the plane of the sheet, but approaching a perpendicular direction to the axis of stretch. Such conditions occur, with higher alkyl esters of cellulose[2] and with polyvinyl acetate, when alignment of optical density, by side chains, may be greater transverse to the backbone spacings of the chain molecules. With partly hydrolyzed polyvinyl acetate, the optical birefringence $n_\gamma - n_\beta$ decreases with decreasing —OH content from positive to negative, going through a zero value at about 6 percent hydroxyl (cf. Fig. 9).

DISCUSSION

The change from a well-marked *linear* relation (over a considerable range) to a non-linear one may well indicate something like a phase transition, such as occurs in the "crystallization" of rubber upon high elongation.[3] In the case of polyvinyl alcohol, a sample at some 250 percent elongation gave such a well-marked fiber pattern (cf. Fig. 10) as to indicate that something of the sort is occurring, and this will be followed up by further x-ray diffraction observations.

In the previous paper it was suggested that the phenomena observed might be accounted for by the formation of oriented chains of hydrogen bonds, relatively rigidly connected with, or integrated in, the long-chain structure of the colloid macromolecules. The outstanding effects which have to be explained are:

1. Absence of effect with purely organophile (hydrophobe) colloids (polymers). It appears that Wood's interpretation in terms of a differential dielectric capacity along and across an axis of fibering, while a relevant, and, in a sense, obligatory concomitant, is not a sufficient cause.

2. It is thought that the role of effective —OH groups, whether derived from constitutional hydroxyls (and perhaps amino- or imino-groups in proteins) or from these reinforced by adsorbed water molecules, is to form quasi-electronically conducting chains.

In the case of polyvinyl alcohol an idealized image of a parallel group of such chains, part of the molecules, is shown in Fig. 11.

In the dry material it is supposed that the chain molecules are aligned, side by side, with alternate hydrophobe ($-CH_2$) and hydrophile —OH adjacent alignment.† The extreme ease of lengthwise splitting supports this view.

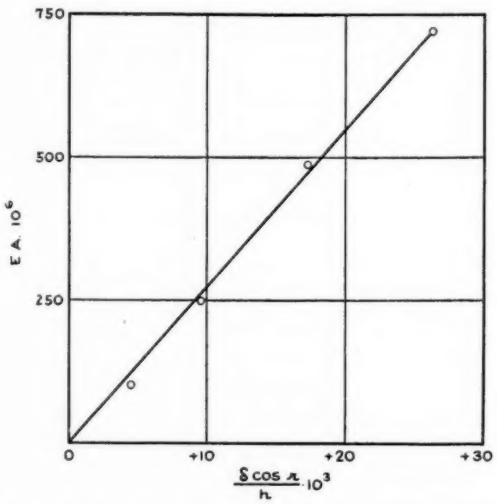

FIG. 8. Relation between electrical anisotropy and optical birefringence of polyvinyl alcohol.

A recent x-ray study of the structure of (crystalline) polyvinyl alcohol[4] indicates that some modification of this picture may be neces-

[2] J. Spence, J. Phys. Chem. **43**, 865 (1939); **45**, 401 (1941).

[3] H. Mark, Ind. Eng. Chem. **34**, 1343 (1942).

† *En bloc*, as compared with a plane, some complications of the arrangement might occur.

[4] Rose C. L. Mooney, J. Am. Chem. Soc. **63**, 2828 (1941).

sary, at any rate for well-crystallized material. It was not stated how the material was prepared but merely that "well-oriented samples can be obtained, the fiber periodicity is short, and the chemical composition known and simple." The structure concluded to represent the observations best did not accord with the assumption just made that the hydrogens are lying (as bridges) between successive oxygens in the same plane. This would not explain the 2.72A separation between oxygens of adjacent chains, and would give "a hydrogen bond distance somewhat shorter than is usual in alcohols. A more reasonable arrangement is that illustrated in Fig. 2 [our Fig. 12]. This shows *paired* vinyl alcohol chains projected in the 101 plane. The structure, as deduced from x-ray diffraction, is considered to consist of pairs of long-chain molecules, held together by hydrogen bonds. These double chains all lie along the fiber axis, but in random orientation about it. . . . Each chain has a zigzag carbon planar configuration, with glycol units in the 1, 3 position."

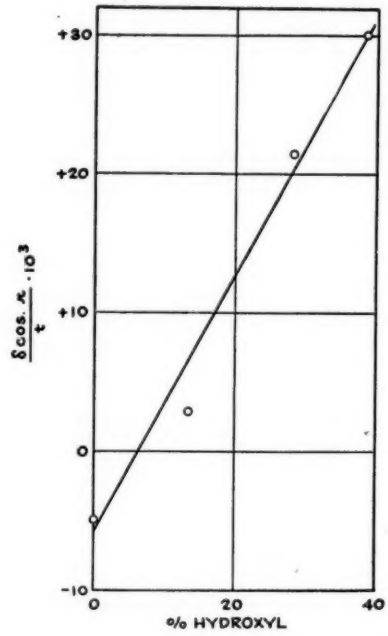

FIG. 9. Effect of hydroxyl content on the optical birefringence of hydrolyzed polyvinyl acetates at 225 percent elongation.

It appears that this paired structure would still permit of continuous hydrogen-bond chains.

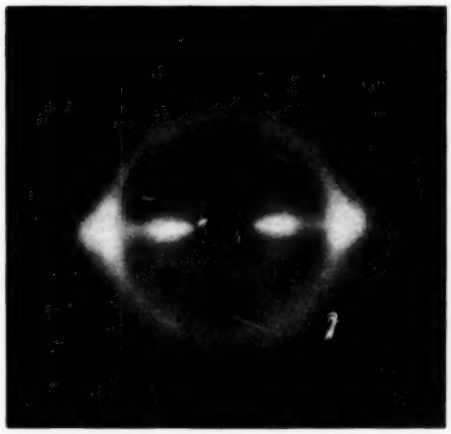

FIG. 10. Diffraction diagram, Cu $K\alpha$ of polyvinyl alcohol at 250 percent elongation, parallel to plane of sheet and perpendicular to direction of elongation.

The ease of splitting longitudinally observed in our specimens would still be possible, provided the double chains were not in too random orientation about the fiber axis. Also it is possible, as already mentioned, that crystallization occurs rather abruptly as a function of elongation and orientation. Insofar as H-bonding and conductance are concerned, the two molecular chains constitute only one shared H-bond chain.

A kind of electronic conduction could take place along the macromolecular chain by way of a quantum molecular resonance process; the hydroxyl can be regarded as resonating between the states symbolized below:

$$-OH \leftrightarrow -O^- \cdots H^+ \leftrightarrow -OH \leftrightarrow \text{etc.}$$

In an electric field a torque would be produced proportional to V^2, to the total current capacity of the conductors, and to $\sin\theta\cos\theta$ ($\propto \sin 2\theta$),

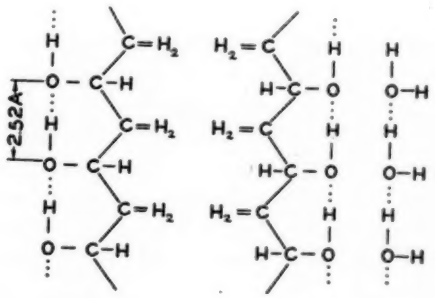

FIG. 11. Formation of chains of hydrogen bonds in polyvinyl alcohol (adsorbed water may form a separate chain as shown).

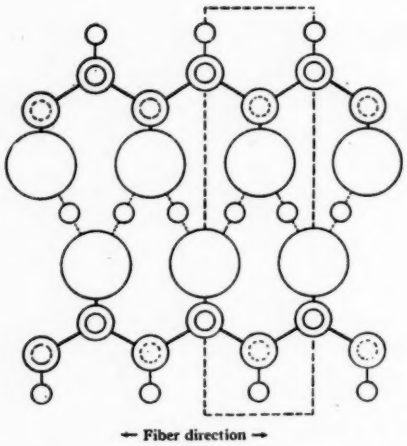

FIG. 12. [From Rose C. L. Mooney, J. Am. Chem. Soc. **63**, 2828 (1941).] Polyvinyl alcohol chains projected on the 101 plane. The circles, in descending order of size, represent oxygen, carbon, and hydrogen. The dotted and solid circles distinguish between hydrogens on alternate sides of the chains.

where θ is the angle between the axis of the conductor, and that of the electric field. The "independence of length" for polyvinyl alcohol, etc., seems somewhat at variance with the effect of adsorbed water with partly hydrolyzed polyvinyl acetates. In this case, evidently *gaps* would exist in the molecular chains, consisting of residual acetyl groups. It appears that these can be "bridged" by adsorbed water molecules. Beyond a certain composition, the nearer this latter approaches 100 percent polyvinyl alcohol, the less effective are the additional water molecules.

Considering again a completely stretched cellulose macromolecule or chain, then according to x-ray and other indications[5] it appears that while the two secondary —OH groups in one glucosan unit can possibly supply an H bond between themselves, it would be quite difficult for a primary —OH of one glucosan to bridge to a secondary —OH of a contiguous glucosan. Only by adsorption of water molecules could the two chains of H bonds be formed, as compared with the *one* chain feasible for polyvinyl acetates (cf. Fig. 13). This seems a reasonable explanation why the E. A. of partly hydrolyzed polyvinyl acetates increases linearly at first with the density of adsorbed water molecules, while with cellulose a power (initially 2) of the adsorption density seems involved. Exact relations are improbable, particularly for cellulose, because thermal and other conditions would affect the strength of individual hydrogen bridges, or, conversely, the interval necessary. Certainly for resonance and conductance along the chain, the strength of the H bond would have to be limited possibly up to 2.9A.[6] This could be satisfied readily enough in polyvinyl alcohol itself and probably without much difficulty in the "gaps" for hydrolyzed polyvinyl acetates, but in cellulose both the stereochemical and the energetic

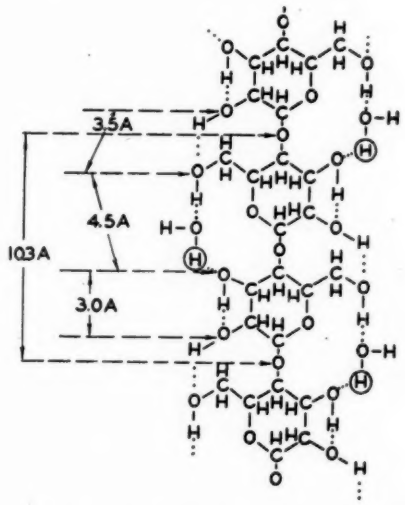

FIG. 13. Continuous hydrogen bonding in cellulose by the addition of one mole of water per glucose residue (bonds contributed by water are indicated by circles).

conditions for the adsorption are considerably more complicated. The figure given (Fig. 13) is based on the configuration deduced in the paper of Meyer and Misch[7] of 1937. In a recent paper by P. H. Hermans, J. de Booys, and C. J. Maan[8] certain modifications are suggested, which are of importance in regard to the regain of moisture (water adsorption) and to the bearing of this upon electrical anisotropy. These changes are

[5] K. H. Meyer and H. Mark, *Der Aufbau der hochpolymeren organischen Naturstoffe* (Akad. Verlagsges. m.b.H., Leipzig, 1930).

[6] L. Pauling, *The Nature of the Chemical Bond and the Structure of Molecules and Crystals* (Cornell University Press, Ithaca, New York, 1940), second edition, p. 289.

[7] K. H. Meyer and L. Misch, Helv. Chim. Acta **20**, 232 (1937).

[8] P. H. Hermans, J. de Booys, and C. J. Maan, Kolloid Zeits. **102**, 169 (1943).

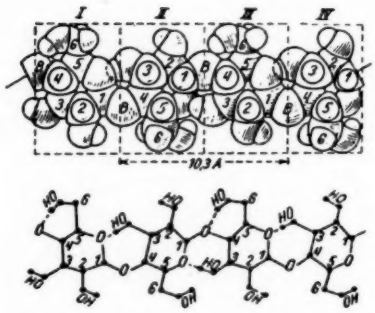

FIG. 14. [From P. H. Hermans, J. de Booys, and C. J. Maan, Kolloid Zeits. **102**, 177 (1943).] (a) Stuart model of the cellulose chain with spatial puckering viewed from above (oxygen atoms shaded). (b) Diagram of the corresponding nuclear structure.

largely based upon a remodelling using van der Waals radii (according to Stuart) for the atoms, and instead of a planar pyranose (hexose) ring, a puckered one, according with the "armchair" form of the cyclohexane ring.

In Fig. 14 is shown their "most probable configuration of the straight, stretched cellulose molecule with spatial buckling, and using Stuart's atom-models (van der Waals radii) viewed from above. It will be seen that the bridge oxygen between nuclei II and III lies somewhat downward, and, between I and II, or equally III and IV, somewhat upward [of a median plane] while the horizontal buckling factor is clearly evident. The model also shows that a horizontal buckling in the opposite sense would lead to steric hindrance." *

"Herewith only the choice of position of the —CH_2OH groups is left free. In Fig. 12 these [groups] are placed alternately in the 'normal' and the 'reverse' positions. —OH group 3 is given a particular position with respect to the ring-oxygen atom of the adjacent ring, such as to give a hydrogen bond. Likewise, such an H-bond is possible between the —OH in normal position at C-atom 6, and the glucosidic bridge-oxygen. By these additional ring systems, the stretched position of the chain might be further strengthened, since rotation about the glucoside bridges would be hindered."

The authors also point out this notable peculiarity of the β-glucose configuration [as adopted, cf. Figs. 2 and 3 of their article]. "All the hydroxyl groups find themselves on the side of the ring extension, while above and below only hydrogen-carrying valences project. The cellulose chain has actually a somewhat flattened shape and *therewith two* [2] *hydrophobe and two* [2] *hydrophile sides.*† With no other hexose than β-glucose can such a relation be obtained.

It is apparent that the configuration suggested by these authors would involve somewhat different conditions for the adsorption of water vapor, and for its effect upon electrical anisotropy, from those deducible from the earlier Meyer-Mark chain macromolecule. However, evidently in one important respect they are alike, *viz.*, in predicating a duplex or twofold array of adsorption "sites" for water to form continuous H-bond chains. The temperature coefficient of adsorption, or, more precisely, the differential adsorption heat, would seem likely to be of different magnitude and trend for the two cases, and may help to decide between them. The newer model, especially if the preferred formation of H bridges between glucosan —OH groups and bridge oxygens be accepted, would appear to require longer chains of oriented adsorbed water molecules than the earlier one.

We may note in this connection that S. Baxter[9] has suggested that the electrical conduction of textile fibers, e.g., wool, involves a mechanism other than electrolytic. He suggests an electronic conduction, as in a semiconductor. It is assumed that "the dry wool fiber is an almost perfect insulator, and that adsorbed water molecules cause 'impurity centers' giving rise to electronic conduction." We are not convinced, for reasons which will be discussed elsewhere,** that much of the direct (macro) conductance is not electrolytic, but agree in part with Baxter for an inner, residual electronic portion. The actual mechanism of this we consider to be by way of a hydrogen-bond resonance process, as indicated here.

A study of the temperature coefficients is contemplated, as well as of other factors, in the relation of electrical anisotropy to electrical conductance.

* Between hydrogens of successive glucosans.

† Our italics.

[9] S. Baxter, Trans. Faraday Soc. **39**, 207 (1943).

** In connection with the conductance of gelatin.

Letters to the Editor

PROMPT publication of brief reports of important discoveries in physics may be secured by addressing them to this department. The closing date for this department is the third of the month. Because of the late closing date for the section no proof can be shown to authors. The Board of Editors does not hold itself responsible for the opinions expressed by the correspondents. Communications should not in general exceed 600 words in length.

Photography of Crystal Structures

MAURICE L. HUGGINS
Eastman Kodak Company, Rochester, New York
November 1, 1944

AS shown by the writer[1] several years ago, Sir Lawrence Bragg's[2] method of photographic summation of Fourier series by addition of the proper patterns of light and dark bands can be improved in accuracy and speed by the use of a previously prepared set of masks.

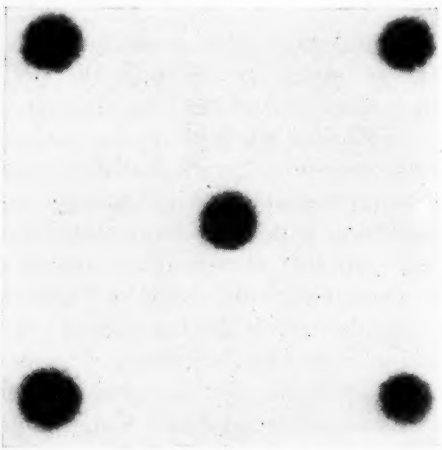

FIG. 1. Photograph, looking along one of the crystallographic axes, of the body-centered cubic unit of α-iron, from x-ray data by Armstrong.

With the assistance of the Physics Department of these Laboratories, an improved set of 316 masks for this purpose has recently been made. Using these, electron density photographs of crystal structures and Patterson summations are easily and rapidly made from the appropriate x-ray data. Examples are shown in Figs. 1–3. The magnification is of the order of 100,000,000 in each case.

Most of the background density, between the atoms, in Fig. 3[3] is not real, but is a result of inaccuracies in the x-ray data and in the masks and incompleteness of the former. The relative positions and approximate relative densities of the atomic peaks are correctly shown, however. In Fig. 1,[4] the background was removed by a short treatment with Farmer's reducer solution. In Fig. 2[5] the background has been practically all removed by reprinting.

The shape of the molecule in Fig. 2 is somewhat distorted, both because the plane of the molecule is not parallel to the plane of the projection and because the projection, as obtained, is a square, whereas the true projection of the unit cell is not. The latter cause of distortion can readily be removed, if desired, by adding another optical step or in other ways. For purposes of structure analysis, however, this is not necessary.

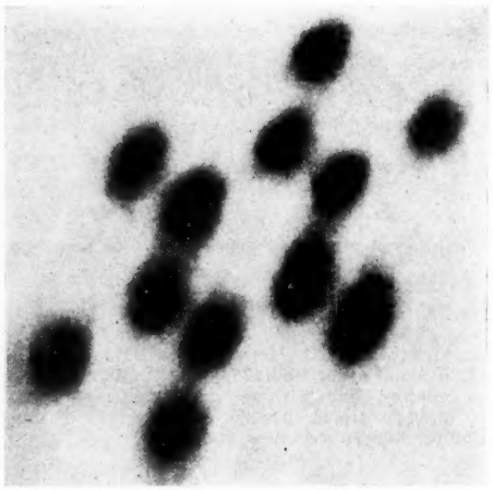

FIG. 2. Photograph of the hexamethylbenzene molecule, using x-ray data from the crystal, by Brockway and Robertson.

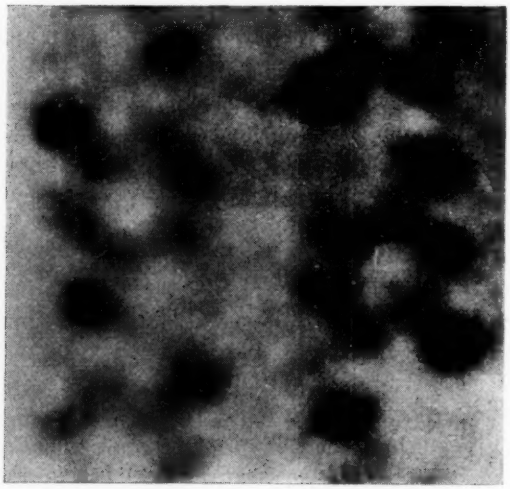

FIG. 3. Photograph of a β-resorcinol (*meta*-dihydroxybenzene) crystal, using x-ray data by Robertson and Ubbelohde. Two complete molecules, with parts of others, are shown.

We hope soon to be able to furnish duplicate copies of the improved set of masks, at a nominal cost, to others engaged in crystal structure analysis.

[1] M. L. Huggins, J. Am. Chem. Soc. **63**, 66 (1941).
[2] W. L. Bragg, Zeits. f. Krist. **A70**, 475 (1929); *The Crystalline State* (The Macmillan Company, London and New York, 1934), p. 229.
[3] J. M. Robertson and A. R. Ubbelohde, Proc. Roy. Soc. **A167**, 122 (1938).
[4] A. H. Armstrong, Phys. Rev. **34**, 931 (1929).
[5] L. O. Brockway and J. M. Robertson, J. Chem. Soc., p. 1324 (1939).

Errata : On the Statistical Mechanics of Liquids, and the Gas of Hard Elastic Spheres

[J. Chem. Phys. 12, 1 (1944)]

O. K. RICE
University of North Carolina, Chapel Hill, North Carolina
November 2, 1944

PAGE 4: Third and fourth lines above Eq. (3) and elsewhere on the page. The "dodecahedron" is actually a figure with twelve vertices but fourteen sides (six squares and eight triangles). The volumes are given correctly.

Page 11: Eq. (24). Second term in bracket,

$$\frac{1}{2}\frac{\sigma^3}{r_1^3\sigma^3}, \quad \text{should be} \quad \frac{1}{2}\frac{\sigma^3}{r_1^3\zeta^3}.$$

Page 16: Left-hand side of displayed unnumbered equation should be

$$[e^{1/3}T/\Theta(a_0)](2^{1/2}/2^{1/6}).$$

Page 18: In line following first equation in Appendix, "free space" should read "portion of the total length."

Note: It may be remarked that the term "cubic close-packed" and derivatives thereof are used in two senses. Sometimes they refer to a cubic close-packed array of hard spheres in mutual contact, which thus occupy the smallest possible volume. In other cases they refer rather to the type of lattice, without demanding that the spheres be in actual contact, the possibility of displacements about the average positions which form the lattice points being visualized. The actual usage in any given instance should be clear from the context.

Erratum: The Chain Photolysis of Acetaldehyde in Intermittent Light

[J. Chem. Phys. 10, 445 (1942)]

W. L. HADEN, JR., AND O. K. RICE
University of North Carolina, Chapel Hill, North Carolina
November 2, 1944

IN the abstract the energies of activation for reactions (2) and (3) are interchanged. They are given correctly in Table III.

Bond Moments of Higher Valence States

R. SAMUEL
The Illinois Institute of Technology, Chicago, Illinois, and the Hebrew Institute of Technology, Haifa, Palestine
November 10, 1944

IN a recent article[1] additive bond moments have been calculated for non-aromatic first-order molecules formed by a central atom in its maximal state of valency. This has been done on the basis of classical formulae. One point apparently has not been made sufficiently clear, as it has subsequently been raised in a number of discussions. This is, whether the new values in reality are not those of the semipolar double bonds. In other words, whether, for example, the value of 4.4D ascribed to the bond between pentacovalent nitrogen and oxygen in the nitro group, does not constitute in reality the value for the semipolar double bond between the same two atoms. In this letter it will be shown that this is not so.

On the basis of the resonance interpretation of the semipolar double bond, the nitro group is a hybrid of the two forms

$$O=\overset{|}{\overset{+}{N}}-\overset{-}{O} \qquad (1a)$$

and

$$\overset{-}{O}-\overset{|}{\overset{+}{N}}=O. \qquad (1b)$$

On account of the rigorous energetical degeneracy each form contributes 50 percent. Indeed, if no other similar molecule existed, the value of 4.4D could easily be associated with this mixture.

But in the azoxy compounds the two corresponding forms are

$$-N=\overset{|}{\overset{+}{N}}-\overset{-}{O} \qquad (2a)$$

and

$$-\overset{-}{N}-\overset{|}{\overset{+}{N}}=O. \qquad (2b)$$

These constitute two different terms of the molecule, and according to their energetical difference (2a) will contribute x_1 percent and (2b) y_1 percent. To obtain the value of 4.4D for the mixture, the energy difference must be such that x_1 and y_1 just have the required values. This would be an entirely fortuitous coincidence, as this energy of excitation depends on both parts of the molecule equally and not on the nitrogen-oxygen part alone.

Again the *N*-ethers of oximes would be mixtures of x_2 percent of

$$>C=\overset{|}{\overset{+}{N}}-\overset{-}{O} \qquad (3a)$$

and y_2 percent of

$$>\overset{-}{C}-\overset{|}{\overset{+}{N}}=O, \qquad (3b)$$

and if fortuitously the energy difference between these two terms is such that x_2 and y_2 obtain the required ratio the value of 4.4D may result for the moment of this bond. The same would be true of nitrous oxide, which would be a mixture of x_3 percent of

$$N\equiv\overset{|}{\overset{+}{N}}-\overset{-}{O} \qquad (4a)$$

and y_3 percent of

$$\overset{-}{N}=\overset{|}{\overset{+}{N}}=O. \qquad (4b)$$

This is only half of the problem. A very great number of molecules are interconnected by having one or the other bond in common. Thus, the same bond between C and N of the *N*-ethers occurs again with the same moment in the

diazo compounds which would be mixtures of x_4 percent and y_4 percent of two forms. The ratio of x_4 and y_4 must be such as to obtain the same value of 2.6 D for the bond between C and N as in the *N*-ethers. But for the latter the percentage ratio of x_2 and y_2 has already been fixed according to the requirements of the bond between N and O. The difference between the two energy levels of the *N*-ethers and hence the ratio of x_2 and y_2 must be such as to obtain for this mixture of two forms the same moment of the nitrogen-oxygen bond as in the nitro group, of the nitrogen-carbon (double) bond the same as in the diazo compounds, and of the nitrogen-carbon (single) bond the same as in the nitrates. The argument must not be elaborated. But it is very difficult to see how the excitation energies of the molecules can be consistent with so many different and simultaneous conditions.

To sum up: The problem which confronts us cannot be solved by means of philology but is a genuine problem in the realm of physics. On the basis of the classical formulae we expect in first approximation constant and additive moments of the individual bonds, and we find them. On the basis of the resonance interpretation of the theory of the semipolar double bond we really cannot expect additive and constant bond moments, but we find them nevertheless. Hence we have to explain each of them by a whole series of fortuitous coincidences, which in the framework of this theory remain unexplained freaks of nature. As has been pointed out, such a state of affairs cannot be directly disproved by a physico-chemical experiment, because the percentage ratio is a variable factor in the latter theory. But it would appear that the classical concepts are superior by virtue of the principle of economy of hypotheses.

[1] R. Samuel, J. Chem. Phys. **12**, 380 (1944).

Author Index to Volume 12

References with (L) are to Letters to the Editor.

Alfrey, Turner, Jr. Molecular theory of the viscoelastic behavior of an amorphous linear polymer—374

—— **and G. Goldfinger.** Copolymerization of systems of three and more components—322(L)

—— **and G. Goldfinger.** Mechanism of copolymerization—205

Amdur, I., Margaret McCormack Jones, and H. Pearlman. Accommodation coefficients on gas covered platinum—159

Andersen, Holger C. and E. R. Van Artsdalen. Bromination of hydrocarbons. II. Photochemical bromination of ethane and ethyl bromide. Carbon-hydrogen bond strength in ethane—479

Aston, John G., Saul Isserow, George J. Szasz, and Robert M. Kennedy. Empirical correlation and method of calculation of barriers hindering internal rotation—336

—— **G. W. Moessen, H. C. Hardy, and G. J. Szasz.** Heat capacity of gaseous butadiene-1,3—458

Auluck, F. C. and R. N. Rai. Surface tension and van der Waals' equation—321(L)

Beck, Clifford. Infra-red absorption of solid ammonium chloride and ammonium bromide—71

Branson, Herman (see Simha, Robert)—253

Brown, Sanborn C., John W. Irvine, Jr., and M. Stanley Livingston. Cyclotron targets: preparation and radiochemical separation. II. Krypton—132

Carr, Howard. Thermal diffusion in liquids—349(L)

Cassel, Hans M. Condensation and supersaturation of adsorbed phases—115(L)

Cleveland, Forrest F. Raman spectra of hydrocarbons. IV. 2,5-Dimethyl-1, 5-hexadiene and 2,5-dimethyl-2,4-hexadiene—53

—— (see Hamilton, Dwight T.)—249

—— (see Meister, Arnold G.)—393

—— (see Murray, M. J.)—156

—— **and M. J. Murray.** Erratum: Raman spectra of acetylenes. VII. Symmetrical-top acetylenes—320

Coggeshall, Norman D. Discrimination in mass spectrometer ion sources—19

Cross, Paul C., R. M. Hainer, and Gilbert W. King. Asymmetric rotor. II. Calculation of dipole intensities and line classification—210

Dodgen, Harold W. (see Rollefson, G. K.)—107

Doty, Paul M. Dissociation of methyl chloride on a hot filament—399

—— (see Zimm, B. H.)—203(L)

—— **and Joseph E. Mayer.** Electron affinity of bromine and a study of its decomposition on hot tungsten—323

——, **B. H. Zimm, and H. Mark.** Some light scattering experiments with high polymer solutions—144(L)

Duncan, A. B. F. (see Lawson, Martha)—329

Dunicz, Boleslaw Ludwik. Application of probability considerations to the mechanism of the photochemical polymerization of acetylene—37; Erratum—204(L)

Dwyer, R. J. and O. Oldenberg. Dissociation of H_2O into H+OH—351

Flory, Paul J. Thermodynamics of heterogeneous polymer solutions—114(L)

—— Thermodynamics of heterogeneous polymers and their solutions—425

—— **and John Rehner, Jr.** Effect of deformation on the swelling capacity of rubber—412

Gemant, Andrew. Potentiometric measurements of hydrogen ion concentration in solutions of low dielectric constant—79

Glockler, Geo., John F. Haskin, and Claire C. Patterson. Depolarization of Raman lines. A further simplification of method—349(L)

Goldfinger, G. (see Alfrey, Turner, Jr.)—205, 322(L)

Gunning, H. E. and E. W. R. Steacie. Mercury photosensitized polymerization and hydrogenation of butadiene—484

Haden, W. L., Jr., and O. K. Rice. Erratum: Chain photolysis of acetaldehyde in intermittent light—521(L)

Hainer, R. M. (see Cross, Paul C.)—210

Hamilton, Dwight T. and Forrest F. Cleveland. Raman spectra of hexachloroethane and hexabromoethane—249

Hardy, H. C. (see Aston, J. G.)—458

Harker, David. Crystal structure of Ni_4Mo—315

Harkins, William D. (see Jura, George)—113(L), 114(L)

—— **and George Jura.** Decrease (π) of free surface energy (γ) as a basis for the development of equations for adsorption isotherms; and the existence of two condensed phases in films on solids—112(L)

Haskin, John F. (see Glockler, Geo.)—349(L)

Hennig, Gerhart R. and George E. Kimball. Kinetics of the electroreduction of acetone—415

Herman, R. C. (see Shaffer, W. H.)—494

Hill, Terrell L. Electrostatic contribution to hindered rotation in certain ions and dipolar ions in solution. III—56; IV—147

Huggins, Maurice L. Photography of crystal structures—520(L)

Irvine, John W., Jr. (see Brown, Sanborn C.)—132

Isserow, Saul (see Aston, John G.)—336

James, T. H. Charge effect in photographic development: Role of the gelatin—453

Jansen, E. F. (see Shaw, T. M.)—439

Jones, Margaret McCormack (see Amdur, I.)—159

Chemistry Library

THE JOURNAL OF CHEMICAL PHYSICS

VOLUME 12 NUMBER 12

DECEMBER, 1944

Published by the
AMERICAN INSTITUTE OF PHYSICS
incorporated
Lancaster Pa. and New York, N. Y.

The Journal of Chemical Physics

ADVISORY EDITORIAL BOARD

R. T. Birge — Irving Langmuir
A. H. Compton — John T. Tate
Lewis Franck — Harold C. Urey

BOARD OF EDITORS

Joseph E. Mayer, *Editor*

Associate Editors

Term ending December 31, 1944	*Term ending December 31, 1945*	*Term ending December 31, 1946*
Charles O. Beckman	L. O. Brockway	I. Fankuchen
Hatch L. Crawford, Jr.	Ronald W. Gurney	Paul J. Flory
F. Daniels	Kenneth S. Pitzer	Joseph H. Frazer
David Harker	Alfred L. Sklar	Joseph O. Hirschfelder
Bryce H. Weatherwax	E. W. H. Stracie	W. F. Libby
	Hugh S. Taylor	Walter H. Stockmayer

The Journal of Chemical Physics is published monthly by the American Institute of Physics. Its purpose is to bridge a gap between journals of physics and journals of chemistry. The artificial boundary between physics and chemistry has now been in actual fact completely eliminated, and a large and active group is engaged in research which is as much the one as the other. It is to this group that the Journal is rendering its principal service and makes its greatest appeal, both as a prompt and efficient medium for publication of research and as a convenient and carefully edited assemblage of pertinent information.

Subscription Rates

The United States and Possessions, Canada and Mexico $10.00
Elsewhere 11.00

Back Numbers

Complete set: Vol. 1, 1933—Vol. 11, 1943 ..... $110.00
Yearly rate: $11.00.
Single copies: $1.00 each.

The Journal of Chemical Physics is published monthly by the American Institute of Physics, 57 East 55th Street, New York 22, New York.

Entered as second class matter December 1933 at the post office at Lancaster, Pa., under the Act of August 24, 1912, acceptance for mailing at special rate of postage provided for in paragraph 4, Section 538, P. L. & R. authorized [illegible]

THE AMERICAN INSTITUTE OF PHYSICS

INCORPORATED

ADMINISTRATIVE STAFF

HENRY A. BARTON, *Director*

MADELINE M. MITCHELL, *Publications Manager*

JOHN T. TATE, *Advisor on Publications*

Office: 57 East 55 Street, New York 22, New York

JOURNALS

THE PHYSICAL REVIEW
REVIEWS OF MODERN PHYSICS
JOHN T. TATE, *Editor (on leave)*
J. W. BUCHTA, *Acting Editor*

JOURNAL OF THE OPTICAL SOCIETY OF AMERICA
GEORGE R. HARRISON, *Editor*

THE JOURNAL OF THE ACOUSTICAL SOCIETY OF AMERICA
FLOYD A. FIRESTONE, *Editor*

AMERICAN JOURNAL OF PHYSICS
DUANE ROLLER, *Editor*
JOSEPH D. ELDER, *Assistant Editor*

THE REVIEW OF SCIENTIFIC INSTRUMENTS
GAYLORD P. HARNWELL, *Editor*

THE JOURNAL OF CHEMICAL PHYSICS
JOSEPH E. MAYER, *Editor*

JOURNAL OF APPLIED PHYSICS
ELMER HUTCHISSON, *Editor*

GOVERNING BOARD

PAUL E. KLOPSTEG, *Chairman*
Northwestern University

GEORGE B. PEGRAM, *Secretary*
Columbia University

For the American Physical Society:

L. A. DUBRIDGE
University of Rochester

GEORGE B. PEGRAM
Columbia University

JOHN T. TATE
University of Minnesota

For the Optical Society of America:

K. S. GIBSON
National Bureau of Standards

R. C. GIBBS
Cornell University

A. G. WORTHING
University of Pittsburgh

For the Acoustical Society of America:

FLOYD A. FIRESTONE
University of Michigan

WALLACE WATERFALL
The Celotex Corporation

HARVEY FLETCHER
Bell Telephone Laboratories

For the Society of Rheology:

R. B. DOW
Aberdeen Proving Ground

HERMANN MARK
Brooklyn Polytechnic Institute

N. W. TAYLOR
Minnesota Mining & Manufacturing Company

For the American Association of Physics Teachers:

PAUL E. KLOPSTEG
Northwestern University

T. D. COPE
University of Pennsylvania

L. W. TAYLOR
Oberlin College

The American Institute of Physics is a membership corporation of which five societies are the founding members. These five societies are the principal national societies devoted to pure and applied physics in America. Their officers and those of their representatives who form the Governing Board of the Institute, are given above. The principal product of the Institute is the publications sponsored by the societies or by itself. The boards and the editors of the journals are listed above.

The broad purpose of the Institute is to represent, in all matters of wide or common interest, the five thousand or more members and subscribers associated with the Founder Societies and the journals. It aims to advance the science and profession of physics, and to promote cooperation between pure research, the applied sciences, and the industries. To achieve these aims, it is greatly in need of an endowment and is empowered by law to administer grants and funds of any kind.

CONTENTS

THE JOURNAL OF CHEMICAL PHYSICS, Vol. 12, No. 12 DECEMBER, 1944

Sensitization of Hydrocarbons. I. Photochemical and Thermal Bromination of Methane and Methyl Bromide; Carbon-Hydrogen Bond Strength in Methane . . . . . G. B. KISTIAKOWSKY AND E. R. VAN ARTSDALEN 469

Sensitization of Hydrocarbons. II. Photochemical Bromination of Ethane and Ethyl Bromide. Carbon-Hydrogen Bond Strength in Ethane . . . . . HOLGER C. ANDERSEN AND E. R. VAN ARTSDALEN 479

Mercury Photosensitized Polymerization and Hydrogenation of Butadiene . . . . . H. E. GUNNING AND E. W. R. STEACIE 484

Tetrahedral XY_2 Molecular Models. Part I. Classical Vibration Problem . . . . . W. H. SHAFFER AND R. C. HERMAN 494

Infra-Red Spectra of Heat XY_2 Molecules. Part I. Vibration-Rotation Energies . . . . . W. H. SHAFFER AND R. F. SCHUMAN 504

Electrical Anisotropy of Solutions of Hydrophilic Colloids. Part II . . . . . S. E. SHEPPARD AND P. T. NEWSOME 513

Letters to the Editor:

Photography of Crystal Structures . . . . . MAURICE L. HUGGINS 499

Rigorous Theory of Molecular Orientation: On the Statistical Mechanics of Dipoles, and the Gas of Hard Elastic Spheres . . . . . O. K. RICE 501

Fluorescence, The Chain Hypothesis of Autoionization in Intermittent Light . . . . . W. L. HARDIN, JR., AND O. K. RICE 503

Photodissociation of Hydrogen-Halogen Mixtures . . . . . E. ROTHSTEIN 505

Abstract Issue to Volume 12 523

Analytic Subject Index to Volume 12 535

Volume Table of Contents iii

LANCASTER PRESS, INC., LANCASTER, PA.